COMBUSTION & FLAME

Quarterly Journal of The Combustion Institute

Contents

VOLUME 1 NO. 4 DECEMBER 1957

	Page
MECHANISMS FOR THE FORMATION OF IRONS IN FLAMES. *H. F. Calcote*	385
STUDIES ON THE OXIDATION OF HYDROCARBONS UNDER EXTREMELY CLEAN EXPERIMENTAL CONDITIONS. *Z. G. Szabó and D. Gál*	404
DETERMINATION OF BURNING VELOCITY OF PENTABORANE-OXYGEN-NITROGEN MIXTURES. *W. G. Berl, E. L. Gayhart, E. Maier, H. L. Olsen and W. T. Renich*	420
AN ISOTOPIC TRACER STUDY OF CARBON FORMATION IN HYDROCARBON FLAMES. *R. E. Ferguson*	431
A THEORY OF FLAME PROPAGATION LIMITS DUE TO HEAT LOSS. *E. Mayer*	438
EXTINCTION OF FIRES IN LIQUIDS BY COOLING WITH WATER SPRAYS. *D. J. Rasbash and Z. W. Rogowski*	453
INTERPRETATION OF THE SAMPLE TAKEN BY A PROBE IN A LAMINAR CONCENTRATION GRADIENT. *A. A. Westenberg, S. D. Raezer and R. M. Fristrom*	467
RECENT DEVELOPMENTS AND NOTES. *W. A. Kirkby*	479
PUBLICATIONS	487
INDEX	489

Published quarterly. Annual subscription including postage—U.K. £5 5s. 0d.; U.S.A. $16.00. Combined subscription with FUEL*—U.K. £8 8s. 0d.; U.S.A. $25.00. Editorial Offices, Showroom, Binding and Trade Departments:* 4-5 Bell Yard, Temple Bar, London, W.C.2. *Publishing and Advertisement Offices:* 88 Kingsway, London, W.C.2. *Telephone:* Holborn 6900. *U.S.A. Distributors: Interscience Publishers Inc., 250 Fifth Avenue, New York 1, N.Y.*

BUTTERWORTHS SCIENTIFIC PUBLICATIONS

Mechanisms for the Formation of Ions in Flames

H. F. CALCOTE*

The status of our understanding of the mechanisms of ion formation in flames is summarized, including not only a review of the literature but also some new proposals on cumulative and chemi-ionization. The high observed concentrations of ions in the combustion zone cannot be accounted for by thermal ionization of impurities, of equilibrium species existing at the flame temperature, or of non-equilibrium species. Ionization of carbon particles may account for the ions in high temperature-rich hydrocarbon flames, but experimental evidence is poor. This explanation is unsatisfactory for flames in lean mixtures. Ionization via translational energy or a simple extension of the high-energy tail of the Boltzmann curve is too slow. The most probable mechanism except for high temperature flames where thermal ionization predominates is cumulative excitation by processes such as

$$CO(^1\Pi) + C_2(^1\Sigma_u^+) \rightarrow CO(^1\Sigma^+) + C_2^+ + e^-$$

or chemi-ionization by processes such as

$$C_2(^3\Pi_g) + O_2 \rightarrow CO(^1\Sigma^+) + CO^+ + e^-$$

The most critical problem in this field is the actual identification of the ion.

IT HAS been known for a long time that flames possess a high electrical conductivity and can be distorted by an electric field. In fact, in 1801, A. VOLTA used a flame to discharge the electricity from the surface of a non-conductor[1] and, in 1802, G. ERMAN[2] obtained currents from flames by inserting two wires in them. The mechanism by which the ions are produced is not completely understood except in high temperature flames where a thermal process probably predominates.

As early as 1906 F. L. TUFTS[3] suggested that ions arose in some fashion from the chemistry of the combustion process. This might be taken as the first and apparently only consideration of chemi-ionization, a kinetic process, until recently[4,5]. Most suggestions have involved a thermal process where the problem reduces to finding a species of sufficiently low ionization energy so that thermodynamics, via Saha's equation, can be employed to calculate the ion concentrations. Thus S. W. SAUNDERS and associates[6-8] from 1926 to 1929 as well as J. A. J. BENNETT[9], 1927, argued for a thermal process without proposing the species being ionized. K. F. BONHOEFFER and F. HABER[10,11] in 1928 suggested that radicals such as CC and OH might have sufficiently low ionization potentials to account for the electrical properties of flames. C. TANFORD[12] in 1946 pointed out that nitric oxide has a low ionization potential and in equilibrium concentrations could be the species thermally ionized. B. LEWIS and G. VON ELBE[13] quote O. STERN as suggesting that polymerized carbon atoms, C_4, C_6, etc., might have ionization potentials approaching the work function of graphite, or that even small carbon particles might be responsible. V. I. TVERDOKHLEBOV[14] assumes that C_nH_m or C_n containing a large quantity of internal energy is

*Present address: AeroChem Research Laboratories Inc., P.O. Box 12, Princeton, New Jersey.

ionized by collision with electronically excited OH. Impurities such as sodium with low ionization potentials are frequently suggested. Lewis and von Elbe[13] even suggest that friction of the gas flowing past the tube walls may produce the ions. More recently E. SAENGER, P. GOERCKE and I. BREDT[15] have argued for a mechanism by which the chemical energy is first released as translational energy which is transferred to ionization via collisions before thermal equilibrium is obtained. H. BEHRENS[16,17] suggests that molecular ions may be formed by recombination of excited atoms.

The various mechanisms will be evaluated in this paper with the object of arriving at the most acceptable within the framework of our present knowledge.

EXPERIMENTAL OBSERVATIONS

The experimental observations of importance for this study can be summarized by stating that: (*a*) some flames, depending upon the type of fuel, can be strongly deflected by electric fields[4,5,18–21] and in some instances can be extinguished[11,22–26] or stabilized[4,5]; and (*b*) the ion concentration is greater in the combustion zone than in the hot gases immediately after it[28–32]. This latter observation was made very early in the century, 1906, by F. L. TUFTS[28] and J. F. DAVIDSON[27]. From the relative electrical conductivity in the reaction zone and in the gases immediately behind this zone where the ion concentration has been accurately measured, it is possible from the old literature to deduce an ion concentration in the reaction zone of hydrocarbon–air flames of greater than 4×10^{10} ions cm^{-3}. From deflection of flames in electric fields[4] and from estimates from the flame pressure with an applied field[5] the concentration is approximately 10^{12} ions cm^{-3}. These values have been confirmed by more careful measurements employing Langmuir probes[32].

THERMAL IONIZATION

The most obvious source of ions is thermal, i.e. equilibrium ionization determined by the concentrations of species of low ionization potential and the flame temperature. The equilibrium constant for this process was derived by Saha in 1920 and the significance of Saha's 'chemical constant' made clear by R. H. FOWLER[33].

For a singly ionized species

$$M \rightleftharpoons M^+ + e^-$$

the equilibrium constant K_N for concentrations (N_o, N_+ or N_-) expressed in atoms (molecules), ions, or electrons per cubic centimetre is given by the relation

$$\log K_N = \log [(N_+ N_-)/N_o]$$
$$= \log G + 15{\cdot}38 + 1{\cdot}5 \log T - 5040\, V_i/T$$

where $G = (g_+ g_-)/g_o$ and the gs are the statistical weights, T is the absolute temperature, and V_i = ionization potential in electron volts (eV). Thus by means of straightforward thermodynamics employed to calculate the adiabatic flame temperature and equilibrium concentrations in a flame it is possible to calculate the equilibrium concentrations of ions. Since the

calculation of ion concentration usually does not alter the concentrations of other species it is adequate to employ the equilibrium constant for ionization calculated by Saha's equation to predict the thermal ionization of a particular species.

There are several possibilities for ion formation by thermal means—these are ionization of: (*a*) impurities, (*b*) equilibrium species existing at the flame temperature, (*c*) non-equilibrium species existing at the flame temperature, and (*d*) carbon particles. Each of these possibilities will be treated.

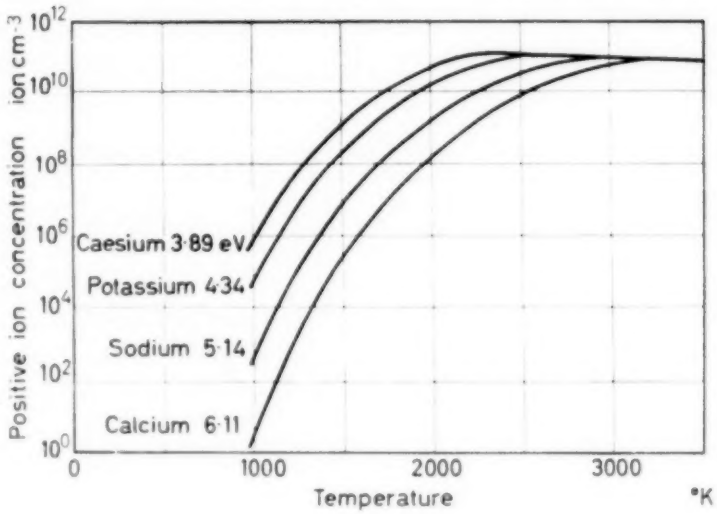

Figure 1. Effect of temperature and ionization potential on the thermodynamic ion concentration. Calculated by Saha's equation assuming an initial species concentration of 1×10^{12} *atoms* cm^{-3} *at 298° K*

Impurities

Any impurities having low ionization potentials such as the alkali metals or alkaline earths will contribute to ionization, particularly at higher temperatures. Since only trace quantities are required this source must be carefully considered. K. E. SHULER and J. WEBER[34] observe that the potassium doublet always appears in spectroscopic studies of flames at the Applied Physics Laboratory and interpret the data to indicate a concentration at 3000°K of 10^{10} to 10^{12} potassium atoms cm^{-3}. In addition, R. M. MOYERMAN and K. E. SHULER[35] in an extensive literature review conclude that the concentration of sodium atoms in the atmosphere is of the order of 10^{10} to 10^{12} atoms cm^{-3}. Assuming 10^{12} atoms cm^{-3} at room temperature the contribution to ion concentration from possible impurities is indicated in *Figure 1*. No account has been taken of the equilibria of the atoms with their oxides or salts which would tend to reduce the ion concentration. The formation of negative ions would reduce the number of electrons and slightly increase the number of positive ions[36–58].

In high temperature flames such as hydrogen–oxygen and acetylene–oxygen, where the adiabatic flame temperatures approach 3000°K and

3360°K respectively, the ionization in the outer cone might certainly be due primarily to impurities in the atmosphere such as sodium. Actually, the concentrations of sodium estimated for atmospheric air would hardly be expected to apply when the gases are taken from high pressure cylinders. Nevertheless, at 1400°K, a potassium atom impurity of 10^{12} potassium atoms cm^{-3} would give $7{\cdot}8 \times 10^{7}$ ions cm^{-3} and 10^{12} sodium atoms cm^{-3} would give $2{\cdot}6 \times 10^{6}$ ions cm^{-3}. This compares[32, 39] with an experimental value in a propane–air flame at this temperature of about 10^{10}.

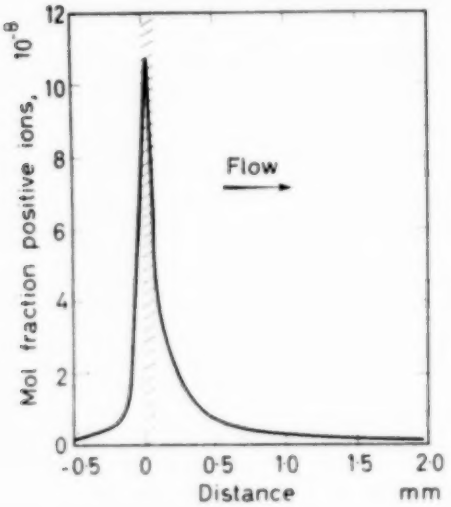

Figure 2. Ion concentration through a typical combustion wave. Propane, equivalence ratio =0·84, 13·2 mol per cent. Oxygen +86·8 mol per cent nitrogen, 1 atm, T_b=1535°K flat flame on 8·9 cm burner, probe diameter=0·005 cm, platinum—40 per cent rhodium

The major ionization in a flame occurs in a very thin zone (*Figure 2* and refs. 4, 5, 31, 32, 40) corresponding to the reaction zone. This is sufficient proof in itself that ionization is not due to impurities such as sodium because the gas temperature remains high past the reaction zone and in fact usually rises slightly. If impurities were responsible for the majority of ions the ion concentration would follow closely to the gas temperature; but it does not, and the ion concentration falls rapidly (*Figure 2*). It is this phenomenon that allows one to use ionization as a means of observing the position of the flame front in turbulent flame studies[40–42]. It should be noted, however, that salted flames also show a higher conductivity in the combustion zone than behind the combustion zone[3, 27] and that A. G. GAYDON and H. G. WOLFHARD[36] find abnormal excitation of metal atoms in the combustion zone. The difference between the relative ion concentrations in the inner cone and just above the inner cone of salted and unsalted flames is striking (*Table 1*).

Table 1. Relative conductivities in combustion zone and just above combustion zone for salted and natural flames

	Salted flame	*Unsalted flame*
Combustion zone[3b]	10	1000
Above combustion zone	1	1
Combustion zone[27]	1·5	20
Above combustion zone	1	1

The numbers in the two columns bear no relation to each other; the conductivity for the sodium chloride salted flame was much greater than for the unsalted flame

Other arguments against thermal ionization due to impurities in the flame front of hydrocarbon flames were presented by H. F. CALCOTE and C. R. KING[32]. Flames of carbon disulphide and hydrogen sulphide contain very small concentrations of ions. Were contaminants responsible, these flames ($T_b = 2265°$ and 2100°K) would be expected to afford ion concentrations comparable to hydrocarbon flames.

Another argument against impurities in hydrocarbon flames is the observation that in relatively cool flames respectable concentrations of ions are observed[32]. Thus[32,39], in a fuel lean propane–air flame at an equivalence ratio* of 0·467 where the calculated adiabatic flame temperature is 1330°K, the ion concentration in the reaction zone is roughly 2×10^{10} ions cm^{-3}. The theoretical concentration for an uncontaminated flame is roughly 10^{-4} ions cm^{-3}. The experimental value is 10^{14} times greater than the theoretical value. To account for this concentration by sodium contaminant would require 10^{17} sodium atoms cm^{-3}—an unrealistic quantity.

Therefore, it can be concluded that impurities are not responsible for ionization in the reaction zone of hydrocarbon–air flames.

Reaction intermediates and products

Thermal ionization may be reasonably expected for any species present in the flame front with a low ionization potential. Reaction intermediates

Table 2. Some ionization potentials of molecules

Molecule	*Ionization potential eV*	*Ref.*	*Molecule*	*Ionization potential eV*	*Ref.*
CO	14·1		$CH_2=CH_2$	10·5	47
CO_2	13·8		$CH_3-C\equiv CH$	10·4	48
NO	9·25	43	$CH_3-CH=CH_2$	9·73	43
NO_2	12·3	43	$CH_3-CH_2-CH=CH_2$	9·8	49
N_2O	12·9	43	$CH_3-CH=CH-CH_3$	9·3	49
NH_3	10·2	43	$CH_3-CH_2-C\equiv CH$	10·2	48
O_2	12·2		$(CH_3)_2C=CH_2$	9·4	49
O_3	12·8	44	$(CH_3)_2C=O$	10·3	50
H_2O	12·6		cyclo*Propane*	10·1	43
HCOOH	11·5	45	cyclo*Hexane*	9·88	43
CH≡CH	11·2	46	cyclo*Hexene*	8·95	43

and products either present in equilibrium or non-equilibrium concentration might contribute to ionization. *Tables 2* and *3* summarize the ionization potentials for a number of such species. The ionization potentials for some of the radicals are certainly low but still greater than for the alkali metals. Radicals with low ionization potentials were first suggested by Bonhoeffer and Haber[10,11] in 1928 as the source of ions in flames. Radicals,

*Stoichiometric air/fuel ratio divided by actual air/fuel ratio.

however, will not account for ionization in the flame front of hydrocarbon–air flames, as indicated in *Table 4*. The required concentrations are much greater than is reasonable.

Table 3. Some ionization potentials of radicals

Radical	*Ionization potential eV*	*Ref.*	*Radical*	*Ionization potential eV*	*Ref.*
OH	12·7	51	$CH_2=CH-CH_2$	8·16	60
HO_2	11·5	52	$(CH_3)_2CH$	7·90	59
CH	11·1	53	$CH_2=C(CH_3)CH_2$	8·03	61
CH_2	11·9	54	$CH_3-CH=CH-CH_2$	7·71	61
CH_3	9·88	55	$C_6H_5CH_2$	7·73	58
C_2	12	56, 57	$CH_3C_6H_5CH_2$		47
C_2H	11·3	53	para	7·46	
$CH_2=CH$	8·16	58	ortho	7·61	
CH_3-CH_2	8·78	59	meta	7·65	
$CH\equiv C-CH_2$	8·25	59			

Table 4. Required species concentration (per cm³) to produce thermally the experimental positive ion concentration in flames (Reference Figure 4)

Species ionized	V_i	*At the equivalence ratio*		
		0·70 *Lean*	1·0 *Stoichiometric*	1·5 *Rich*
CC	12	1×10^{32}	1×10^{29}	3×10^{31}
$CH_2=CH$	8·2	7×10^{21}	2×10^{20}	6×10^{21}
$C_6H_5CH_2$	7·73	4×10^{20}	2×10^{19}	4×10^{20}
$CH_3-CH=CH-CH_2$	7·71	3×10^{20}	2×10^{19}	3×10^{20}

Carbon particles

It was first suggested by O. Stern (see ref. 13) that carbon particles are responsible for the ions observed in flames. He reasoned that the ionization potential would lie between the work function 4·35 eV, and the ionization potential, 11·3 eV of gaseous carbon. This view was supported by K. E. Shuler and J. Weber[34] for very rich acetylene–air flames, by V. I. Tverdokhlebov[62] for hydrocarbon flames, and has been used by T. M. Sugden and B. A. Thrush[63] and by H. Einbinder[64] to study the ionization of free carbon in acetylene–air flames. J. K. McNeely and collaborators[65] observed in studies of flame distortion by d.c. electric fields in diffusion flames that 'if the amount of free carbon in a flame may be judged by the colour of the flame, the ionization as measured by the current bears a direct relation to the free carbon'. T. Kinbara and J. Nakamura[66] observe that sooty flame fuels, such as benzene, toluene, and acetylene, are very conductive while the conductivity of methyl and ethyl alcohol and hydrogen flames is comparatively low. Deflection of propane–air flames in an electric field has been interpreted by M. J. Saunders and A. G. Smith[67] in terms of ionized carbon particles. However, an electric wind explanation of this same phenomenon is more satisfying[1, 3]. Tufts[3], in 1906, had

noted that in diffusion flames the maximum conductivity occurs in the lower part of the flame and not in the luminous part.

T. KINBARA and associates[66, 68, 69] have made a careful study of ionization in diffusion flames. They interpret their results as indicating that the ions are produced at the base of the diffusion flame in a region corresponding to premixed gaseous combustion. In a spectroscopic investigation of this bright green zone they find it similar to the inner cone of a premixed bunsen flame with CC bands preceding both CH bands and the peak in electron concentration. This is interpreted as evidence that ions are produced in the reactions consuming or de-activating the excited C_2 radicals. *Figure 3*

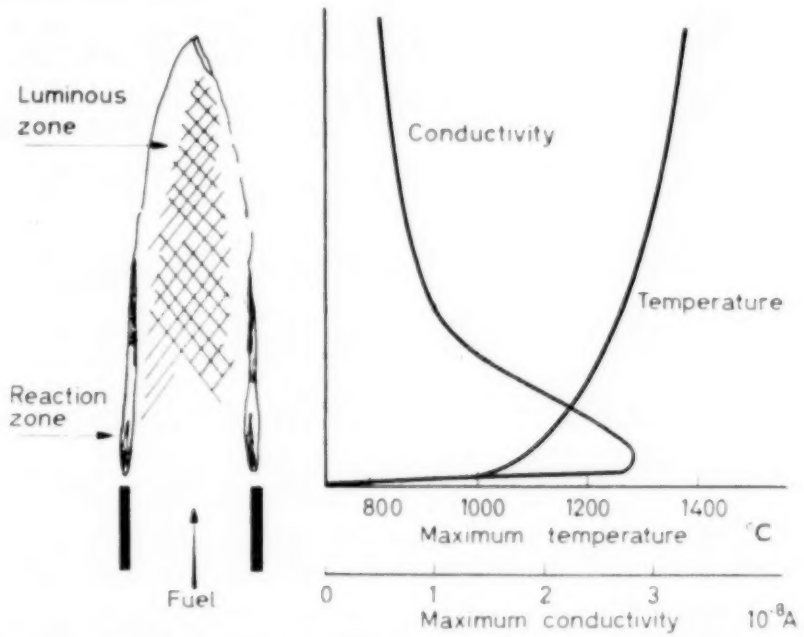

Figure 3. Electrical conductivity and temperature in a hydrocarbon diffusion flame (after T. KINBARA *and* J. NAKAMURA[66])

was constructed from data in their paper[66]. The current was measured between two pointed electrodes 1·2 mm apart with 1·5 V applied between them and the temperature was measured with a platinum–rhodium thermocouple without making radiation corrections. If the ion concentration is proportional to the conductivity, it can be stated that the concentration of ions is less in the luminous part of a diffusion flame, i.e. where carbon particles are prevalent, than at the base of the flame where luminous carbon particles have not yet formed. This seems true in spite of the fact that the temperature reaches its maximum in the yellow-luminous-diffusion zone. It would be difficult to interpret the ionization in such flames as due to carbon particles.

In another study T. KINBARA and H. IKEGAMI[69] determined the mobilities of the positive and negative ions in diffusion flames by measuring the electrical potential through electrode sheaths. The positive ion mobilities were found to be of the order of, or less than, 1 $cm^2\ s^{-1}\ V^{-1}$ in agreement

however, will not account for ionization in the flame front of hydrocarbon–air flames, as indicated in *Table 4*. The required concentrations are much greater than is reasonable.

Table 3. Some ionization potentials of radicals

Radical	*Ionization potential eV*	*Ref.*	*Radical*	*Ionization potential eV*	*Ref.*
OH	12·7	51	$CH_2=CH-CH_2$	8·16	60
HO_2	11·5	52	$(CH_3)_2CH$	7·90	59
CH	11·1	53	$CH_2=C(CH_3)CH_2$	8·03	61
CH_2	11·9	54	$CH_3-CH=CH-CH_2$	7·71	61
CH_3	9·88	55	$C_6H_5CH_2$	7·73	58
C_2	12	56, 57	$CH_3C_6H_5CH_2$		47
C_2H	11·3	53	para	7·46	
$CH_2=CH$	8·16	58	ortho	7·61	
CH_3-CH_2	8·78	59	meta	7·65	
$CH\equiv C-CH_2$	8·25	59			

Table 4. Required species concentration (per cm³) to produce thermally the experimental positive ion concentration in flames (Reference Figure 4)

Species ionized	V_i	*At the equivalence ratio*		
		0·70 *Lean*	1·0 *Stoichiometric*	1·5 *Rich*
CC	12	1×10^{32}	1×10^{29}	3×10^{31}
$CH_2=CH$	8·2	7×10^{21}	2×10^{20}	6×10^{21}
$C_6H_5CH_2$	7·73	4×10^{20}	2×10^{19}	4×10^{20}
$CH_3-CH=CH-CH_2$	7·71	3×10^{20}	2×10^{19}	3×10^{20}

Carbon particles

It was first suggested by O. Stern (see ref. 13) that carbon particles are responsible for the ions observed in flames. He reasoned that the ionization potential would lie between the work function 4·35 eV, and the ionization potential, 11·3 eV of gaseous carbon. This view was supported by K. E. Shuler and J. Weber[34] for very rich acetylene–air flames, by V. I. Tveridokhlebov[62] for hydrocarbon flames, and has been used by T. M. Sugden and B. A. Thrush[63] and by H. Einbinder[64] to study the ionization of free carbon in acetylene–air flames. J. K. McNeely and collaborators[65] observed in studies of flame distortion by d.c. electric fields in diffusion flames that 'if the amount of free carbon in a flame may be judged by the colour of the flame, the ionization as measured by the current bears a direct relation to the free carbon'. T. Kinbara and J. Nakamura[66] observe that sooty flame fuels, such as benzene, toluene, and acetylene, are very conductive while the conductivity of methyl and ethyl alcohol and hydrogen flames is comparatively low. Deflection of propane–air flames in an electric field has been interpreted by M. J. Saunders and A. G. Smith[67] in terms of ionized carbon particles. However, an electric wind explanation of this same phenomenon is more satisfying[1,5]. Tufts[3], in 1906, had

noted that in diffusion flames the maximum conductivity occurs in the lower part of the flame and not in the luminous part.

T. KINBARA and associates[66, 68, 69] have made a careful study of ionization in diffusion flames. They interpret their results as indicating that the ions are produced at the base of the diffusion flame in a region corresponding to premixed gaseous combustion. In a spectroscopic investigation of this bright green zone they find it similar to the inner cone of a premixed bunsen flame with CC bands preceding both CH bands and the peak in electron concentration. This is interpreted as evidence that ions are produced in the reactions consuming or de-activating the excited C_2 radicals. *Figure 3*

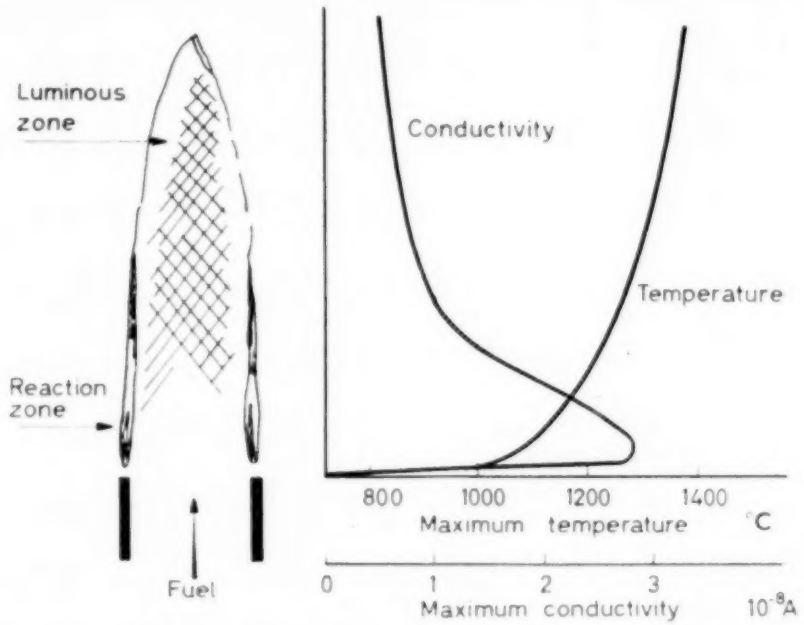

Figure 3. Electrical conductivity and temperature in a hydrocarbon diffusion flame (after T. KINBARA *and* J. NAKAMURA[66])

was constructed from data in their paper[66]. The current was measured between two pointed electrodes 1·2 mm apart with 1·5 V applied between them and the temperature was measured with a platinum–rhodium thermocouple without making radiation corrections. If the ion concentration is proportional to the conductivity, it can be stated that the concentration of ions is less in the luminous part of a diffusion flame, i.e. where carbon particles are prevalent, than at the base of the flame where luminous carbon particles have not yet formed. This seems true in spite of the fact that the temperature reaches its maximum in the yellow-luminous-diffusion zone. It would be difficult to interpret the ionization in such flames as due to carbon particles.

In another study T. KINBARA and H. IKEGAMI[69] determined the mobilities of the positive and negative ions in diffusion flames by measuring the electrical potential through electrode sheaths. The positive ion mobilities were found to be of the order of, or less than, 1 $cm^2\ s^{-1}\ V^{-1}$ in agreement

with previous studies on premixed flames[70–73]. It is pertinent to this discussion to point out that the mobilities of alkali ions in flames are of this same order of magnitude[72,73] so that the flame ion cannot be very much larger than an alkali ion. The negative ion mobilities were found to be of the order of 10^3, again in agreement with previous studies, which indicates that they are free electrons. Beyond the yellow tip, however, the negative ion mobility decreased to 1 showing that electron attachment occurred.

Ionization of carbon particles is certainly a possibility in high temperature-rich flames where copious quantities of carbon are produced although experimental evidence is extremely weak. This hypothesis requires further examination.

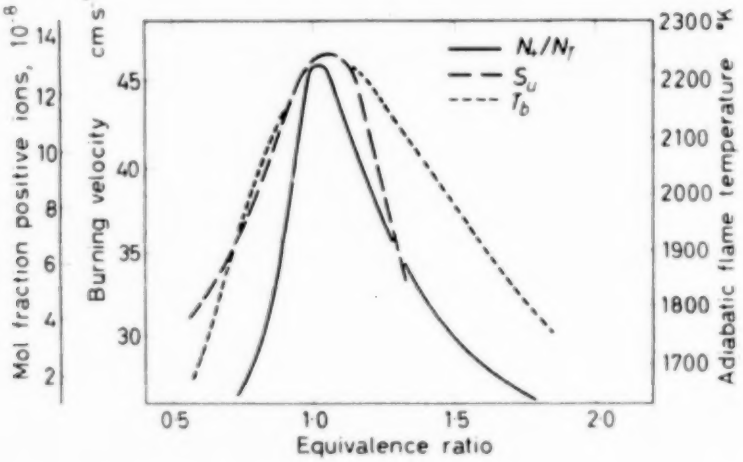

Figure 4. Maximum ion concentration, flame temperature and burning velocity for a propane air flame at 0·3 atm. Ion concentration obtained with a 0·01cm diameter platinum–40 per cent rhodium probe, burning velocity at 1 atm, flame temperature from R. W. Smith, Jr, J. Manton *and* S. R. Brinkley, Jr[74a]

More carbon would be expected in rich flames than in lean flames and is in fact observed only in rich flames. Even if the carbon is produced in unobservable concentrations or in the form of large carbon-rich molecules, more would be expected on the rich side of stoichiometric than on the lean side. Therefore, employing a thermal mechanism, more ions would be expected in rich flames than in lean flames of the same temperature. This is indeed the argument employed by Shuler and Weber[31]. In fact, it is difficult to see how ions might be produced by this process in lean flames.

Examination of *Figure 4* shows that about the same number of ions are observed in rich propane–air flames and in lean flames at the same temperature. However, at a reduced pressure the ion maximum is displaced toward leaner mixtures (*Figure 5*). What is even more impressive is the observation that in acetylene–air flames, *Figure 6*, the ion concentration peaks on the lean side of the maximum temperature and is more in agreement with the maximum burning velocity than with the maximum

temperature. It is interesting to note that B. LEWIS and C. D. KREUTZ[76] found that lean mixtures exhibited a greater temperature change when exposed to a d.c. electric field than did rich mixtures. It would then seem that there is nothing unique about ionization in rich flames.

A calculation of the number of ions produced by ionization of carbon particles assuming every carbon atom in the flame is part of a carbon particle is also informative. Shuler and Weber[34] consider particles of diameter 100 to 1000 Å. Einbinder[64] calculates the particle diameters to

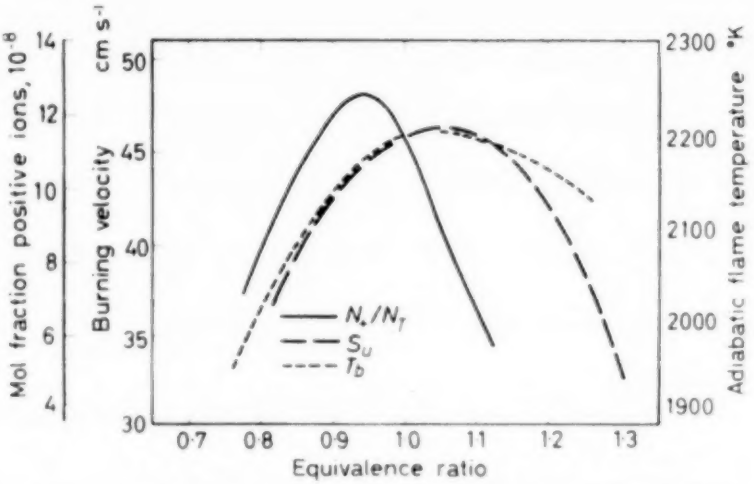

Figure 5. Maximum ion concentration, flame temperature and burning velocity for a propane–air flame at 0·076 atm; all other conditions as for Figure 4

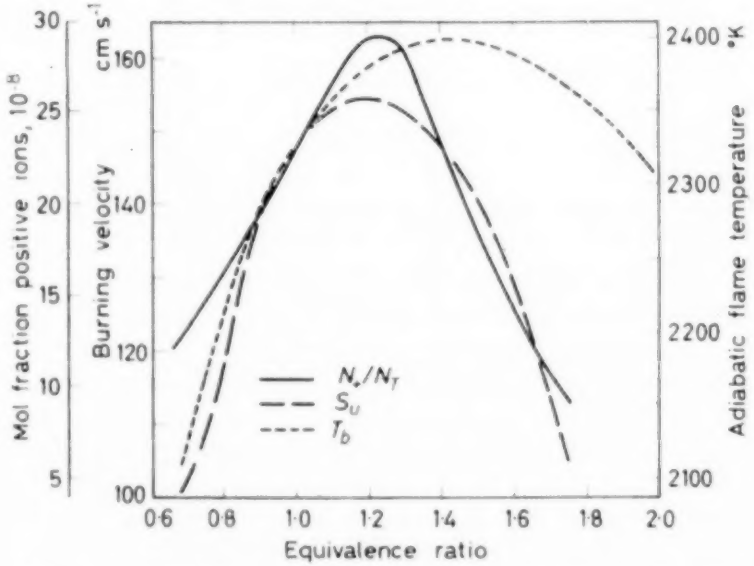

Figure 6. Maximum ion concentration, flame temperature and burning velocity for an acetylene–air flame at 0·03 atm. Ion concentration obtained with a 0·014 cm diameter platinum probe, burning velocity at 1 atm, flame temperature from R. W. SMITH, Jr, J. MANTON *and* S. R. BRINKLEY, Jr[74b]

be 55 to 85 Å, and Sugden and Thrush[63] use a carbon particle radius of 200 Å that is derived from electron microscopy for their acetylene–air flames. Taking a particle of 100 Å diameter as the basis of our calculation the particle volume would be $(4/3)\pi r^3 = 5{\cdot}2 \times 10^{-19}$ cm^3 and each particle would contain (with C density of graphite = 2·25 g cm^{-3}) $5{\cdot}9 \times 10^4$ atoms.

The total carbon atom concentration in a propane–air flame at an equivalence ratio of 0·47, including all of the carbon atoms in the feed and, thus, all of the carbon atoms available to form all carbon-forming molecules, e.g. carbon dioxide and carbon monoxide, is $3{\cdot}3 \times 10^{17}$ cm^{-3}. The absolute maximum concentration of carbon particles of 100 Å radii that could be present if no other carbon-containing species were present is $5{\cdot}6 \times 10^{12}$ cm^{-3}. Such a flame contains approximately 2×10^{10} ions cm^{-3}. At a flame temperature of 1330°K with a work function for carbon of 4·35 eV the maximum ion concentration would be 2×10^8 ions cm^{-3}. Application of Einbinder's equations for the ionization of solid particles[64] shows that they would be only singly ionized at this temperature. Thus, there are roughly 100 times more ions than could be accounted for by particles if *every* carbon atom were tied up in a carbon particle of 100 Å radius.

IONIZATION VIA TRANSLATIONAL ENERGY

Saenger, Goercke and Bredt[19] have attempted to explain ionization in rocket exhausts and flames by assuming that the total energy of the combustion process is released in the form of kinetic energy of translation and that the higher-velocity tail on the Boltzmann distribution possesses sufficient energy to account for the observed ionization. They assume that, before this energy can reach equilibrium with the rotational and vibrational degrees of freedom, ions are produced by collisions of fast-moving neutral species and that the ions so formed persist to build up a high concentration. In their treatment the overall reaction energy is distributed over all of the products in translational energy only, and the high-velocity tail of the Boltzmann distribution is rapidly replaced. Eventually, of course, rotational and vibrational equilibrium is obtained. For present purposes let it be assumed that exothermic elementary chemical reactions release their energy initially as kinetic energy of translation—this will be questioned subsequently. There are several serious difficulties with the concept of ionization in flames via translational energy.

First, a classical treatment of ionization by collision of neutral species[77], considering the conservation of energy and momentum before and after collision, shows that only about half the kinetic energy is available for ionization. The maximum kinetic energy, $K.E.$, which can be transferred to internal potential energy, E_i, when species of mass m_A collide with species of mass m_B, i.e. $A + B \rightarrow A + B^+ + e^-$ is

$$E_i/K.E. = m_B/(m_B + m_A)$$

This has been demonstrated in a study of the ionization of helium atoms by helium atoms where ionization set in at 49·5 eV, which is exactly twice

the ionization energy of helium[77]. The critical potential for ionization is even greater than twice the ionization potential if the non-ionized collision partner is heavier than the ionized partner.

Secondly, for ionization by collision of neutral species the efficiency of ionization increases very slowly with increasing energy of the collision partners above the threshold energy for ionization[77]. This is to be contrasted with the very rapid increase in ionizing efficiency for electrons as electron energies exceed the ionization potential. This may be explained by the large mass and thus low speed of the molecule relative to the Bohr theory velocity of the electron in its orbital. Thus, the duration of the collision is very much longer than the classical period of revolution of an electron, so the electron can adjust its position while momentum is exchanged between the collision partners. Thus, R. G. FOWLER[78a] states that 'theory and experiment agree that the cross sections for massive impacts compare with corresponding electron impacts on an equal velocity basis'. It should be noted, however, that massive impact must be the mechanism by which ions are produced in a shock wave, and even there the cross sections for direct ionization by atom–atom collisions are too small by several orders of magnitude to account for the rapid ionization near the shock. Much remains to be learned about such interactions.

An example will serve to demonstrate the objection to Saenger's assumption. For a propane–air flame at an equivalence ratio of 0·47, $T_b = 1330°K$, $N_+ = 2 \times 10^{10}$ ions cm^{-3}. The heat release per mole of product is 99·5 kcal which corresponds to a translational flame temperature (heat per molecule = 1·5 kT) of 3210°K. The equivalent translational flame temperature for a stoichiometric mixture is 6800°K. The number of molecules with kinetic energy at least equal to 2 V_i, i.e. the number, N_i, of molecules having sufficient energy to cause ionization upon collision, is given by

$$N_i/N_t \sim \exp(-2V_i/kT)$$

which gives approximately 0·2 and 3 ions cm^{-3} respectively for a flame at equivalence ratios of 0·47 and 1·0.

This analysis has assumed a Boltzmann distribution of translational energy such that every particle with energy above 2 V_i will ionize a molecule, but we have not allowed for replacement of the higher energies in the distribution as they lose energy in producing ions. The situation might be imagined that as ions are formed the high velocity distribution is replenished while the reverse process of ion recombination is slow. The problem then reduces to a comparison of the relative rates of ionization and of transfer of translational energy to rotation and vibration. Since these last two processes are relatively fast compared to the rate of energy transfer to electronic excitation it is reasonable to assume that the energy will be converted rapidly to rotation and vibration, reducing the translational temperature, before much ionization occurs. This seems especially true in view of the small number of molecules initially possessing sufficient energy to ionize by collision. Thus, the high translational energy tail of the Boltzmann distribution would have to be replenished some 10^{10} times to

produce the required number of ions. This would certainly be sufficient time for the energy to become distributed in rotation and vibration.

As an alternative, it might be considered that in a highly exothermic elementary reaction the energy goes *all* to translation and then, by collision, into ionization before becoming distributed in rotation and vibration. The elementary reaction step

$$C_2 + O_2 \longrightarrow 2CO + 287{\cdot}5 \text{ kcal mol}^{-1}$$

is highly exothermic and it can be assumed for the sake of argument that all of the heat of reaction goes into translational energy as the products fly apart. Then assume that ionization occurs on collision with a molecule of low ionization potential. How efficient is this process? If the high kinetic energy molecule or atom were to lose its energy on the first collision as far as ionization capabilities are concerned, the number of molecules ionized would be dependent upon the number of collisions with species (to the first approximation) where the energy exceeds $2V_i$. In the particular reaction, $\Delta H = 12{\cdot}5$ eV, so that only those species possessing an ionization potential of 6 eV or less would be ionized. The real candidates are the alkali metals, particularly sodium. Assuming a concentration of 1×10^{10} sodium atoms cm^{-3} and, assuming the number of collisions with sodium to be proportional to the number of sodium atoms present, the rate of ion formation is

$$\frac{N_{Na}}{N_I} = \frac{1 \times 10^{10}}{3{\cdot}3 \times 10^{18}} = 3 \times 10^{-9}$$

times the rate of $C_2 + O_2 \longrightarrow 2CO$. For C_2 in the $^3\Pi_u$ state the energy available is 14·9 eV and species with $V_i \leqslant 7{\cdot}5$ eV might be ionized. The alkali metals and some free radicals would now become possibilities, but the situation is little different.

It would seem therefore that any simple mechanism by which the energy is first released as translational energy and then produces ionization is inefficient. This proposition has been considered at some length because the result can be generalized to say that any simple mechanism by which the energy goes into ionization via other degrees of freedom will probably be inefficient. As a corollary, any distortion in the high energy tail of the Boltzmann distribution of total energy will be inadequate to explain ionization in flames.

CUMULATIVE EXCITATION

It is certainly reasonable to suppose that an electronically excited species might undergo a number of elastic collisions before finding the proper partner with which to react. Efficiency of energy transfer from electronic states to vibrational, rotational, or translational, states is small. Energy is most easily transferred in single quanta and this cannot be done with relatively large spacing between electronic energy levels as compared with closely spaced vibrational and rotational levels. If the molecule does not lose its energy by radiation it will have a good chance of retaining its energy for a number of collisions. Gaydon and Wolfhard[36] estimate that

with a radiative life of 10^{-8} seconds a molecule will suffer about fifty collisions during its excited lifetime. Thus collisions of the second kind where the excitation energy of one atom or molecule is transferred to another to cause ionization can be a probable process.

The transfer of electronic energy from one molecule to an electronic level in a receiving partner would be a frequently occurring efficient process, especially when the energy levels are nearly equal. This is better stated as the Franck resonance rule[78b] that the most probable process is the one resulting in the least increase in total kinetic energy. When A. G. GAYDON and H. G. WOLFHARD[79] employ the relative intensities of lines in the iron emission spectrum to indicate abnormal excitation in flames, collisions of the type considered here must be important between iron atoms and excited species from the combustion process. V. G. ALELSEEVA and S. L. MANDELSHTAN[80] had previously observed that in an acetylene–air flame the relative intensities of the lines from tin, sodium, lithium, potassium and thallium indicated a Boltzmann distribution of excited states in the outer separated cone but not in the inner cone where each atom also gave a different line reversal temperature. Cumulative excitation to ionization might then be a reasonable source of ions. Several possibilities are listed in *Table 5* where the excitation energy above the ground state is given below each species and the starred (*) product would contain the indicated excitation energy. This is to be compared with the ionization energy, V_i, just below the subject species.

Table 5. Possible cumulative excitation reactions leading to ionization

Energy in kcal mol^{-1}

$CO(^1\Pi) + C_2(^1\Sigma_u^+) \rightarrow CO(^1\Sigma^+) + C_2^*$			
186	$123{\cdot}5 + a$		$309 + a = 324$
		$V_i = 276$	
$CO(^1\Pi) + C_2(^1\Pi_g) \rightarrow CO(^1\Sigma^+) + C_2^*$			
186	$98{\cdot}0 + a$		$284 + a = 299$
		$V_i = 276$	
$C_2(^1\Sigma_u^+) + C_2(^1\Sigma_u^+) \rightarrow C_2(^1\Sigma_g^+) + C_2^*$			
$123{\cdot}5 + a$	$123{\cdot}5 + a$		$247 + 2a = 277$
		$V_i = 276$	
$CO_2(^3\Pi) + C_2(^1\Sigma_u^+) \rightarrow CO_2 + C_2^*$			
130	$123{\cdot}5 + a$		$253 + a = 268$
		$V_i = 276$	
$CO(^1\Pi) + OH(^2\Sigma^+) \rightarrow CO(^1\Sigma^+) + OH^*$			
186	93·5		280
		$V_i = 314$	

Excitation energy taken from K. J. LAIDLER and K. E. SHULER[81]. The energy of the $^1\Sigma_g^+ \rightarrow {}^3\Pi_u$ transition to the ground state for C_2 is not specified; this is estimated by G. HERZBERG[82] to be 15 kcal mol^{-1}.

From a study of acetylene–air flames at 30 to 50 mm of mercury Tverdokhlebov[14] proposes a specific cumulative excitation mechanism for the production of ions in flames. He measured the current to a small spherical platinum probe as a function of position in the flame. The formation of positive and negative ions is assumed to occur in the reaction zone by

$$M + OH^* \longrightarrow M^+ + OH^-$$

where M represents a hydrocarbon molecule or radical of the type C_nH_m or C_n with a large internal energy. The electronically excited OH* is assumed to have 4 eV excitation energy and the electron attachment energy $EA(OH) = 3$ eV is taken from the work of T. M. SUGDEN[83] and F. M. PAGE[84].

This type of reaction is reasonable because the ionization potentials of radicals are lower than for molecules, compare *Tables 2* and *3*. Tverdokhlebov assumes values between 8 and 12 eV as reasonable. With $OH(^2\Sigma^+) = 4{\cdot}1$ eV excitation energy, $EA(OH) = 2{\cdot}8$ eV[83, 84] and $V_i = 7{\cdot}5$ eV (*Table 3*), the internal energy content of M which presumably must be transferred from vibration to electronic excitation is 0·6 eV. This is the order of the energy of only one classical vibrational degree of freedom at flame temperature and thus seems reasonable. Larger positive ions are assumed by Tverdokhlebov to be produced by a process of polymerization to yield particles with diameters between 100 and 500 Å. This would reduce the mobility of positive ions and, he assumes, account for the observed reduction in positive ion current behind the flame front. This is to be contrasted with the idea of recombination of ions (employed in the next section) to calculate rates of ion recombination.

The main difficulty with Tverdokhlebov's hypothesis is that the mobilities of C_nH_m or C_n should be smaller than those observed in flames. It has already been pointed out that the mobility of flame ions is of the same order of magnitude as the mobility of the alkali metals. Another objection arises because the mobility of the negative species in flames indicates that they are free electrons[1, 73, 85, 86]. Tverdokhlebov assumes that the second step is

$$C_2(^1\Pi_g) + OH(^2\Sigma^+) \longrightarrow C_2^+ + OH^-$$

or

$$\longrightarrow M_iOH + e^-$$

If this last reaction were fast it could remove the difficulty.

Actually, it seems unnecessary to assume that the species ionized is a large molecule or radical; various other possibilities exist when cognizance is taken of the electron attachment energy of OH. For example

$$C_2(^1\Pi_g) + OH(^2\Sigma^+) \longrightarrow C_2^+ + OH^-$$

would have 11·8 eV available for ionizing C_2; only 12 is required†.

†The ionization potential of C_2 is not known very accurately and this must be taken into account when it is considered in reactions as above.

CHEMI-IONIZATION

It was originally argued that ions in flames are due to 'chemi-ionization'[4, 5] without specifically defining what was meant. It now becomes necessary to define the process. This can be done best by referring to potential-energy surfaces employed in the theory of absolute reaction rates[87, 88]. *Figure 7*

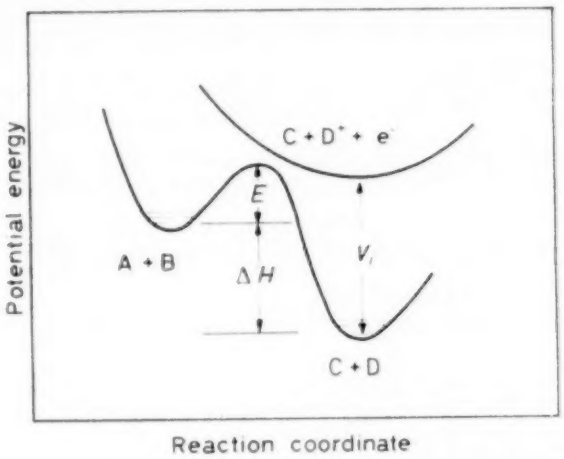

Figure 7. Potential energy curve for chemi-ionization in the reaction
$A+B \rightarrow C+D^{+}+e^{-}$

represents a cross section through the valley of a typical potential-energy surface for the general reaction $A+B \longrightarrow C+D$. The potential energy of the system is plotted as a function of reaction coordinate. This represents the variation in total potential energy as the system moves from left to right, i.e. from reactants to activated complex at the top of the barrier to products on the far right. The lower solid curve represents the lowest electronic state for reactants and products while the broken horizontal lines would represent vibrational levels when only single diatomic molecules are involved. Other curves would be employed to represent higher electronic states for reactants and products. The upper curve on this diagram represents the potential energy of the products when one of the products is an ion, i.e. $C+D^{+}+e^{-}$. Any projection of this curve upon the surface containing the ground state reaction coordinate would lie above the curve representing the ground state by the ionization potential, V_i, of the species ionized. Examination of *Figure 7* shows that the energy available for ionization is the heat of reaction, ΔH, and the activation energy, E. Thus, when the potential energy curve of an ionized product crosses or approaches the potential energy curve of the ground state and $\Delta H + E > V_i$, there will be a possibility of forming an ionized product. When one of the reactants is in an excited electronic state, that energy is also available, as of course is some of the vibrational energy in the reactants.

Thus, for chemi-ionization, elementary reactions possessing the above characteristics must be sought, i.e. $V_i < \Delta H + E$. For the present the criteria that the potential energy surfaces of the ionized product and reactants must cross or approach each other and that the probability of the reaction crossing from one surface to another will be great, will be ignored. Then, elementary reactions possessing sufficient energy will be sought. These will have to be confirmed by theoretical analyses and experiments. Several possibilities are

listed in *Table 6*. For all of the reactions which involve either free radicals or atoms the activation energy would be expected to be low, so the only energy available would be the heat of reaction. In the examples cited this is never in itself sufficient, so it is necessary to assume that one of the reactants is electronically excited. This is not entirely unreasonable since it is well known that flames contain electronically excited species. The primary question that is thus raised concerns the concentration of excited species—is it sufficient to account for the rate of formation of ions?

Table 6. Possible chemi-ionization reactions

Reaction	*Heat of reaction (Product in ground state), kcal mol*$^{-1}$		V_i *(Product) kcal mol*$^{-1}$
	Ground state reactants	*Excited reactants*	
(1) $C_2+O_2 \rightarrow CO(^1\Sigma^+)+CO^+ + e^-$	287·5	342·7 *for* $C_2(^3\Pi_g)$*	325
(2) $CH+CH \rightarrow CH{=}CH^+ + e^-$	230	321 *for* $CH(^2\Sigma+)$	268
		304 $(^2\Sigma-)$	
		296 $(^2\triangle)$	
(3) $CH+H_2 \rightarrow CH_3^+ + e^-$	110	201 *for* $CH(^2\Sigma+)$	229
(4) $CO+O \rightarrow CO_2^+ + e^-$	126·9	313 *for* $CO(^1\Pi)$	318

*This is the electronically excited state from which Swan bands are emitted ($A^3\Pi_g \rightarrow {}^3\Pi_u$). When other excited states are considered the available energy becomes even greater.

Excitation energies from K. J. LAIDLER and K. E. SHULER[51].

The rate of ion formation can be estimated by observing that at the maximum value of ion concentration in a flame front, i.e. at the peak in *Figure 2* the rate of ion formation must equal the rate of recombination. If we further assume that the ions are formed in the reaction zone and that beyond the reaction zone the ions disappear by recombination, it is possible to determine the rate of recombination

$$-dN_+/dt = \alpha N_+ N_- = \alpha N_+^2$$

since $N_+ = N_-$. Integration of this equation gives

$$1/N_+(t) = \alpha t + 1/N_+(0)$$

where $N(t)$ and $N(0)$ represent the ion concentration at times t and 0 respectively, and α is the usual coefficient of recombination. A plot of $1/N(t)$ against t should give a straight line of slope α if this recombination law is followed. Such a plot where $t=0$ at the peak of the ion concentration–distance curve does give a straight line. A typical slope gives $\alpha = 2 \times 10^{-7}$. Then for $N_+ = 10^{11}$ ions cm^{-3}, $-dN_+/dt = 2 \times 10^{15}$ ions cm^{-3} s^{-1} which is equal to the rate of formation of ions. Wilson[73], using the rather detailed theory of the potential drop in the cathode sheath and measurements of sheath thickness, obtained a rate of ion formation of 5×10^{12} ions cm^{-3} s^{-1}.

The concentration of reactants necessary to give such rates can be estimated by assuming that every collision between appropriate pairs is

effective in causing reaction. This is a reasonable assumption for such reactions because, as previously indicated, the activation energy is expected to be small. The number of collisions is

$$Z_{AB}=2(2\pi)^{\frac{1}{2}}N_A N_B\{\tfrac{1}{2}(\sigma_A+\sigma_B)\}^2(RT/\mu)^{\frac{1}{2}}$$

where σ_A and σ_B are the diameters of the reactants and the reduced mass is $\mu=M_A M_B/(M_A+M_B)$.

If we assume $\sigma_A=\sigma_B\sim10^{-8}$ cm, the molecular weight of A and B to be 30, and $T=2000°$K, the number of collisions is $8\times10^{-15}N_A N_B$. This requires that the concentration of reactants shall be rather high, i.e. 10^{15} cm^{-3}, or 10^{12} and 10^{18} cm^{-3}. There are at 2000°K, $3{\cdot}6\times10^{18}$ total species cm^{-3}. A. G. GAYDON and H. G. WOLFHARD[89] estimate that in an acetylene–oxygen flame at 1 atm ($T=3320°$K) there are $7{\cdot}5\times10^{11}$ excited C_2cm^{-3}. R. R. JOHN and M. SUMMERFIELD[90] estimate that excited CH and C_2 are present to the extent of only about 5×10^7 cm^{-3}; however, their actual rate of production is high, of the order of 3×10^{11} radicals cm^{-3} s^{-1}. A more detailed comparison of ion concentrations and rates of ion production should be made with possible reactant concentrations and rates of radical production after the ionized species is identified.

Behrens[17] has pointed out that application of the principle of microscopic reversibility to dissociative recombination of molecular ions and electrons leads to the possibility of ionizing recombination of excited atoms or radicals

$$A^*+B^*\longrightarrow AB^++e^-$$

V. S. ROSSIKHIN and associates[91] studied the electrical conductivity of transient flames and concluded from the dependence of current on the square of the pressure that the process leading to ionization was bimolecular. They interpreted the non-correspondence of changes in current with composition and temperature of the flame as evidence of the important role chemical reactions play in the ionization process.

W. JOST and H. G. WAGNER[92] have looked for chemi-ionization in cool ether–oxygen flames at temperatures of about 400°C and pressures in the range of 200 to 700 mm of mercury. Appreciable chemi-ionization was not found. The ion concentrations were small, approximately 2×10^4 ions cm^{-3}.

The basic question that is raised by the above description of chemi-ionization is: In what form does the energy appear in the products of a highly exothermic reaction? It has been assumed in this discussion that all of the energy goes into one electronic degree of freedom to ionize the product. This requires experimental and theoretical justification. It is obvious that before real progress can be made on the mechanism of ionization in flames the actual species ionized must be identified. This can be done by a mass spectroscopic study of ions in flames. Such a study is planned by the author. With the identification of the ionized species further studies of ions in flames should lead to a better understanding of elementary reactions and collision processes at high temperatures.

This work was sponsored by Project SQUID which is supported by the Office of Naval Research, Department of the Navy, under Contract

N6–ori–105, T.O. III, NR–098–038. The experimental data which are reported here for the first time were obtained by I. R. King.

Experiment Incorporated,
Richmond, Virginia

(Received August 1957)

REFERENCES

[1] THOMSON, J. J. and THOMSON, G. P. *Conductivity of Electricity Through Gases* Vol. I, 3rd ed. Cambridge University Press: London, 1928
[2] ERMAN, G. *Ann. Phys., Lpz.* 11 (1802) 150
[3a] TUFTS, F. L. *Phys. Rev.* 21 (1905) 409
[3b] TUFTS, F. L. *Phys. Rev.* 22 (1906) 193
[4] CALCOTE, H. F. *Third Symposium on Combustion, Flame and Explosion Phenomena*, p 245. Williams and Wilkins: Baltimore, 1949
[5] CALCOTE, H. F. and PEASE, R. N. *Industr. Engng Chem. (Industr.)* 43 (1951) 2726
[6] GARNER, W. E. and SAUNDERS, S. W. *Trans. Faraday Soc.* 22 (1926) 281
[7] SAUNDERS, S. W. and SATO, K. *Trans. Faraday Soc.* 23 (1927) 248
[8] GARNER, W. E. and ROFFEY, F. *J. chem. Soc.* (1929) 1123
[9] BENNETT, J. A. J. *Trans. Faraday Soc.* 23 (1927) 307
[10] BONHOEFFER, K. F. and HABER, F. *Z. phys. Chem. A* 137 (1928) 263
[11] HABER, F. *S.B. preuss. Akad. Wiss.*, Phys. Math. 11 (1929) 162
[12] TANFORD, C. Private communication, 1946
[13] LEWIS, B. and VON ELBE, G. *Combustion, Flames and Explosions of Gases*, pp 206–07. Academic Press: New York, 1951
[14] TVERDOKHLEBOV, V. I. *J. exp. theor. Phys., Moscow* 30 (1956) 252
[15] SAENGER, E., GOERCKE, P. and BREDT, I. *Z. phys. Chem.* 199 (1952) 46; Translation as *Tech. Memor. Nat. Adv. Comm. Aero., Wash. No. 1395* (1951)
[16] BEHRENS, H. *Z. phys. Chem.* 195 (1950) 24
[17] BEHRENS, H. *Naturwissenschaften* 38 (1951) 187
[18] HABER, F. *Z. angew. Chem.* 42 (1929) 745
[19] MALINOVSKII, A. E., ROSSIKHIN, V. S. and TIMKOVSKII, V. P. *Phys. Z. Sowjet.* 5 (1934) 212
[20] MALINOVSKII, A. E. *Phys. Z. Sowjet.* 9 (1936) 264
[21] MALINOVSKII, A. E. and JEGEROW, K. E. *Acta phys.-chim. U.R.S.S.* 4 (1936) 929
[22] BERNATSKII, V. K. and ROTANOV, A. P. *J. Soc. phys.-chim. russe*, Phys. Pt 60 (1928) 503
[23] LEWIS, B. *J. Amer. chem. Soc.* 53 (1931) 1304
[24] SKALOV, B. and SOKOLIK, A. *J. phys. Chem., Moscow* 5 (1934) 617
[25] MALINOVSKII, A. E. *J. Chim. phys.* 21 (1924) 469
[26] MALINOVSKII, A. E. and JEGOROW, K. E. *Phys. Z. Sowjet.* 5 (1934) 453
[27] DAVIDSON, J. F. *Phys. Z.* 7 (1906) 108
[28] HABER, F. and LACY, B. S. *Z. phys. Chem.* 68 (1909) 726
[29] EPSTEIN, F. and KRASSA, P. *Z. phys. Chem.* 71 (1910) 28
[30] VOGT, K. *Ann. Phys., Lpz.* 12 (1932) 433
[31] HEUMANN, T. *Spectrochim. Acta* 1 (1940) 293
[32] CALCOTE, H. F. and KING, I. R. *Fifth Symposium (International) on Combustion*, p 473. Reinhold: New York, 1955
[33] FOWLER, R. H. *Statistical Mechanics*, 2nd ed., p 372. Cambridge University Press: London, 1936
[34] SHULER, K. E. and WEBER, J. *J. chem. Phys.* 22 (1954) 491
[35] MOYERMAN, R. M. and SHULER, K. E. *Science* 118 (1953) 612
[36] GAYDON, A. G. and WOLFHARD, H. G. *Flames, Their Structure, Radiation and Temperature*, Chapman and Hall: London, 1953
[37] SUGDEN, T. M. *Proc. Roy. Soc. A* 119 (1953) 204
[38] SUGDEN, T. M. *Disc. Faraday Soc.* 19 (1955) 68
[39] KING, I. R. and CALCOTE, H. F. *J. chem. Phys.* 23 (1955) 2203
[40] DENNISTON, D. W., Jr, OXENDINE, J. R., KNAPSCHAEFER, D. H., BURGESS, D. S. and KARLOVITZ, B. *J. appl. Phys.* 28 (1957) 70
[41] KARLOVITZ, B., DENNISTON, D. W., KNAPSCHAEFER, D. H. and WELLS, F. E. *Fourth Symposium (International) on Combustion*, p 613. Williams and Wilkins: Baltimore, 1953
[42] SUMMERFIELD, M., REITER, S. H., KEBELY, V. and MASCOLO, R. W. *Jet Propulsion* 25 (1955) 377
[43] WATANABE, K. *J. chem. Phys.* 26 (1957) 542
[44] WARREN, J. W. *Nature, Lond.* 165 (1950) 810
[45] MORRIS, J. D. and NICHOLSON, A. J. C. *J. chem. Phys.* 20 (1952) 1021

[46] KOSCH, P., HUSTRULID, A., and TATE, J. T. *Phys. Rev.* 52 (1937) 843
[47] FARMER, J. B., LOSSING, F. P., MARSDEN, D. G. H. and MCDOWELL, C. A. *J. chem. Phys.* 24 (1956) 52
[48] WATANABE, K. and NAMIOKA, T. *J. chem. Phys.* 24 (1956) 915
[49] HONIG, R. E. *J. chem. Phys.* 16 (1948) 105
[50] DUNCAN, A. B. F. *J. chem. Phys.* 3 (1935) 131
[51] TSUCHIYA, T. *J. chem. Phys.* 22 (1954) 1784
[52] FONER, S. N. and HUDSON, R. L. *J. chem. Phys.* 23 (1955) 1364
[53] ELTENTON, G. C. *J. chem. Phys.* 15 (1947) 455
[54] LANGER, A., HIPPLE, J. A. and STEVENSEN, D. P. *J. chem. Phys.* 22 (1954) 1836
[55] OSBERGHOUS, D. and TAUBERT, R. *Z. Phys. Chem.* 4 (1955) 264
[56] KALLMAN, H. and ROSEN, B. *Z. Phys.* 61 (1930) 332
[57] CHUPKA, W. A. and INGHRAM, M. G. *J. chem. Phys.* 21 (1953) 1313
[58] *Applied Mass Spectrometry*, p 102. Institute of Petroleum: London, 1954 (Conference in London, October 1953)
[59] FARMER, J. B. and LOSSING, F. P. *Canad. J. Chem.* 33 (1955) 861
[60] LOSSING, F. P., INGOLD, K. U. and HENDERSON, I. H. S. *J. chem. Phys.* 22 (1954) 621
[61] MCDOWELL, C. A., LOSSING, F. P., HENDERSON, I. H. S. and FARMER, F. B. *Canad. J. Chem.* 34 (1956) 345
[62] TVERDOKHLEBOV, V. I. *Dokl. Akad. Nauk S.S.S.R.* 103 (1955) 1049; *Chem. Abstr.* 50 (1956) 7569[f]
[63] SUGDEN, T. M. and THRUSH, B. A. *Nature, Lond.* 168 (1951) 703
[64] EINBINDER, H. *J. chem. Phys.* 26 (1957) 948
[65] MCNEELY, J. K., BROWN, O. A. and CROSNO, C. W. *Iowa St. Coll. J. Sci.* 5 (1931) 269 and 6 (1931) 1
[66] KINBARA, T. and NAKAMURA, J. *Sci. Pap. Coll. gen. Educ., Univ. Tokyo* 4 (1954) 9; *Fifth Symposium (International) on Combustion*, p 285. Reinhold: New York, 1955
[67] SAUNDERS, M. J. and SMITH, A. G. *J. appl. Phys.* 27 (1956) 115
[68] KINPARA, T. and NAKAMURA, J. *Sci. Pap. Coll. gen. Educ., Univ. Tokyo* 4 (1954) 21
[69] KINBARA, T. and IKEGAMI, H. *Sci. Pap. Coll. gen. Educ., Univ. Tokyo* 4 (1956) 129; *Combustion & Flame* 1 (1957) 199
[70] WILSON, H. A. *Trans. Roy. Soc. A* 216 (1916) 63
[71] WATT, J. S. *Phys. Rev.* 25 (1925) 69
[72] BECKER, A. *Handbuch der Experimentalphysik* Vol. 13. Leipzig, 1929
[73] WILSON, H. A. *Rev. mod. Phys.* 3 (1931) 156
[74a] SMITH, R. W. Jr. MANTON, J. and BRINKLEY, S. R. Jr. *Rep. Invest. U.S. Bur. Min. No. 4983* (1953)
[74b] SMITH, R. W. Jr, MANTON, J. and BRINKLEY, S. R. Jr. *Rep. Invest. U.S. Bur. Min. No. 5035* (1954)
[75] SAUNDERS, S. W. *Trans. Faraday Soc.* 23 (1927) 256
[76] LEWIS, B. and KREUTZ, C. D. *J. Amer. chem. Soc.* 55 (1933) 934
[77] VON ENGEL, A. *Ionized Gases*, p 49. Oxford University Press: London, 1955
[78a] FOWLER, R. G. *Handbuch der Physik*, Vol. 21, p 223. Springer: Berlin, 1956
[78b] FOWLER, R. G. *Handbuch der Physik*, Vol. 21, p 236. Springer: Berlin, 1956
[79] GAYDON, A. G. and WOLFHARD, H. G. *Proc. Roy. Soc. A* 205 (1951) 118
[80] ALELSEEVA, V. G. and MANDELSHTAN, S. L. *J. exp. theor. Phys., Moscow* 17 (1947) 759; *Chem. Abstr.* 42 (1948) 1503
[81] LAIDLER, K. J. and SHULER, K. E. *Industr. Engng Chem. (Industr.)* 43 (1951) 2758
[82] HERZBERG, G. *Molecular Spectra and Molecular Structure. I. Spectra of Diatomic Molecules*, p 454. Van Nostrand: New York, 1950
[83] SUGDEN, T. M. *Fifth Symposium (International) on Combustion*, p 406. Reinhold: New York, 1955
[84] PAGE, F. M. *Disc. Faraday Soc.* 19 (1955) 87
[85] LENARD, P. *Ann. Phys., Lpz.* 9 (1902) 642
[86] WILSON, H. A. and BRYAN, A. B. *Phys. Rev.* 23 (1924) 195
[87] GLASSTONE, S., LAIDLER, K. J. and EYRING, H. *The Theory of Rate Processes*. McGraw-Hill: New York, 1941
[88] LAIDLER, K. J. *The Chemical Kinetics of Excited States*. Oxford University Press: London, 1955
[89] GAYDON, A. G. and WOLFHARD, H. G. *Proc. Roy. Soc. A* 201 (1950) 570
[90] JOHN, R. R. and SUMMERFIELD, M. *Jet Propulsion* 27 (1957) 169
[91] ROSS'KHIN, V. S., PROTOPOPOV, A. K., MARTYNYUK, L. A. and TSYKORA, I. L. *Nauch Zap Dnepropetrovsk Univ. Sborn. Rabot Fiz.-Mat. Fak.* 41 (1953) 9; *Chem. Abstr.* 49 (1955) 9991
[92] JOST, W. and WAGNER, H.-G. *Naturwissenschaften* 40 (1953) 435

Studies on the Oxidation of Hydrocarbons under Extremely Clean Experimental Conditions

Z. G. SZABÓ and D. GÁL

Investigations on the oxidation of hydrocarbons have not led, hitherto, to unequivocal results because (i) of lack of extreme purity in experimental conditions (ii) of the great number of parallel and consecutive elementary reactions in the oxidation of hydrocarbons, and (iii) the oxidation processes have frequently stopped before their initial reaction constituent(s) are completely consumed. By making use of certain catalytic effects we tried to increase the amounts of the single intermediates selectively and from the mode of action of the catalyst we could make deductions on the mechanism of the original reaction and on the nature of the catalysed elementary step(s).

The experiments were carried out in an all-glass apparatus, employing Bodenstein glass valves and a quartz manometer as null instrument. The experimental curves have been plotted in the non-stationary range. The characteristics ($\tau_{max.}$ and φ) reflect the essence of the process, thus facilitating probable deductions to be made on the single elementary acts. Ethane, ethylene and acetylene were chosen as model substances. The catalytic effects of water, iodine, methylamine and nitric oxide were examined.

INVESTIGATION of the reaction kinetics of the oxidation of hydrocarbons has great theoretical and practical importance. These processes belong to a special group of branching chain reactions and the establishment of the rules governing them leads to further development of the theory of chain reactions. Knowledge of the details of oxidation processes is, from the practical point of view, significant in regard to the control of the processes, and the preparation of intermediates and end products.

Although theoretical and experimental work dealing with the oxidation of hydrocarbons forms a considerable part of the literature on reaction kinetics, our knowledge of the mechanism and even of the kinetics of the processes is rather scanty and contradictory. To illustrate the problems involved, it is sufficient to mention the initiating reaction which, in spite of a great number of experiments and several theories, is not yet fully settled.

The solution of this outstanding complex problem, or at least an approximation to it, can only be reached by determining and eliminating most of the causes of the contradictions.

First and foremost is the lack of extreme purity attained so far in the experiments. Minimal impurities present in the apparatus or in the reacting substances greatly influence the course of the reaction, especially

branching chain reactions. Also N. N. SEMENOFF[1] regarded the effects of trace catalysis as a criterion of such branching chain reactions.

Another cause of difficulty is that in the oxidation of hydrocarbons an extraordinarily large number of parallel and consecutive elementary reactions occur in which many different intermediates, frequently very short-lived and in small quantities, are formed. Consequently, they escape analytical detection and without knowledge of them, no proper view of the number and character of the constituents of the overall reaction can be developed.

The third phenomenon, which does not occur in other chain reactions and which has not so far been interpreted in the general theory of chain reactions, is that these oxidation processes frequently stop—or at least their rate decreases—just before the initial reaction components, or even one of them, are wholly consumed. It should also be mentioned that some strange kinetic curves, frequently observed in the oxidation of hydrocarbons, differ fundamentally from the normal form of rate functions which also occur in common chain reactions. These drop with decreasing concentration. Undoubtedly, the mechanism of the oxidation of hydrocarbons cannot be cleared up until this experimental fact is interpreted.

Because of these difficulties in our theoretical and experimental investigations on the oxidation of hydrocarbons we tried to find a new way. By making use of certain catalytic effects we tried to increase or decrease selectively the amount of the single intermediates or of the processes arising from them as being active centres. In arranging the experiments and evaluating the results our principal aim was to get some information on the mechanism of the original, non-catalysed reactions and on the nature of the catalysed elementary step or steps.

From what has been said it follows that the experiments must be carried out under the cleanest conditions possible where there are neither uncontrollable catalytic actions nor mutual interactions between catalysts. However, if it is impossible to eliminate such an interaction, it must be elucidated and taken into account. The existence of such catalytic interactions is usually responsible for the lack of proper evaluation of investigations made so far.

On the basis of the foregoing one theoretical and one practical requirement will affect the planning of the experiments. Theoretically, only homogeneous catalytic actions can be considered. Their interpretation is much simpler than that of heterogeneous catalytic phenomena. Under conditions of extreme purity the homogeneous catalytic action can be controlled better and more easily reproduced than the heterogeneous one. In other words, in homogeneous catalysis it is possible to vary the extent of the selective actions by varying the concentration of the catalyst.

The practical requirement is that the investigations must be carried out with the purest possible substances so that the measurements following the reaction should not influence the chemical conversion. Consequently the experiments were arranged by the static procedure, where the whole kinetic curve could be plotted within one reaction, the freezing-in could

be applied at any time, so giving some information on the stabilization of radicals and, by measuring the pressure, also on the fine variations in the state of the reaction mixture.

EXPERIMENTAL

Apparatus

Our apparatus corresponding to the above conditions was as follows.

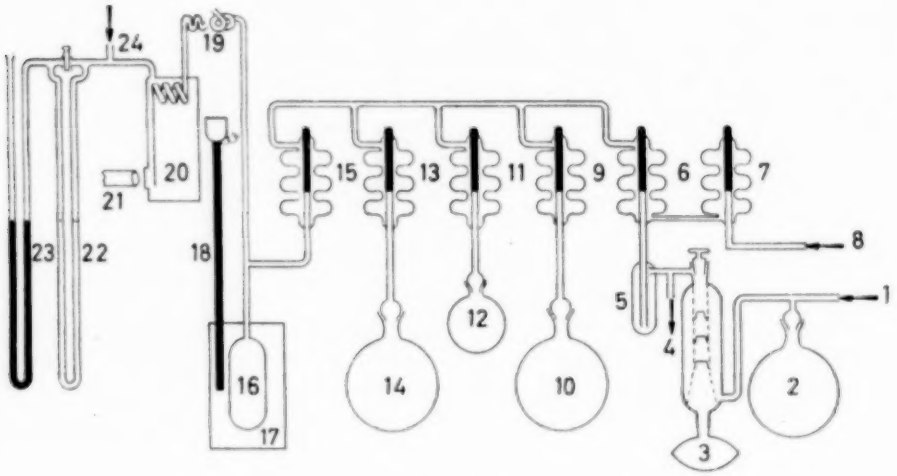

Figure 1. Arrangement of apparatus (schematic)

The reacting substances kept in vessels 10, 12 and 14 were introduced into the reaction vessel 16 pumped out by means of the mercury diffusion pump 3 through the system of Bodenstein glass valves 6, 9, 11, 13 and 15. Progress of the reaction was followed with the aid of a differential manometer 22, filled with 2-bromonaphthalene, and with a mercury manometer 23, applying simultaneously Bodenstein quartz glass manometer 20 as null instrument.

Choice of hydrocarbons

The theoretical aim of these investigations being to draw some conclusions on the mechanism of the processes from formal kinetic data, the obviously model substances to choose were simple hydrocarbons which, though showing the general characteristics of the oxidation of hydrocarbons, might yield possibly only a few kinds of intermediates. On the other hand, it is known that the structure of a hydrocarbon molecule greatly influences the quality of attachment with oxygen and later reactions. The detailed treatment of this complex problem may lead us a long way towards elucidation of the relation between reactivity and chemical kinetics, this relation being one of the most important factors in modern chemistry. Consequently, it seemed best to choose hydrocarbons which differ only in their bond type while having equal numbers of carbon atoms. Therefore ethane, ethylene and acetylene were selected.

Catalysts

The choice of the catalysts proved to be more difficult, primarily due to the lack of a uniform theory on the catalysis. Thus choice of the most suitable catalyst for a given process was nearly always made empirically. Catalysts can be arranged, according to their action and structure, in the following groups: (*i*) inert gases operating by physical catalysis; (*ii*) halogens and their compounds, the action mechanism of which is relatively the simplest. They catalyse, especially at higher temperatures, by starting the chains through dissociation of halogen atoms. Also, the dissociated halogen atoms, e.g. iodine, undergo reaction with the free radicals, keep them from rupturing, and thus exert their catalysing action. Therefore, iodine was chosen as one of the catalysts.

(*iii*) The most interesting homogeneous catalysts are those which, depending on the ratio of the concentrations, exert a double effect, for either positive or negative catalysis. It seemed appropriate to examine this double effect under conditions of extreme purity, and nitric oxide was selected for testing. (*iv*) In the practical oxidation of hydrocarbons, 'anti-knocks' play an important part, although their reaction mechanism cannot yet be regarded as having been determined. Methylamine was chosen for this examination.

(*v*) Oxidation of hydrocarbons is affected autocatalytically by the intermediates formed. No catalyst of this nature was used because the intermediate catalyst can only be properly studied if the kinetic considerations and the analytical measurements are collated. Since the present investigations are not intended to follow the reactions analytically, examination of these intermediate catalysts has been omitted.

(*vi*) The action of mercury should be noted. Mercury vapour destroys peroxides most efficiently—consequently all the investigations carried out directly with mercury manometers may seem to be rather illusory, as also those where insufficient care was taken to ensure elimination of mercury vapour, the peroxides being important intermediates in the oxidation of hydrocarbons.

(*vii*) Last but not least, the catalytic role of water must be mentioned. Although the effect of water has already been studied by various authors, no overall view has been developed so far, mainly because in previous experiments perfectly water-free starting substances were not used. In addition, other impurities were present in the apparatus at the same time and affected the experiments made to measure the effect of water. Since we set out to attain conditions of extreme purity, it seemed desirable to settle the question of catalysis by water too. As water is a poor catalyst, it may be expected to exert some small effect and that only on very few elementary reactions and without influencing later steps; that is, there was a prospect of establishing to a high degree the specific character of the water effect. All these assumptions were fully justified by later experiments.

There are two fundamental kinds of catalytic action which we may regard as plausible. One manifests itself in terms of the stabilization of free radicals, first suggested six years ago[2]. The catalyst molecule reacting

with, and stabilizing, the intermediate radicals, may lead to two kinds of result: the radical may escape destruction and be preserved, either free or in its stabilized form, when it reacts, thus increasing the conversion. Alternatively, a mutual interaction may occur between the stabilized and non-stabilized radicals, causing them to recombine. In this case there is no contribution to the conversion, and therefore a decrease of rate. The other method has been mentioned above and depends on radical production catalysed by iodine. With some catalysts the effects may be additive, which results in a double effect. Qualitative and quantitative interpretations of this were given in a lecture to the International Congress on Catalysis, Philadelphia, in 1956[3]. Double catalysis has been found during oxidation of ethane, ethylene and acetylene.

RESULTS

Kinetic curves

To facilitate evaluation of the results obtained, thorough analysis of the kinetic curves has been undertaken. The kinetic curve, whether expressed as rate/concentration or rate/time, certainly reflects the essence of the process; corresponding clues must be found to interpret its real meaning. These clues are the characteristics of the kinetic curves. As the kinetic curves are of rather high order, they have several characteristic data, such as shape of curve, slope of ascendant and descendant branches, place of maximal rate, i.e. the induction period (although instead of this in the

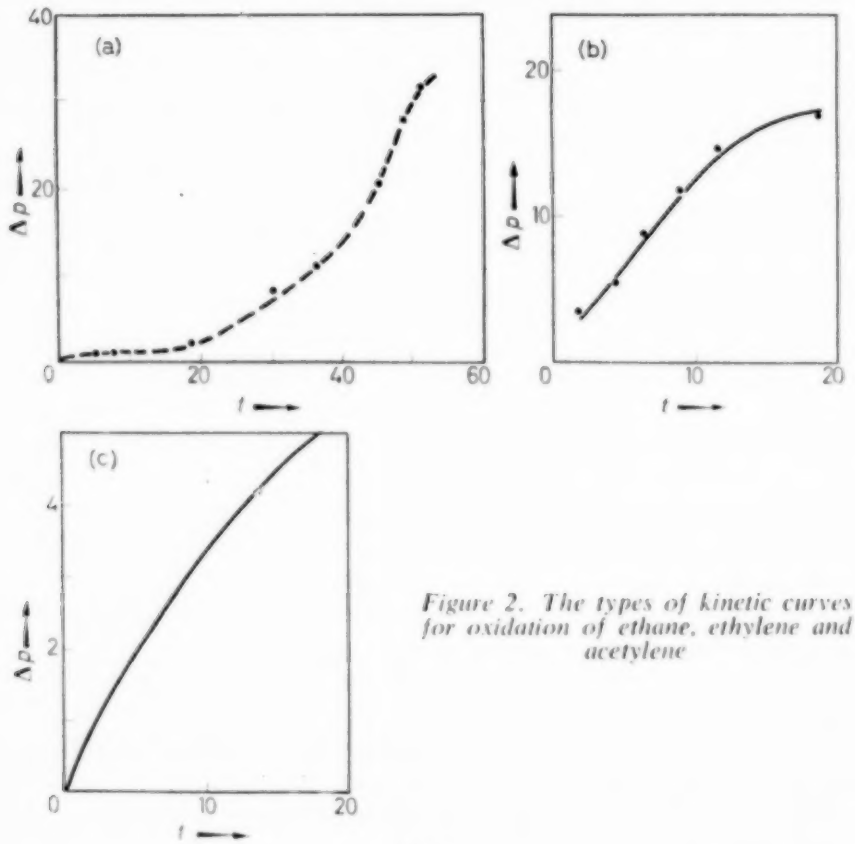

Figure 2. The types of kinetic curves for oxidation of ethane, ethylene and acetylene

oxidation of hydrocarbons it is better to take running-up time into account), and finally the extent of conversion. These characteristics will be further denoted, according to the formal kinetic terms of Semenoff[1], by ϕ and $\tau_{max.}$. $\tau_{max.}$ is, in general, characteristic of the development of the whole process, but it also gives information on the nature of the initiating reaction, as the temperature coefficient of $\tau_{max.}$ gives the best approximation to the activation energy of this phase. In the reactions once started, the extent of the branchings, or more strictly the change of ratio of branchings to rupturings, can be determined by the examination of ϕ.

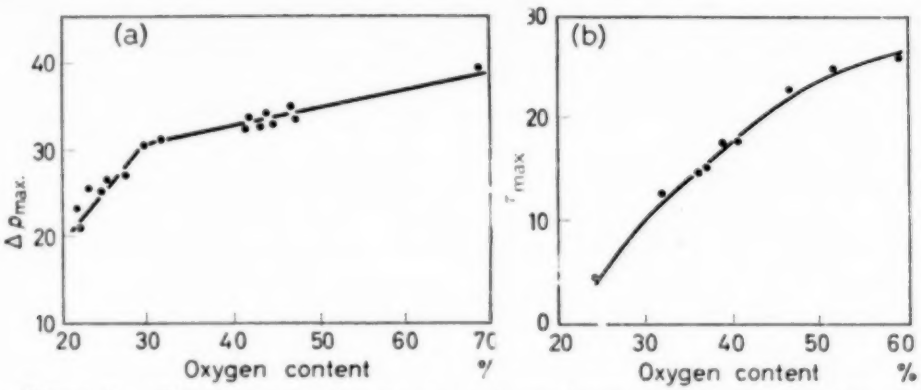

Figure 3. Change of total pressure and running-up time as a function of concentration for oxidation of ethane

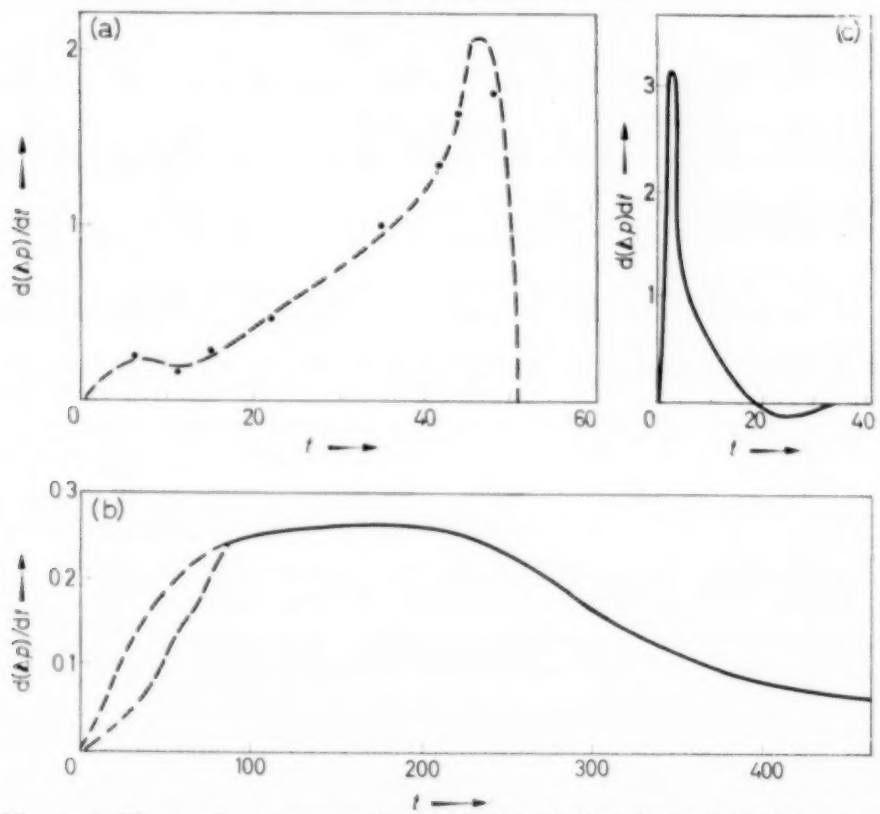

Figure 4. Shape of rate curves for oxidation of (a) *ethane,* (b) *ethylene and* (c) *acetylene*

The value of $\tau_{max.}$ can be seen directly from the kinetic curve, while ϕ can be calculated on the basis of the equation $\Delta p = N_0 \exp \phi t$. As $\tau_{max.}$ and ϕ are functions of composition, pressure and temperature, derivations according to these variables give further valuable information.

In the establishment of the mechanism the energetic data play the main governing role. It is, therefore, essential that unequivocal energetic data shall be available, not subject to uncontrolled catalytic actions.

In our experiments the kinetic curves were plotted in the non-stationary range at a measurable rate for the three gases, and the change of total pressure as a function of time showed the shapes indicated in *Figure 2*. The form and extent of the curve also varies with composition and total pressure. This is illustrated in *Figure 3*. The corresponding velocities behaved as indicated in *Figure 4* for the three gases tested.

$\tau_{max.}$ may be regarded as the reciprocal of the average velocity and it shows, of course, a similar dependence on composition and total pressure. On the basis of the model gases examined, the relation between $\tau_{max.}$ and total pressure—as the graphs show—can be described in simple mathematical terms. With ethane, the dependence on the total pressure is linear, while with ethylene log $\tau_{max.}$ is proportional to log p_0.

The branching factor may be computed from the function log $p \rightarrow t$ and its value is dependent on the total pressure as expressed by $\phi = kP_0^{x}$. Naturally, with ethane, this expression varies with composition; and it is

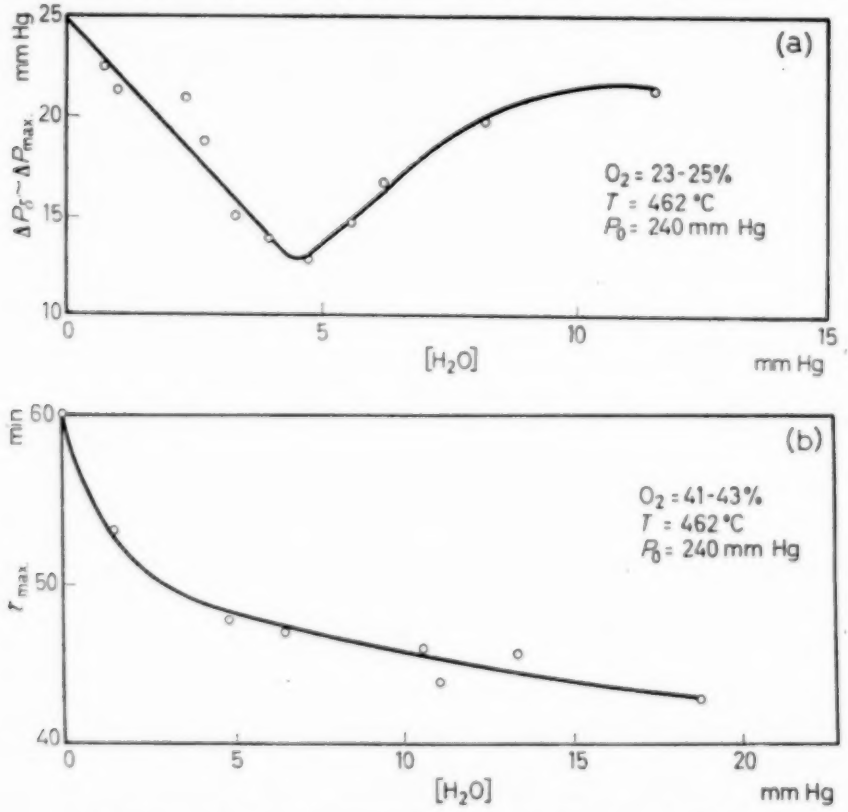

Figure 5. Effect of presence of water on oxidation of ethane

known that ϕ also is a function of temperature. This relation may be given by the equation $\phi = k \exp(-E/RT)$. It is therefore worth while examining the temperature dependence of $\tau_{max.}$.

Table 1. Summarizing table of kinetic parameters

Parameter	C_2H_6 $\tau_{max.} = -aP + b$			C_2H_4 $\tau_{10} = k\,p^{-x}$	
$\tau_{max.} = F(P)$ ($T = 462$ °C)	20 % O_2	$a = 0{\cdot}711$	$b = 205{\cdot}7$	$\tau_{max.} = 33$ min ($P_0 = 240$ mm Hg)	$x = 3{\cdot}3$
	40 % O_2	$a = 0{\cdot}335$	$b = 146{\cdot}1$	$\tau_{max.} = 60$ min ($P_0 = 240$ mm Hg)	
$\phi = F(P) = kP^x$ ($T = 462$ °C)	20 % O_2	$k = 1{\cdot}7 \times 10^{-13}$	$x = 4{\cdot}9$	$\phi = 0{\cdot}083$ ($P_0 = 240$ mm Hg)	$x = 3{\cdot}7$
	40 % O_2	$k = 1 \times 10^{-7}$	$x = 2{\cdot}42$	$\phi = 0{\cdot}058$ ($P_0 = 240$ mm Hg)	
$\phi = k \exp(-E/RT)$	20 % O_2	$E = 62\,081$ cal			
	40 % O_2	$E = 65\,108$ cal			$E = 27\,918$ cal
$\tau_{max.} = c \exp(E_{eff.}/RT)$	20 % O_2	$E_{eff.} = 75\,813$ cal			
	40 % O_2	$E_{eff.} = 60\,419$ cal			$E = 31\,204$ cal
	Catalyst: H_2O				
$\tau_{max.}$ ($P_0 = 240$ mm Hg)	20 % O_2	$\tau_{max.} = 38$ min		$\tau_{10} = 8{\cdot}5$ min (H_2O: 0–20·5 mm Hg)	
	40 % O_2	$\tau_{max.} = 50$–59 min			
ϕ ($P_0 = 240$ mm Hg)	20 % O_2	$\phi = 0{\cdot}080$		$\phi = 0{\cdot}29$ (H_2O: 0–20·5 mm Hg)	
	40 % O_2	$\phi = 0{\cdot}05$–$0{\cdot}07$			
$\phi = k \exp(-E/RT)$	40 % O_2	$E_{eff.} = 55\,122$ cal			
$\tau_{max.} = c \exp(E_{eff.}/RT)$	40 % O_2	$E_{eff.} = 56\,338$ cal			
	CH_3NH_2				
$\tau_{max.} = c \exp(E_{eff.}/RT)$	40 % O_2	$E_{eff.} = 31\,000$ cal			

Effect of water

Summarizing, for ethane, the effect of water depends on how the reaction takes place. If there is less than 30 per cent of oxygen present, and if the values of $\tau_{max.}$ and ϕ are constant, the total pressure change forms a minimum curve. If there is more than 30 per cent of oxygen present, catalysis takes place, and the saturation value is readily reached. In water-catalysed cases the temperature coefficient is the same for $\tau_{max.}$ and ϕ (see *Table 1*).

We must remember that in the non-catalysed case the two kinetic characteristics are fundamentally different. The catalytic action of water not only decreases the value of activation energies, as is usual with catalysed reactions, but it compensates them too. If the compensation is caused by a greater decrease in the temperature coefficient of the branching factor than in that of the apparent activation energy, water will exert its effect in the reactions leading to branching and is thus a volume effect, i.e. the probability of branching would be increased. Alternatively the decrease of the probability of breaking must not be excluded; this would be equivalent to poisoning the wall. Further experiments must be made to determine

whether the decrease of the activation energy of branchings or the increase of that of the rupturing reaction is responsible for the effect mentioned.

From the effect of water on the oxidation of ethane the most important conclusion can be drawn; at the same time it provides direct evidence of the mechanism. This is as follows. When the oxidation of ethane is water-catalysed in the presence of a small amount of oxygen, $\tau_{max.}$ and φ do not change. The same effect was observed when ethane was replaced by ethylene. It was therefore concluded that the oxidation ranges of ethane differ from each other, from the point of view of mechanism, according to the percentage of oxygen present. While the first step is the same (proved directly also for the effect of iodine, see below)

$$C_2H_6+O_2=C_2H_5+HO_2 \quad \ldots.[1]$$

the decisive difference is in the second step. In the presence of a small quantity of oxygen this is followed by the reaction

$$C_2H_5+C_2H_5=C_2H_4+C_2H_6 \quad \ldots.[2]$$

whereas, in the presence of a large quantity of oxygen, it is more likely that collisions between ethyl radicals and oxygen molecules will lead to the formation of peroxide. Consequently, with small concentrations of oxygen the oxidation of ethane is really an ethylene oxidation, preceded by a double dehydrogenation.

As already mentioned, water does not exert any effect on the oxidation of ethylene with respect to the running-up time, the branching factor, or the total pressure change (conversion $\Delta p_\searrow$). This is shown by the constancy of the time taken for a 10 mm of mercury pressure change to occur, by the extent of the change of pressure during the course of the reaction, and further by the similarity of the curves plotted for different amounts of water.

Water has an inhibiting effect on the oxidation of acetylene; the velocity and running-up time similarly decrease. On comparing this experimental fact with the premise of Bone and Andrew, which states that the presence of water produces an increase in the amount of acetaldehyde, the mechanism suggested by M. BODENSTEIN[1] becomes very likely. Supposing that water promotes formation of acetaldehyde but at the same time results in inhibition, it is reasonable to assume that two parallel processes act. In one these water takes part—the reaction leading to glyoxal, which is known to be non-chain-carrying. The reaction thus bypasses the main chain and leads directly to formaldehyde and carbon dioxide.

Effect of iodine

The effect of iodine on the oxidation of ethane was studied in mixtures containing 40 per cent oxygen. In this range it was found that iodine exerts a positive catalytic effect on the oxidation of ethane, definitely connected with the running-up time or induction period. Since the branching factor does not change on this occasion, it follows that iodine accelerates the start reaction.

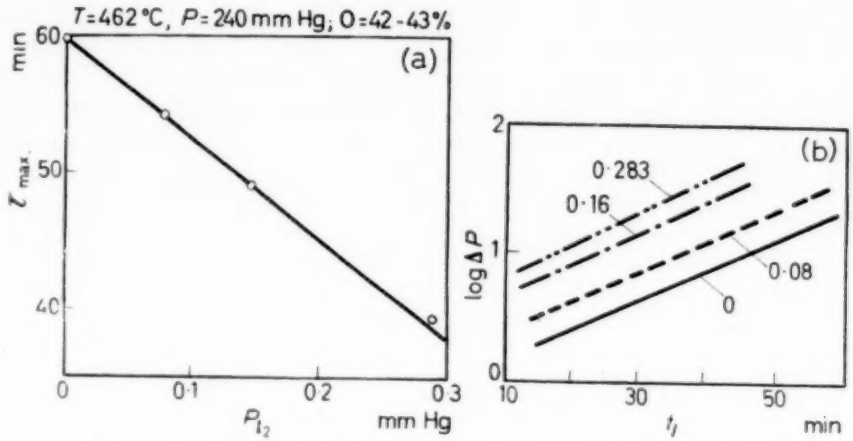

Figure 6. Effect of iodine concentration on oxidation of ethane

To describe this effect quantitatively, the rate equation of the branching chain reaction, the effect of iodine only referring to the start reaction, takes the following form

$$d\Delta p/dt = n_0 v(1 + c[I_2]) + \phi\Delta p \quad \ldots . [3]$$

After integration and reasonable simplification the value of $\tau_{max.}$ as a function of the concentration of iodine, is

$$\tau_{max.} = (2{\cdot}303/d)\tau_{0,\,max.}\{\log B - \log(1 + c[I_2])\} \quad \ldots . [4]$$

Values of $\tau_{max.}$ computed on the basis of this equation are listed with those found experimentally in *Table 2*. The good agreement of the numerical

Table 2. Experimental and calculated (equation 4) values of $\tau_{max.}$ for oxidation of ethane catalysed by iodine

No.	I_2 *taken* mm Hg	$\tau_{max.}$ (min)	
		Found	*Calc.*
113	*Nil*	60	—
137	0·08	54	55·12
141	0·16	48	46·90
142	0·283	39	39·02

data undoubtedly proves that the catalytic action of iodine manifests itself in the dehydrogenating start-reaction. The I—I bond is relatively weak: therefore at the temperature of our experiments iodine is in a rather dissociated state. This is supported further by considerations of energy balance. According to the data of N. J. H. SMALL and A. R. UBBELOHDE[5], the strength of the hydrogen bond in the ethane molecule is 97·5 kcal, while for the H—I it can be taken as 70 kcal. Accordingly, the above reaction is 27·5 kcal endothermic. On the other hand, as stated by Small and Ubbelohde[5], the formation energy of HO_2 is 46 kcal. A. D. WALSH[6] reports a value between 50 and 60 kcal. This is, at any rate, much lower than that of the formation of hydrogen iodide. Thus the catalytic effect of iodine on the start-reaction can easily be understood.

Iodine has a weaker, but more complicated, effect on the oxidation of ethylene, than it has on that of ethane. The running-up time decreases relatively slightly with increasing concentration of iodine, while the values of ϕ increase to a small extent. In an analogous computation carried out with ethane the action of iodine must be taken into account in connection with the branching factor in the rate equation. The decrease of the running-up time can be described—by the effect on ϕ—on the basis of the following equation

$$d\Delta p/dt = n_0 v + (\phi + a[I_2])\Delta p \quad \ldots\ldots [5]$$

hence

$$\tau_{10} = \tau_{0\cdot10}/\{1 + b[I_2]\} \quad \ldots\ldots [6]$$

The values of the running-up time computed from this equation and those found experimentally are given in *Table 3*. The values agree well. Consequently, iodine does not take part in the start-reaction of ethylene oxidation owing to the fact that the process does not start with dehydrogenation but most likely with the formation of peroxide, i.e. with the addition of oxygen where, however, iodine is unable to exert any promoting effect. It must be supposed therefore that iodine prevents the destruction of some free radicals through undergoing a reaction with them, thus keeping them from recombination.

Table 3. Experimental and calculated (equation 6) values of τ_{10} for oxidation of ethylene catalysed by iodine

No.	I_2 *taken* mm Hg	τ_{10} (min)	
		Found	*Calc.*
281	*Nil*	11·3	—
309	0·053	10·9	10·88
307	0·283	9·4	9·38
308	0·471	8·4	8·4

Effect of methylamine

We tried to use methylamine as a well known 'anti-knock' agent in our experiments and expected to decrease the velocity of reaction. The results showed, however, a radically different effect. The cause of this contradiction could only be found when the action of nitric oxide on ethylene was also studied.

Otherwise, the action of methylamine on the oxidation of ethane was studied with two compositions. The results are shown in *Figures 7* and *8*.

It can be seen that the action of methylamine, at least regarding its character, does not depend on the composition. The difference observable is only quantitative. The altered shape of the curves points to a great change with respect to the kinetic parameters $\tau_{max.}$ and ϕ. The effect is rather complex, and on dealing with certain amounts of methylamine two rate maxima may occur. The second maximum may be flattened out, or rather indistinct, but the first maximum is always followed by a rather long stationary period. Owing to the fact that, as shown by the rate curves, the

greater part of the conversion is shifted toward the earlier stage of the reaction, it must be assumed that methylamine (or the nitric oxide formed from it which is the effective substance), reinforces the induction period of the pure reaction and makes a side reaction so far of less importance predominate. Therefore, in the light of the results now obtained by these

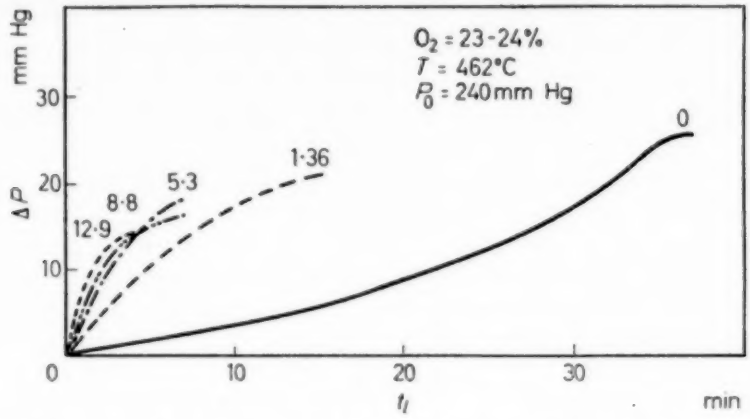

Figure 7. Effect of methylamine concentration on oxidation of ethane

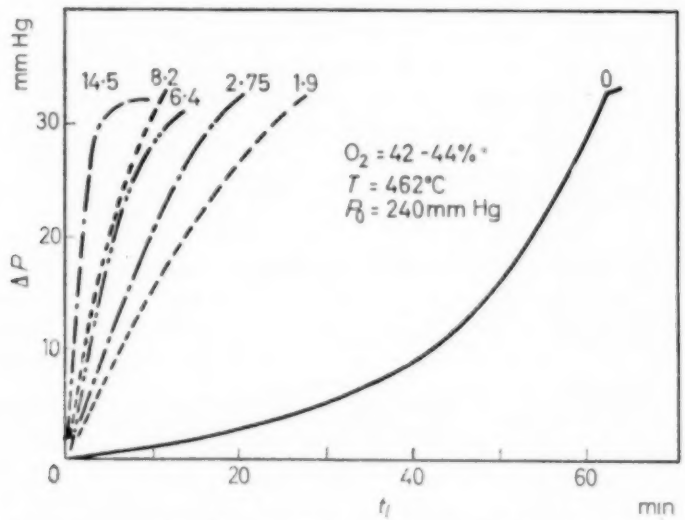

Figure 8. As Figure 7 but with double the oxygen concentration

catalytic reactions, this process, which has often caused only a slight observable rise in the pure oxidation of ethane, must not be regarded as a side reaction but as the first section of the reaction defined by N. N. SEMENOFF[7]. Modification of the rate equation, by adding to it a term kt, leads to a result which interprets the variation of the experimental curve, at least qualitatively. It is worthwhile mentioning here that from the temperature coefficient of the maximum rate of reaction about 31 kcal of effective activation energy can be computed; this is considerably lower than those of the pure or water-catalysed reactions. Compared with the

experimental data obtained with nitrogen dioxide, the effect of methylamine may be interpreted as showing that the latter will be oxidized under the experimental conditions applied, and thus it is not methylamine itself but its products, primarily nitric oxide, which influence the rate of reaction.

More detailed study of the action of methylamine was made in connection with the oxidation of ethylene. Here again, due to the order of introduction of methylamine–oxygen–hydrocarbon, the effective agent is nitrogen dioxide or nitric oxide. Correspondingly, depending on the amount of methylamine applied, both inhibiting and catalysing effects could be expected. As *Figure 9* shows, this double effect is real and the value of $\tau_{10\ mm\ Hg}$ as a function of methylamine concentration clearly shows that catalysis also occurs with ethane, and that the catalyst presumably affects the same elementary reaction. The general theory of homogeneous chain catalysis and inhibition already mentioned[3] was applied to the process of oxidation of ethylene catalysed by methylamine and, taking into account the limiting cases, the constants of the equation

$$F(K) \equiv \frac{v_{(K)}}{v_{(0)}} = \frac{1 + AK}{[1 + 2D_1K + D_2K^2]^{\frac{1}{2}}} \qquad \ldots\ldots [7]$$

were computed stepwise and then, with their aid, the course of the controlling curve of catalysis could be determined. As yet calculations have only been made for approximation of the sections of function varying monotonously, i.e. in the catalytic range where they are more precise and the amount of catalyst introduced is known directly. The values of the influencing factor calculated from the formula

$$F(K) = \frac{1 + AK}{[1 + 2\{A - n_0\}K + \{(A/F_\infty)K\}^2]^{\frac{1}{2}}} \qquad \ldots\ldots [8]$$

of the above equation are in a good agreement with those obtained directly from the data of measurements as shown by *Figure 10* and *Table 4*.

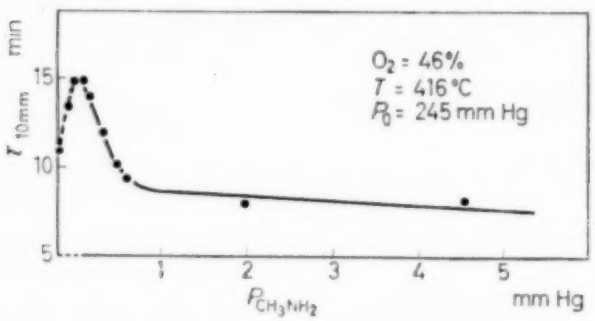

Figure 9. Effect of methylamine concentration on τ_{10} for ethylene oxidation

This good agreement indicates not only the specificity of the catalysis of ethylene, but also points to the fact that the general theory of homogeneous chain catalysis and inhibition can be established on the basis of the stabilization of free radicals.

The action of methylamine on the oxidation of acetylene was not examined.

Effect of nitric oxide

Nitrogen dioxide dissociates at temperatures little higher than room temperature according to the equation

$$NO_2 = NO + \tfrac{1}{2}O_2 \qquad \ldots . [9]$$

At the temperature of our experiments, at any rate, nitric oxide can be taken into account as an acting catalyst. In every case, nitrogen dioxide was introduced into the reaction vessel first and the reacting substances afterwards. Owing to pumping operations, there was always enough time for the dissociation to nitric oxide to reach equilibrium. In essence, our present experiments can be interpreted differently from those in which the catalyst was introduced into the reaction vessel together with the previously prepared mixture.

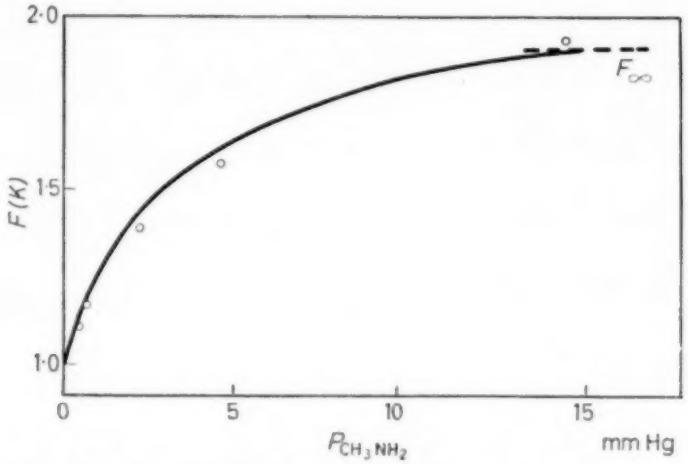

Figure 10. Experimental (o) *and calculated* (——) *values of influencing factor*

Table 4. Experimental and calculated values of the influencing factor

No.	$\tau_{10\ mm\ Hg}$ min	CH_3NH_2 mm Hg	*F(K)*	
			Measured	*Calc. (eq. 8)*
287	9·9	0·47	1·11	1·13
289	9·4	0·58	1·17	1·17
284	7·9	2·20	1·57	1·61
285	5·7	14·5	1·93	1·88

The effect of nitric oxide was, in fact, independent of the composition. This is shown in *Figure 11* which illustrates the rate maxima observed with both small and large percentages of oxygen. The kinetic curves prove that while a small amount of nitric oxide exerts an inhibiting effect, greater amounts have a catalysing effect. This is shown in *Figure 12* in which the time taken to reach 50 per cent conversion is shown as a function of amount of nitrogen dioxide introduced. The part belonging to the range of small concentrations is represented by a broken line. The nitrogen dioxide concentrations belonging to these abscissa values were introduced instead of manometric measurements, with the aid of freezing mixtures, by tension.

The concentrations could not, however, be calculated from the tension formulae because the heat of evaporation undergoes a great change at such low temperatures and the extrapolation leads to quite absurd values. The curve and the part of the abscissa illustrated with a broken line denote that the absolute quantity of nitric oxide introduced is not known. The ordinate values are to be regarded, within the experimental error of course, as precise data. The kinetic curves show very peculiar forms with periodic interruptions; this is, however, a new and real phenomenon pointing to the occurrence of degenerated cold flames.

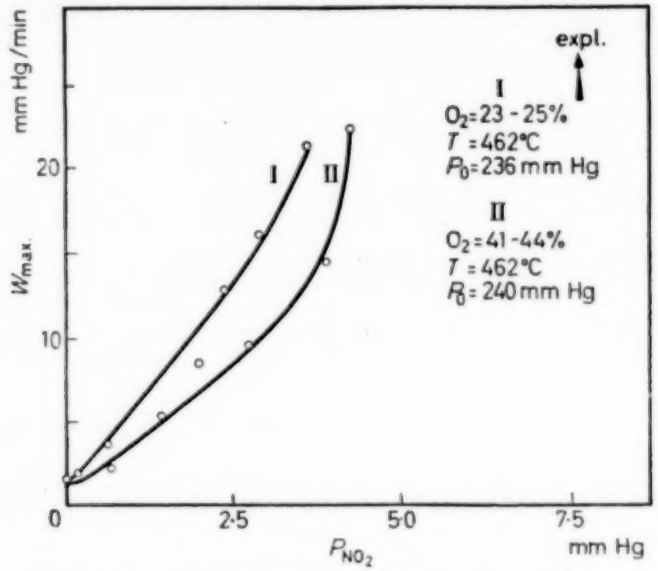

Figure 11. Effect of nitric oxide on rate maxima in oxidation of ethane

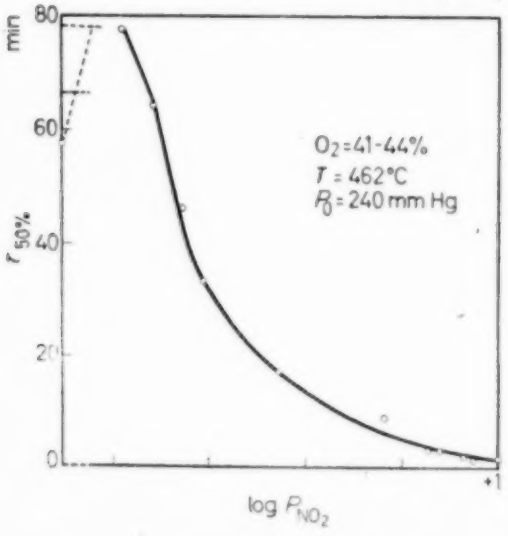

Figure 12. Effect of nitric oxide on half-period of oxidation of ethane

The effect of nitric oxide on the oxidation of ethylene is the same as with ethane. The inhibition observed with small amounts of catalyst becomes catalysis with increasing catalyst concentrations. The course of the kinetic

curves shows that the catalysed reaction also differs qualitatively from the mechanism of the pure reaction.

On comparing the measure of the influence exerted by methylamine with that due to nitric oxide we found that both occur to the same extent at higher concentrations of methylamine. This points to the fact that—assuming full oxidation of methylamine—the concentration of nitric oxide is considerably lower than it is when introduced directly. Consequently, the oxidation presumably leads not only to nitrogen dioxide but also to free nitrogen (which often occurs in the oxidation of amines) so that the amount of nitric oxide formed may be considerably smaller. Accordingly, a certain amount of introduced methylamine is able to cause inhibition at concentrations where the direct effect of nitrogen dioxide presents itself in the form of catalysis.

CONCLUSION

This is a short review of the most important results of our investigations on the oxidation of hydrocarbons under experimental conditions of extreme purity. For the most part, the results and conclusions are drawn directly from the experimental data; they do not, however, facilitate interpretation of the underlying phenomena. Further experiments, arranged under special conditions, are necessary, before a full statement can be made on the essentials of the mechanism. The results obtained so far lead us to hope for a satisfactory outcome; this programme of work will be continued.

A more detailed communication on this subject will be published in Acta Chimica Hungarica.

Institute of Inorganic and Analytical Chemistry,
University of Szeged, Hungary

(*Received July 1957*)

REFERENCES

[1] SEMENOFF, N. N. *Chemical Kinetics and Chain Reactions* Clarendon: Oxford, 1934
[2] SZABÓ, Z. G. *Nature, Lond.* 170 (1952) 246
SZABÓ, Z. G. *Acta chim. hung.* 3 (1953) 139
[3] SZABÓ, Z. G., HUHN, P. and BERGH, A. *Advances in Catalysis,* Vol. IX, pp 343–352. Academic Press: New York, 1957
[4] BODENSTEIN, M. *Z. phys. Chem. B* 12 (1931) 151
[5] SMALL, N. J. H. and UBBELOHDE, A. R. *J. appl. Chem.* 3 (1953) 193
[6] WALSH, A. D. *J. chem. Soc.* (1948) 331
[7] SEMENOFF, N. N. *Some Problems of Chemical Kinetics and Reactivity* Moscow, 1954 (in Russian)

Determination of Burning Velocity of Pentaborane–Oxygen–Nitrogen Mixtures

W. G. Berl, E. L. Gayhart, E. Maier*, H. L. Olsen and W. T. Renich

Pentaborane has been selected as a representative boron hydride in order to obtain burning velocity measurements over a wide range of fuel–air mixtures. Freely propagating laminar flame kernels produced by spark ignition are photographed by the flash schlieren technique, and the burning velocity is derived from the measured rate of growth of these kernels. The pentaborane–air burning velocity reaches a maximum value slightly on the rich side of stoichiometric. The influence of oxygen concentration on burning velocity is reported. Pentaborane flames show pronounced cellular structure of the flame front at all mixture ratios.

The combustion of compounds such as the boron hydrides and their derivatives has received relatively little attention, but the burning properties of these substances have become of increasing interest to fuel technologists because of their high reactivity and heat content. The burning velocities of diborane–air mixtures have been measured by the bunsen burner method over a limited range of composition, and were found to be higher than those of any known fuel burning in air at a corresponding mixture ratio[1,2]. It was considered worth while to obtain burning velocity measurements for other boron hydrides over a wider range of fuel–air mixtures.

The dual factors of the availability of pure pentaborane and its relative stability at room temperature led to its selection as a representative boron hydride. Conflicting information is recorded in the literature concerning the stability of pentaborane–oxygen mixtures at room temperature[3]. There was reason to believe, however, that little or no reaction would occur if fuel–air mixtures in the equivalence ratio range 0 to 1·6 were prepared by rapid addition of oxygen to a pentaborane–nitrogen mixture and subsequent combustion with the smallest possible contact time prior to ignition.

METHOD AND APPARATUS

In view of the expected high combustion rates, burning velocity determinations could not readily be carried out by means of the conventional stabilized bunsen burner methods. This would require burner tubes of 1 mm diameter or less to prevent flashback while maintaining laminar flow, and would also lead to the difficulty of serious flame distortion from solid combustion products being deposited around the burner lip. This technique is also seriously limited in the fuel–air range over which stable flames can be obtained; moreover, if the tube diameter is small, the combustion is affected by diffusion from the surroundings. The constant-pressure explosion method, which uses soap bubbles as a confining means, is

*Now at Carnegie Institute of Technology, Pittsburgh, Pa.

excluded because of the rapid hydrolysis of boron hydrides. Constant volume explosions were rejected because of the risk of reaction during the relatively long contact time of fuel and oxygen between the filling of the bomb and the igniting of the mixture.

A special method of burning velocity measurement, previously applied to hydrogen–air and propane–air mixtures[4,5] and also to acetylene–air and ethylene–air mixtures, has been adopted for the current investigations. This method consists of photographing by the flash schlieren technique the image of freely propagating laminar flame kernels produced by spark ignition. From these photographs, made at successive known intervals of time, the burning velocity is then derived from the measured rate of growth of these kernels.

The apparatus for preparing and metering pentaborane–air mixtures is shown in *Figure 1*. The system is designed in such a way that pentaborane

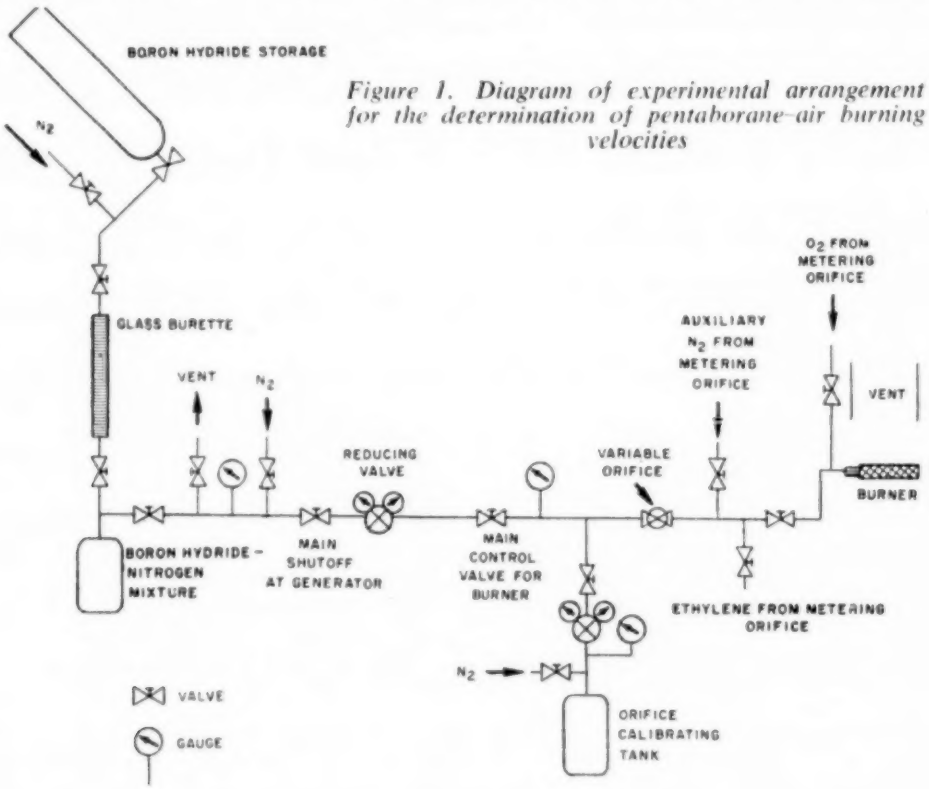

Figure 1. Diagram of experimental arrangement for the determination of pentaborane–air burning velocities

is not exposed to water vapour or air during the filling operation and during storage. The liquid pentaborane is received from the manufacturer* in a steel cylinder under nitrogen pressure. The inverted cylinder is connected to a fuel-mixing tank through a special hydrostatically tested glass burette. The maximum amount of liquid pentaborane that can be fully vaporized in this tank is determined by the ambient temperature and tank volume.

*The Olin Mathieson Chemical Co. has kindly made a gift of several pounds of pentaborane to the Applied Physics Laboratory.

setting a limit to the pentaborane content at any final total pressure. A quantity of liquid pentaborane, not exceeding this maximum, is measured in the burette and run into the fuel-mixing tank. This stainless steel tank, of about 35 l. content, initially contains nitrogen at approximately atmospheric pressure. Additional nitrogen is then added until the nitrogen/pentaborane ratio is equivalent to that in a pentaborane–air mixture of desired equivalence ratio. The mixing of pentaborane–nitrogen is effected by convection produced by an i.r. lamp beamed on one side of the tank for several hours.

This pentaborane–nitrogen mixture passes through a reducing valve to a calibrated variable-area orifice where the rate of the pentaborane–nitrogen flow is established. In the gas line downstream from the variable orifice is a side tube through which more nitrogen may be added. Immediately ahead of a rapid-mixing device, oxygen is injected through seven orifices against the oncoming gas stream at such a rate that the desired oxygen/nitrogen ratio of the final mixture is established. The rapid-mixing device (a short pipe packed with shredded copper foil) ensures uniform composition of the gases.

Traces of water and oxygen contained in the nitrogen coming in contact with pentaborane vapour lead to deposits of solid reaction products inside the flow system. Frequent calibration checks of the metering orifice are therefore required to indicate obstruction therein. (Substitution of super-dry, oxygen-free nitrogen eliminated these deposit problems.) This calibration is accomplished by measuring the rate of pressure drop in a nitrogen-filled calibrating tank. All the valves in the system are either of the packless type or are packed with Teflon. Because of the toxicity of pentaborane all parts of the system have to be made absolutely free of leaks.

The mixed gases flow as a laminar jet into the atmosphere through a 2·5 in.-diameter sintered porous bronze disc (Porex). Composition profiles indicate that no external air enters into the jet within the field of observation. The total gas flow is held to approximately one cubic foot per minute.

The combustion is initiated by means of a small high-voltage spark between two thin electrodes positioned in the centre of the jet and approximately two inches above the porous metal disc and on the axis of the schlieren system. A schlieren image of the resulting flame kernel is photographed by means of a second high-intensity, short-duration spark, the breakdown of which can be accurately timed with reference to the ignition spark by means of a time-delay circuit[6]. The optical arrangement makes use of a wire stop in place of a conventional knife edge to give schlieren images of bilateral symmetry. The intense luminosity of the flame recorded directly by the camera objective completely obscures the schlieren record of the density gradients produced by the flame kernel unless this effect is suppressed by use of an u.v. filter (Wratten 18A), a small aperture stop at the camera objective, and use of Ansco Triple-S Ortho film. The optical magnification of the system is 1·635. The diameter of the field of view is 3 in.

Pictures were taken for any given fuel–air mixture over a range of different delay times. Typical pictures of flame kernels at two delay times and for different fuel/air ratios are shown in *Figure 2*; each photograph is of a separate flame kernel.

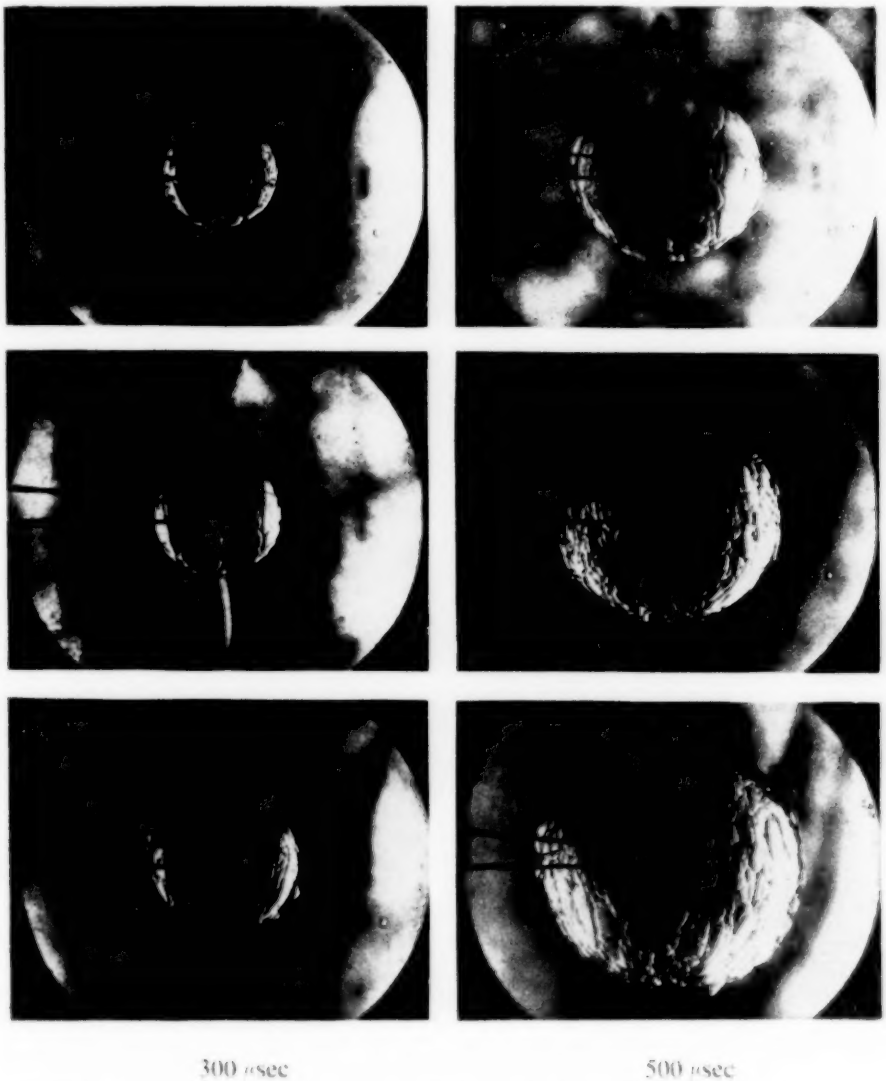

Figure 2. Schlieren pictures of pentaborane–air flame kernels for a variety of mixture ratios (ϕ) and delay times in μsec

The purity of the pentaborane was estimated to be 99·5 per cent. No other hydrides were observable by i.r. analysis*. Although no detailed kinetic information about the rates of oxidation is available, the analysis of the mixture showed that no reaction had occurred in the short period of time (<1 sec) during which a pentaborane–air mixture exists prior to spark ignition in the present apparatus.

*For this information we are indebted to Mr H. Burwasser, Princeton University.

DATA REDUCTION

The method of data reduction is an adaptation of the 'constant pressure' method of F. W. STEVENS[7]. Space velocities are obtained by measuring the position of the flame front with respect to the centre of the kernel as a function of time. A typical example of the measurements is shown in *Figure 3*. The space velocities are the slopes of these curves. Space velocities of a variety of mixtures are tabulated in *Table 1*.

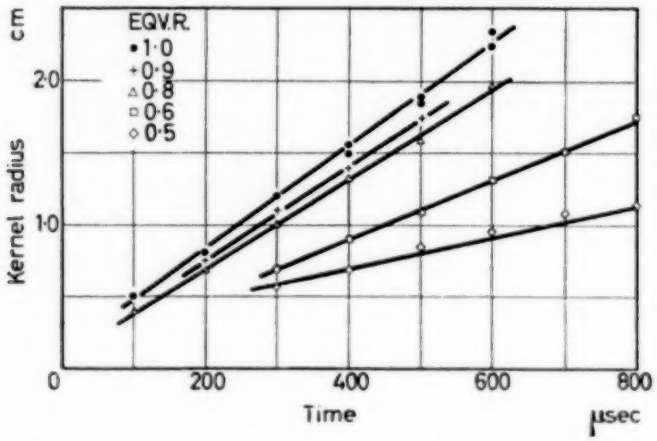

Figure 3. Time/flame kernel radius for several pentaborane–19·4 oxygen–80·4 nitrogen mixtures

Table 1. Space velocities, expansion ratios, and burning velocities as a function of equivalence ratios for a variety of pentaborane–oxygen–nitrogen mixtures

N_2/O_2	ϕ	*Space velocity* cm/s	*Expansion ratio*	*Burning velocity* cm/s
3·00	1·200	10470	9·42	1111
3·50	1·200	8432	9·33	904
3·77	0·200	226	3·92	58
	0·300	580	5·05	115
	0·400	947	5·96	159
	0·400	995	5·96	167
	0·400	1184	5·96	199
	0·500	1769	6·68	265
	0·590	2528	7·18	352
	0·600	2301	7·22	319
	0·700	2708	7·88	344
	0·800	3061	8·42	364
	0·900	4206	8·94	470
	1·000	4653	9·37	497
	1·100	4324	9·67	447
	1·100	5264	9·67	544
	1·200	5273	9·90	533
	1·300	6020	10·08	597
	1·500	3950	10·30	383
	1·600	3635	10·34	352

Laminar burning velocities are obtained by dividing the space velocities by the expansion ratio of the burnt gas relative to the unburnt gas. Thus

$$V_f = V_s/E \qquad \ldots . [1]$$

The expansion ratio is given by the equation

$$E = T_b M_b P_i / T_i M_i P_b \quad \ldots . [2]$$

where T_b denotes adiabatic flame temperature, T_i initial gas temperature, M_b number of moles of burnt gas, M_i number of moles of initial gas, P_i ambient atmospheric pressure, and P_b the pressure inside the kernel. The pressure ratio was obtained from the equation

$$\frac{P_b}{P_i} = 1 + \frac{3\gamma}{2}\frac{(V_s - V_f)^2}{C^2}\left(1 - \frac{1}{g^3}\right)\left(1 - \frac{1}{3g^3}\right) \quad \ldots . [3]$$

where γ denotes the heat capacity ratio of unburnt gases, C is the velocity of sound in the unburnt gas, and g^3 is the density ratio between unburnt and burnt gas.

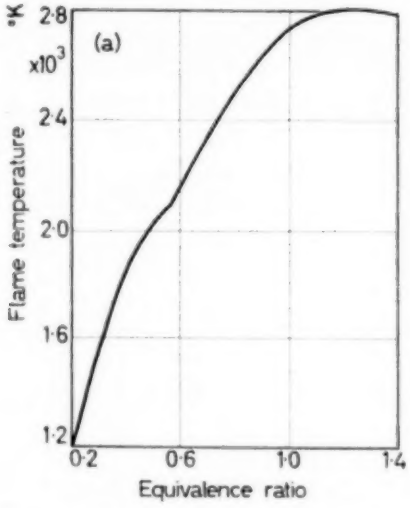

Figure 4a. Mole change for pentaborane – air combustion ($T_0 = 300°$K, $P = 1$ atm, mole change = moles of gaseous products per mole of reactant)

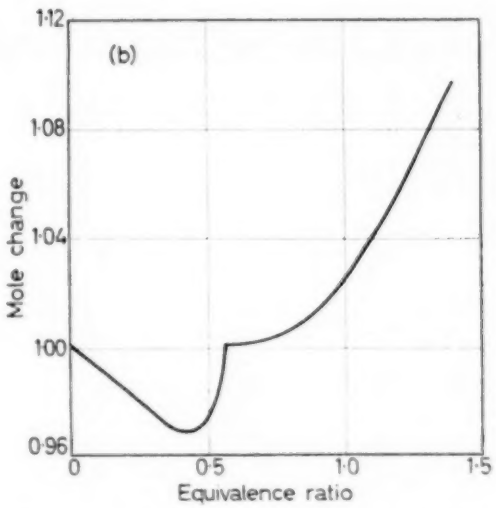

Figure 4b. Flame temperatures of pentaborane–air mixtures (air inlet temperature = 300°K, $P = 1$ atm)

This equation was derived from Stevens[7] by substituting the expansion velocity $(V_s - V_f)$ for the space velocity V_s, which he used as an approximation. It should be noted that for $V_s - V_f$ in excess of 20 m/s, the pressure correction exceeds 1 per cent and should be used. The change in the number of gas moles and final temperature of the gas after combustion are calculated from thermochemical data, and are shown for pentaborane–air in *Figure 4*. Expansion ratios and burning velocities are also listed in *Table 1*.

RESULTS

The burning velocities for a variety of pentaborane–oxygen–nitrogen mixtures are shown as a function of equivalence ratio in *Figure 5*. Burning velocities for hydrogen and acetylene, obtained by the same method, and for propane by a conventional bunsen burner method[8] are included. It is apparent that the pentaborane–air burning velocity is maximum slightly

on the rich side of stoichiometric. The great sensitivity of pentaborane burning velocities to oxygen concentrations is shown in *Figure 6*, which illustrates the behaviour of mixtures containing 20 per cent excess fuel but with a variable oxygen/nitrogen ratio. For comparison, the behaviour of hydrogen is also indicated[9].

All pictures of pentaborane flames show pronounced cellular structure of the flame front. This phenomenon was observed at all mixture ratios. The cell size appears to become smaller for a given size kernel as the expansion velocity increases. The cells are not caused by flow disturbances

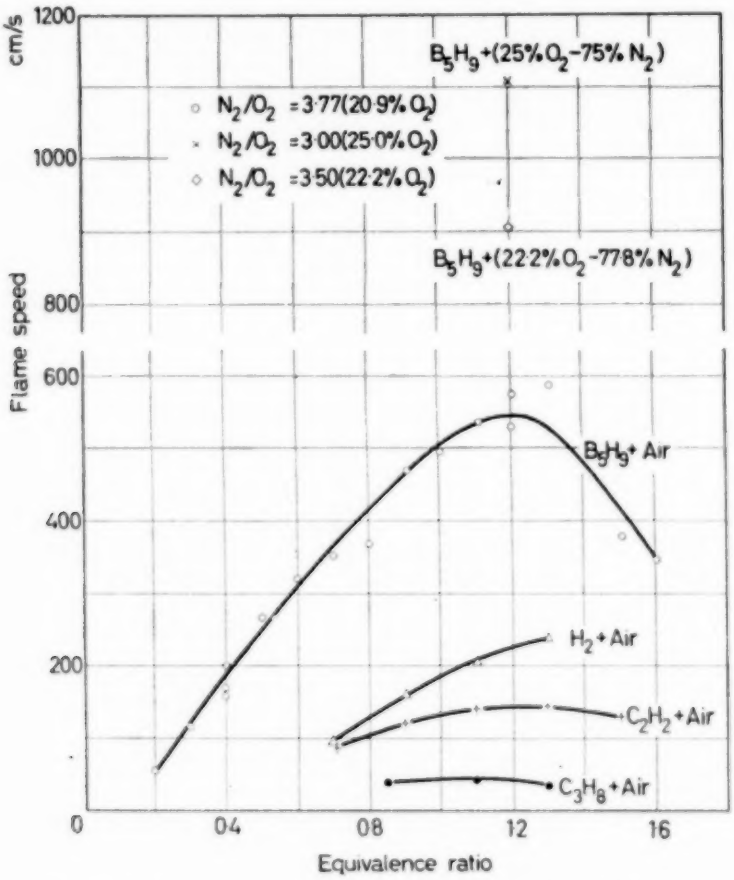

Figure 5. Burning velocity of pentaborane–oxygen–nitrogen mixtures determined by the flame kernel method

in the jet since hydrogen–air kernels of similar propagation rate in the same jet do not show this behaviour. Because of this unevenness of the reaction zone, the exact boundary of the flame could not be determined with high precision. The extent to which the pentaborane burning velocity is affected by the existence of the cells is not known. Localized bulges on the outline were disregarded in obtaining the kernel size. These bulges, which become pronounced for flames showing the highest space velocities, must be caused by regions in which the burning velocity is greater than average.

DISCUSSION

Several aspects of the reduction of space velocities to burning velocities deserve further mention; for example, whether the use of a calculated expansion ratio is permissible in the reduction of space velocity to burning velocity; how reliable the computed expansion ratios are, particularly for fuel-rich mixtures; and considerations of how far the simple mathematical analysis can be carried to high space velocities.

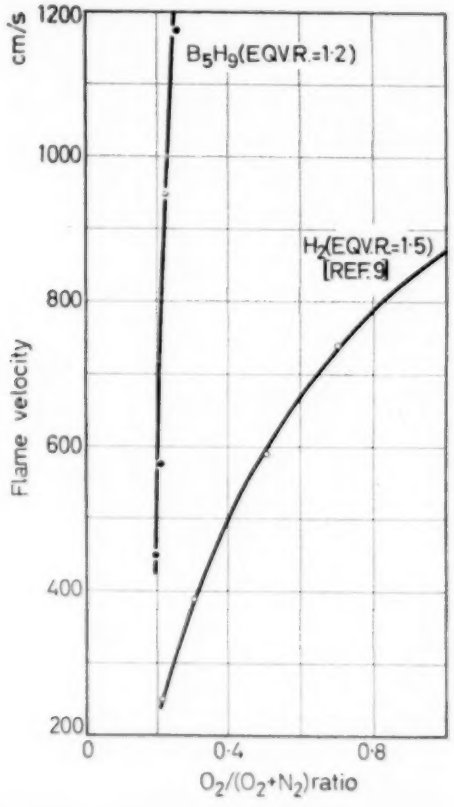

Figure 6. Influence of oxygen/nitrogen ratio on burning velocities of pentaborane–air and hydrogen–air mixtures

The constant pressure method of determining burning velocities[7] which utilizes soap bubbles filled with combustible mixtures and which are centrally ignited requires two measurements: (*a*) the rate of flame expansion, and (*b*) the ratio of final to initial volume. This method, which has also been used by E. F. FIOCK[10–13], J. W. LINNETT[14–16] and others, and by R. A. STREHLOW and J. G. STUART[17], appears to give values of burning velocities in reasonably good agreement with burning velocities determined by other techniques. It resembles the early phase of a constant-volume bomb explosion determination[18].

Comparison of the published data on expansion ratios[14–17] shows that considerable differences exist between the measured and thermodynamically calculated values. There is also considerable scatter in the measured expansion ratio values at any given mixture ratio (*Figure 7*). According to Linnett, Pickering and Wheatley, this scatter may be due to variable heat losses which would affect both the final expansion volume and the rate of

flame propagation, but not necessarily the ratio of the two. It should be pointed out, however, that in closed-volume explosions where no need existed for elaborate devices to blow the soap bubble and to ignite it centrally, adequate agreement could be achieved between measured and calculated bubble size[19]. In the absence of reliable experimental determination of expansion ratio, calculated values for pentaborane flames have been used. An independent determination of gas density within the kernel will ultimately be required to determine the correct expansion ratio.

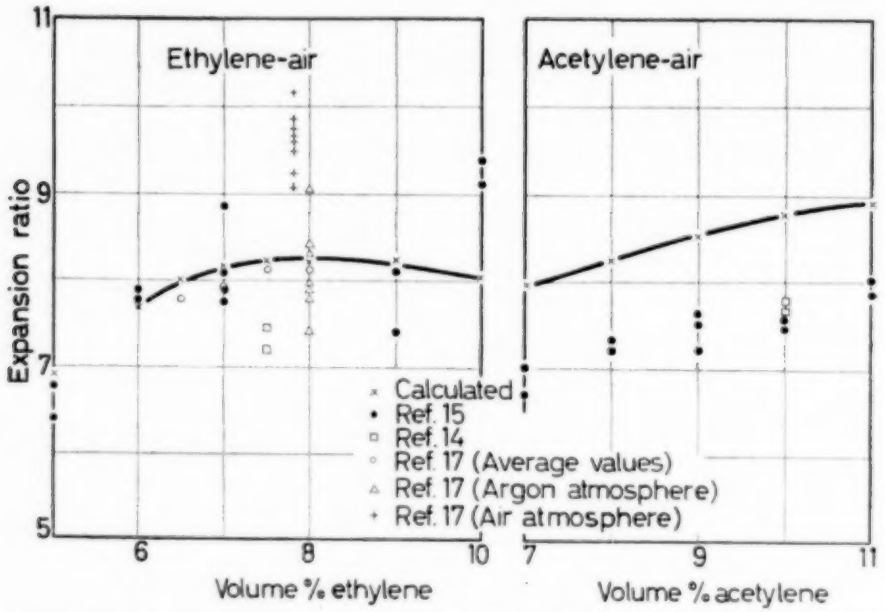

Figure 7. Comparison of experimental and calculated expansion ratios for ethylene–air and acetylene–air mixtures

The technique of photographing the position of the flame front at known time intervals disposes of the problem of a reaction zone of finite thickness. It has been shown[20] that 20 per cent or more of the heat release of a stoichiometric propane–air flame at atmospheric pressure occurs beyond the luminous zone in a region approximately 2 mm thick. Any gradual heat release behind the visible or schlieren reaction zone may lead to difficulties in the determination of the final flame diameter by the Stevens method; the reason for this is that the expansion process would not stop suddenly as soon as the flame front reaches the edge of the combustible region, but would be followed by a zone of relatively slow heat liberation. In the present investigation each measurement offers an independent determination of flame front location. Provided that the kernel diameter is large compared to twice the thickness of the reaction zone, no problems arising from gradual heat-release rates are to be expected. It has been noted previously[4] that in the very early stages of kernel development, where this condition is not met, the propagation rates are indeed lower than the linear, steady-state rate for larger kernels.

The analysis of data on the rich side of stoichiometric is complicated by the lack of adequate knowledge of the equilibria that exist in the boron system in the absence of sufficient oxygen for complete oxidation of all components. Until such information becomes available, the thermochemical calculations were formulated on the basis that all the boron appears as boric oxide (B_2O_3) in the reaction products, the remaining oxygen oxidizing hydrogen to water to the extent of the equilibria existing at the calculated flame temperature. If the less likely assumption that the hydrogen burns preferentially is used, the expansion ratios differ by no more than 4 per cent from the values obtained from the adopted alternative calculations[21]. To the extent of that difference the reported burning-velocity data must be considered tentative on the fuel-rich side of stoichiometric. Preliminary sampling of product gases from fuel-rich flames indicates that the hydrogen content is in fact lower than indicated by the assumption underlying the calculations; if so, somewhat lower expansion ratios and higher burning velocities would result.

The final matter requiring consideration is the permissibility of applying incompressible flow calculations to the present system. The analysis of combustion at constant pressure is based on the original work of Stevens[7] and Silsbee who have determined the flow and pressure conditions within and beyond the kernel bounded by the flame surface. They assume that the gases are incompressible. However, for expansion velocities of the order of 10^4 cm/s, observed for high-speed pentaborane flames, the assumption of incompressibility begins to break down because the speed of the flame front becomes comparable to the velocity of sound. No detailed analysis of the exact velocity and pressure relations both ahead of and behind the combustion wave has as yet been made to indicate the correction terms that should be applied. The compressibility effect is still relatively small at the maximum expansion velocities reported herein (4 per cent change in the static/total-density ratio at Mach 0·3) but increases rapidly as expansion velocities in excess of 10^4 cm/s are reached.

The measurements on pentaborane–oxygen–nitrogen mixtures have demonstrated that this system has the highest burning velocity thus far recorded for laminar flame systems, based on comparable initial and final temperatures. In *Table 2* are shown the maximum burning velocities for hydrogen–air and for acetylene–air, compared with pentaborane–air burning velocities for mixtures having the same calculated final temperatures. In both instances the burning velocity of pentaborane–air is greater than that

Table 2. Burning velocities of hydrogen–air, acetylene–air and pentaborane–air at comparable final flame temperatures

Mixture	*Equivalence ratio*	*Flame temperature* (°K)	*Burning velocity* cm/s
H_2/*air*	1·4	2290	250
B_2H_9/*air*	0·67	2290	370
C_2H_2/*air*	1·3	2605	145
B_2H_9/*air*	0·925	2605	490

of the other two burning velocities. The reason for the high velocities cannot be due entirely to the high flame temperature alone, but must be due in part to the fast reaction rates of the boron hydrides at low temperatures where the rate-determining exothermic reactions are taking place.

This work was supported under Contract NOrd 7386 with the Bureau of Ordnance, U.S. Navy.

Applied Physics Laboratory,
The Johns Hopkins University,
Silver Spring, Maryland

(Received July 1957)

REFERENCES

[1] BERL, W. G. and DEMBROW, D. W. *Nature, Lond.* 170 (1952) 367
[2] PARKER, W. G. and WOLFHARD, H. G. *Fuel, Lond.* 35 (1956) 323
[3] HURD, D. T. *An Introduction to the Chemistry of the Hydrides* Wiley : New York, 1952
[4] OLSEN, H. L., GAYHART, E. L. and EDMONSON, R. B. *Fourth Symposium (International) on Combustion* pp 144–148. Williams and Wilkins : Baltimore, 1953
[5] OLSEN, H. L. and GAYHART, E. L. 'Flame-speed measurements by the flame-kernel method.' *APL/JHU internal Memo. No. CM-855* (1955)
[6] EDMONSON, R. B., GAYHART, E. L. and OLSON, H. L. *Photogr. Engng* 3 (1952) 135
[7] STEVENS, F. W. 'A constant pressure bomb.' *Nat. Adv. Comm. Aero. Rep. No. 176* (1923)
[8] ANDERSON, J. W. and FEIN, R. S. *J. chem. Phys.* 18 (1950) 441
[9] JAHN, G. *Der Zündvorgang in Gasgemischen* Oldenbourg : Berlin, 1934
[10] FIOCK, E. F. and ROEDER, C. H. 'The soap-bubble method of studying the combustion of mixtures of CO and O_2.' *Nat. Adv. Comm. Aero. Rep. No. 532* (1935)
[11] FIOCK, E. F. and ROEDER, C. H. 'Some effects of argon and helium upon explosions of carbon monoxide and oxygen.' *Nat. Adv. Comm. Aero. Rep. No. 553* (1936)
[12] CALDWELL, F. R., FIOCK, E. F., MARVIN, C. F., Jr and ROEDER, C. H. 'Flame speeds and energy considerations for explosions in a spherical bomb.' *Nat. Adv. Comm. Aero. Rep. No. 682* (1940)
[13] CALDWELL, F. R. and FIOCK, E. F. *J. Res. nat. Bur. Stand* 26 (1941) 175
[14] LINNETT, J. W., PICKERING, H. S. and WHEATLEY, P. J. *Trans. Faraday Soc.* 47 (1951) 974
[15] LINNETT, J. W. and PICKERING, H. S. *Trans. Faraday Soc.* 47 (1951) 989 and 1101
[16] LINNETT, J. W. and WHEATLEY, P. J. *Trans. Faraday Soc.* 48 (1952) 338
[17] STREHLOW, R. A. and STUART, J. G. *Fourth Symposium (International) on Combustion* pp 329 336. Williams and Wilkins : Baltimore, 1953
[18] LEWIS, B. and VON ELBE, G. *Combustion, Flames and Explosion of Gases* p 448. Academic Press : New York, 1951
[19] LEWIS, B. and VON ELBE, G. *Combustion, Flames and Explosion of Gases* p 479. Academic Press: New York, 1951
[20] FRISTROM, R. M. *J. chem. Phys.* 24 (1956) 888
[21] RENICH, W. T. *APL/JHU internal Memo.* to W. G. Berl, July 1956

An Isotopic Tracer Study of Carbon Formation in Hydrocarbon Flames

R. E. FERGUSON

In the course of an attempt to investigate experimentally the hypothesis that acetylene is the last stable precursor to carbon in rich premixed hydrocarbon flames, the isotopic composition of the carbon (or soot) formed in closed bomb explosion flames of propane-2-^{13}C has been studied. The results show definitely that carbon does not arise preferentially from a two-carbon piece of the fuel molecule; that is, if acetylene polymerization–decomposition is the actual mechanism of carbon formation, then the acetylene does not contain a carbon pair of the propane and must arise by a process more complicated than simple degradation of the fuel.

Isotopic analyses of gaseous products show that methane and carbon monoxide come equally from all three carbon atoms of the propane, and that the acetylene remaining does in fact contain a nearly random isotope distribution, such as would result from its synthesis in the flame from single-carbon radicals. The composition of other products is given. As a test of whether carbon monoxide participates in carbon formation in hydrocarbon flames, possibly by reaction with existing nuclei, ^{13}CO was burnt in an ordinary propane flame. Neither the carbon collected nor the gaseous products, except carbon dioxide, contained ^{13}C in significant excess over the natural abundance.

OF THE several mechanisms of carbon formation seriously considered at present, one of the most recently favoured, and in many ways the most appealing, has been discussed by G. PORTER[1,2], who postulates that carbon is formed in hydrocarbon flames by the polymerization–decomposition of acetylene produced in the reaction zone. There is much indirect support for this view but, as with most proposed flame reactions, direct evidence is lacking.

This note describes an attempt to investigate the acetylene hypothesis experimentally. As will be seen in what follows, the results do not provide clear evidence for or against the acetylene mechanism, but considerable relevant information was obtained in the study.

The problem was attacked in the following way. Fuel-rich mixtures of oxygen and propane-2-^{13}C were burnt in explosion flames and the isotopic composition of the carbon formed was determined. The object here was to find whether or not the main reaction path (propane→solid carbon) in a premixed flame is through a two-carbon fragment of the fuel, the C—C pair of which survives and appears in the soot deposited. Assuming for simplicity that pure propane-2-^{13}C is burnt, and considering only what happens to the carbon skeleton in the flame, three possibilities seem reasonable:

(*a*) The overall reaction path leading to carbon formation is through a two-carbon piece (provisionally identified as acetylene) of the fuel

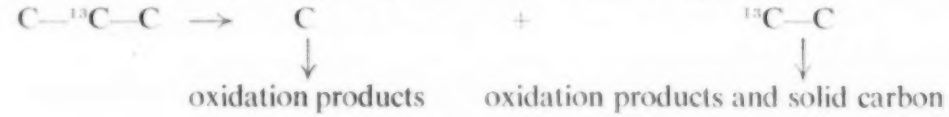

The two-carbon fragment will contain the ^{13}C, and if there is little contribution from single-carbon fragments, the isotope ratio in the solid carbon will be close to $^{13}C/^{12}C = 1$.

(*b*) The propane skeleton decomposes in a series of steps the effect of which is as if complete fragmentation of the chain occurs prior to carbon formation

$$C—{}^{13}C—C \longrightarrow C + {}^{13}C + C \xrightarrow{?} \text{solid carbon}$$

Here it is obvious that the isotope ratio in the solid carbon will be $^{13}C/^{12}C = 1/2$ no matter what the detailed mechanism may be. This scheme would include the case in which acetylene is first synthesized from single-carbon radicals in the flame, then polymerizes, and so on. (Polymerization of the intact propane skeleton would give the same result, but it seems unlikely that the propane survives to participate in carbon formation in premixed flames.)

(*c*) An intermediate case is possible, with mechanism (*a*) operative, but in which an appreciable fraction of the single-carbon radicals combine eventually to form acetylene, etc. This would give an isotope ratio less than unity but greater than a half; the actual value would depend upon the relative rates of recombination and oxidation of the radicals. From what is known about the thermal decomposition of hydrocarbons at high temperatures, this last case would seem off-hand the most likely one if the acetylene mechanism is correct.

The above possibilities are listed mainly for completeness of the discussion. The results point clearly to case (*b*), in which all three carbon atoms of the propane participate equally in carbon formation.

It should be noted that the experiment is not a direct test of the acetylene hypothesis as stated by Porter[2], the validity of which does not depend upon how acetylene is produced in the flame. The result does show that if the acetylene mechanism is correct, then the acetylene in the flame does not contain an original carbon pair of the fuel.

After this initial work, attention was focused on the gaseous products of the explosions. It was found that small quantities of the lower hydrocarbons could be recovered from the burnt mixtures, and in particular it was found possible to isolate sufficient acetylene for isotopic analysis. The acetylene did in fact show a nearly random distribution of ^{13}C among the carbon pairs, which indicates that it does not arise by simple degradation of the propane.

The isotopic composition of other products and also the results of a somewhat unrelated experiment to determine whether carbon monoxide participates in carbon formation will be reported below.

EXPERIMENTAL

Preparation of propane-2-^{13}C

Propane-2-^{13}C was synthesized starting with ^{13}C-enriched barium carbonate by the series of steps

$$^{13}CO_2 \longrightarrow CH_3{}^{13}COOH \longrightarrow \text{Ba salt} \longrightarrow CH_3{}^{13}COCH_3 \longrightarrow CH_3{}^{13}CH_2CH_3$$

Methods previously which have been employed by others[3] were used, with minor modifications, for all but the last step, the reduction of acetone to propane. This was accomplished by reduction of the semicarbazone of acetone with potassium hydroxide in a bomb (other variations of the Wolff–Kishner reaction, such as reduction of acetone hydrazone with sodium methylate, gave unsatisfactory yields). Dry acetone semicarbazone and four times its weight of dry potassium hydroxide were ground together and loaded into a small steel bomb with glass liner. The bomb was evacuated, charged with 3 atm of dry nitrogen, closed off, and heated at 210°C for about 18 hours. The product gases were pumped off slowly through traps containing, in order, sulphuric acid (conc. acid/water = 2/1), Drierite, and Ascarite, into a trap at liquid nitrogen temperature. The crude propane was distilled several times at dry ice temperature to a trap cooled by liquid nitrogen. The yield of propane was 85 per cent for this step, and the overall yield was 46 per cent of theoretical based upon the weight of barium carbonate taken at the start.

Mass spectrometric analysis showed that the sample contained 61·9 per cent propane-^{13}C in excess of the natural abundance. The relative abundance of the $^{12}C^{13}CH_3^+$ and $^{12}C^{12}CH_3^+$ ions indicated that all of the excess ^{13}C was in the 2-position. There was a small excess of $^{13}CH_3^+$ over that expected due to the natural abundance of ^{13}C in the end positions; this has been observed previously and has been attributed to a rearrangement of atoms in the ionization process[4].

Explosions and recovery of carbon

Propane–oxygen mixtures were made by pressure measurement in a fixed volume, mixed by several transfers with a Toepler pump, and then transferred to a previously evacuated 90 cm^3 cylindrical explosion bomb lined with gold foil. After explosion (ignited by a Tesla coil spark across a 1 mm spark plug gap) at 1 atm initial pressure the product gases were pumped off and stored, and the foil with the soot deposit was removed to a fused quartz tube on the vacuum line. The deposit was out-gassed at red heat *in vacuo*, after which carbon dioxide-free oxygen was admitted to the sample. After oxidation the carbon dioxide was recovered and analysed by mass spectrometer for $^{13}C/^{12}C$ ratio. In view of the small sample size (a few milligrammes) considerable care was taken to avoid contamination of the apparatus. Blank runs, which included handling of the foil, etc., showed that the carbon dioxide was possibly contaminated with at most 0·2 per cent of its volume of carbon dioxide from other sources.

Analysis of gaseous products

The product gases of interest were divided into two fractions, one volatile at liquid nitrogen temperature, containing hydrogen, carbon monoxide, and methane, and another condensable at liquid nitrogen temperature but volatile at dry ice temperature. The first fraction was analysed by mass spectrometer directly, and the second, containing C_2 and C_3 hydrocarbons along with carbon dioxide, was separated into its components by gas–liquid partition chromatography. The isotopic compositions of the pure

C_2 hydrocarbons recovered were determined mass spectrometrically by low voltage measurements (only the molecule ions present). The purity of the separated components exceeded 99 per cent in all cases.

RESULTS AND DISCUSSION

Carbon formation

Table 1 shows the composition of the two propane samples used.

Table 1. Composition of propane samples burnt

Component	*Concentration, mole per cent*	
	Sample A	*Sample B*
C—^{13}C—C	61·6	21·3
C—C—C	36·2	76·5
C—^{13}C—^{13}C	1·4	0·5
C—C—^{13}C	0·8	1·7

The composition of sample *A*, the undiluted material, was calculated from the reported ^{13}C excess of 61·9 atomic per cent in the 2-position (i.e. a total of $61{\cdot}9 + 1{\cdot}1 = 63{\cdot}0$ atomic per cent ^{13}C in this position), assuming that the two end carbon atoms show the natural abundance. Sample *B* was prepared by dilution of sample *A* with two volumes of ordinary propane, which contains about 1·1 atomic per cent ^{13}C based on total carbon, assumed to be distributed randomly in the molecule. Propanes present in very small concentration (e.g. ^{13}C—C—^{13}C) are neglected.

Since species other than propane-2-^{13}C are present in the samples, the expected istopic compositions of the carbon deposit will of course be different from those in the idealized example given at the outset. With sample *A* the simplified acetylene mechanism, case (*a*), is expected to give carbon containing 32 atomic per cent ^{13}C; a 'random' mechanism, case (*b*), should yield 21·7 atomic per cent ^{13}C. The difference is still conveniently large.

The results are collected in *Table 2*.

Table 2. ^{13}C content of soot formed in propane-2-^{13}C–oxygen explosions

Run	*Fuel*	*Percentage propane by volume*	*^{13}C in carbon formed, atomic per cent*		
			Calc., C_2H_2 hypothesis	*Calc., random mechanism*	*Observed*
1	*Sample A*	39·8	32·0	21·7	21·5
2	*Sample A*	37·2	32·0	21·7	21·6
3	*Sample B*	39·9	11·4	8·0	7·9
4	*Sample B*	37·2	11·4	8·0	7·8

Runs 1 and 3 were made with mixtures near the rich inflammability limit for spark ignition in the bomb used; they gave copious-appearing soot deposits (4 to 5 mg). Runs 2 and 4 were made with mixtures which barely showed carbon formation (0·05 to 1 mg). Regardless of the difference in conditions the results are practically the same and thus are apparently independent of mixture ratio within the region of carbon formation.

The close agreement between the last two columns of *Table 2* rules out the simplified acetylene mechanism. The conclusion to be drawn from these data is that carbon does not arise preferentially from a two-carbon pair of the propane; if it does arise from acetylene, then the acetylene is not a recognizable fragment of the propane.

The gaseous products

The non-condensable fractions contained mostly carbon monoxide and hydrogen, a small amount of oxygen, and some methane (about 9 mole per cent of the total product). The fractions condensable at liquid nitrogen temperature, which amounted to about 5 mole per cent of the total, contained propane, propene, carbon dioxide, and all three C_2 hydrocarbons. The acetylene concentration was roughly 0·3 mole per cent of the total products, varying slightly with mixture ratio. The analytical results are given in *Table 3*.

Table 3. Isotopic composition of products

Product	*Explosion*	*Total ^{13}C in propane, atomic per cent based on carbon*	*^{13}C content of product, same units*
CO	1 *and* 2	21·7	22·5 *and* 22·2
CH_4	2	21·7	21·1
CO_2	3 *and* 4	8·0	8·4 *and* 8·4
C_2H_2	3 *and* 4	8·0	8·5 *and* 8·8
C_2H_4	3	8·0	8·8
C_2H_6	3	8·0	8·2

At present no significance is attributed to the differences between entries in the last two columns for carbon monoxide and methane. They are small, and therefore the results are taken to mean that the three atoms of the propane contribute about equally to the methane and carbon monoxide formed in the flame.

The discrepancy is larger with the C_2 hydrocarbons. Another table will be useful for discussion of the problem of the origin of these products. It shows the detailed composition of the acetylene sample, which is about the same as that of the ethylene and ethane isolated.

Table 4. Isotopic composition of acetylene in products of propane-2-^{13}–oxygen explosions

Component	*Concentration, mole per cent of C_2H_2*			
	Calculated, arising directly from propane	*Calculated, not a piece of the propane*	*Observed*	
			Run 3	*Run 4*
$H^{12}C{=}{}^{12}CH$	77·4	84·5	83·6	83·0
$H^{13}C{\equiv}{}^{12}CH$	22·4	14·7	15·8	16·3
$H^{13}C{\equiv}{}^{13}CH$	0·25	0·6	0·6	0·7
Overall ^{13}C content, atomic per cent of carbon	11·4	8·0	8·5	8·8

The observed composition is rather close to that in the third column, calculated for a hypothetical mechanism involving the formation of acetylene from single-carbon radicals. The deviation from this random case indicates that some acetylene may be formed by direct degradation of propane, perhaps in the cooler regions near the wall of the bomb. That the walls do have an influence is borne out by the observation that the hydrocarbon content of the products is somewhat increased by the presence of the gold foil liner (hence dead space) in the explosion bomb. On the other hand, the extent of deviation from a random isotope distribution in the C_2 hydrocarbons is very close to that observed, in another study, for the electronically excited C_2 radical in an acetylene flame[5], where there were no 'cooler regions'. There may be some connection between these two observations; the possibility is interesting enough to justify further work.

The data in *Tables 2* to *4* show that the total ^{13}C content of the acetylene produced is somewhat higher than that of the soot formed, whereas the values should be identical if carbon arises from acetylene. However, this discrepancy is not taken at present as evidence against Porter's mechanism, because the acetylene involved in carbon formation may not have exactly the same isotopic composition as that remaining in the cooled products.

The mechanism of the isotopic mixing process is as yet only a subject for speculation. The simplest explanation is that most of the acetylene (also ethane and ethylene) is synthesized in the reaction from single-carbon radicals. This may occur early in the flame front or later in the hot burnt gas, in the presence of carbon particles, reactions which may also contribute to the mixing process. In any case, it is evident that most of the lower hydrocarbon products do not arise by direct degradation of the fuel.

Experiments are now in progress on the thermal decomposition of propane-2-^{13}C in the temperature range ($>1100^\circ K$) where acetylene is a major product. This work may throw some light on the origin of acetylene in a simpler high temperature system.

Propane–oxygen explosions with added ^{13}CO

It has been suggested[6] that carbon monoxide formed in hydrocarbon flames contributes to carbon formation by the Boudouard reaction

$$2CO \rightleftharpoons C \text{ (solid)} + CO_2$$

perhaps by addition of its carbon to existing carbon nuclei started by some other process[7]. It is possible by a simple experiment to determine whether this is so in explosion flames similar to those discussed above.

Briefly, the experiment was as follows. A mixture of 33·2 mole per cent ordinary propane, 8·3 mole per cent ^{13}CO (66·5 atomic per cent ^{13}C based on total carbon), and 58·5 mole per cent oxygen was exploded in the bomb described above. The ^{13}C content of the carbon was determined and the gaseous products were analysed by mass spectrometer. The original mixture contained 5·5 atomic per cent ^{13}C based on total carbon. The ^{13}C content of the soot deposited was 1·2 atomic per cent, not appreciably

above the natural abundance of 1·1 atomic per cent, and there was no evidence that any of the gaseous products excepting carbon dioxide contained ^{13}C. The carbon dioxide in the explosion products showed a ^{13}C abundance of 7 atomic per cent, indicating that the ^{13}CO was not present merely as a diluent. Its oxidation apparently proceeds, as might be expected, independently of the hydrocarbon radical chain reactions occurring simultaneously. Such a small ^{13}C excess in the solid carbon formed could be due to adsorption of carbon oxides on the surface of the carbon during cooling of the bomb contents, followed by reaction of the adsorbed material with carbon during subsequent high temperature outgassing of the deposit.

RÉSUMÉ

Study of the isotopic composition of solid carbon (soot) formed in explosion flames of propane-2-^{13}C has shown that carbon does not arise from a two-carbon fragment of the propane. This means that if acetylene polymerization–decomposition is the mechanism of carbon formation, then the acetylene involved is not a product of simple degradation of the fuel.

Determination of the ^{13}C abundance in methane and carbon monoxide present in the cooled explosion products has indicated that they come approximately equally from the three carbon atoms of the propane. The acetylene recovered contains a nearly random isotope distribution, which means that most of it is formed by a process in which the original C—C bonds of the propane are broken at some stage; the same is true of ethane and ethylene. There is an apparent small difference between the ^{13}C content of the acetylene isolated from the reaction products and that of the soot deposited, but in view of the complexity of the reaction system under study, the results of the work reported are taken to be not inconsistent with the acetylene mechanism of carbon formation.

An investigation of the products of explosion of a (propane + ^{13}CO + oxygen) mixture has provided evidence against the participation of carbon monoxide in carbon formation in typical soot-forming hydrocarbon flames.

The writer is indebted to C. R. Yokley of this laboratory for his help with separations of the hydrocarbon products, and to the Mass Spectrometry Section of the National Bureau of Standards for the isotope analyses.

This research was supported by the United States Air Force Office of Scientific Research under contract No. CSO-680-57-12.

National Bureau of Standards,
Washington 25, D.C. *(Received June 1957)*

REFERENCES

[1] PORTER, G. *Fourth Symposium (International) on Combustion* p 248. Williams and Wilkins: Baltimore, 1952
[2] PORTER, G. *Combustion Researches and Reviews* p 108. AGARD; Butterworths: London, 1955
[3] CALVIN, M. *et al. Isotopic Carbon* Wiley: New York, 1949
[4] STEVENSON, D. P. *J. chem. Phys.* 19 (1951) 21
[5] FERGUSON, R. E. *J. chem. Phys.* 23 (1955) 2085
[6] BEHRENS, H. *Fourth Symposium (International) on Combustion* p 538. Williams and Wilkins: Baltimore, 1952
[7] BEHRENS, H. *Fourth Symposium (International) on Combustion* p 252. Williams and Wilkins: Baltimore, 1952

*A Theory of Flame Propagation Limits Due to Heat Loss**

E. MAYER†

An energy balance equation for the flame front relates the actual flame temperature T_f to the adiabatic temperature T_f^a and a heat loss parameter λ. From this equation real values of T_f are possible only for limited ranges of T_f^a and λ, depending on the character of the heat loss mechanism. Flame propagation limit criteria are deduced for the special cases of (1) *convective heat loss applicable to flame quenching in a circular tube, and* (2) *radiative heat loss applicable to free flames near the composition limit. Illustrative numerical applications are made to hydrocarbon–air data. The theoretical results for both quenching and composition limits are in satisfactory agreement with the observed data.*

WHEN the results of experiments on the flammability of premixed gases are represented in a pressure/composition diagram, the flammable area appears to be limited as illustrated in *Figure 1* for natural gas–air mixtures[1]. At

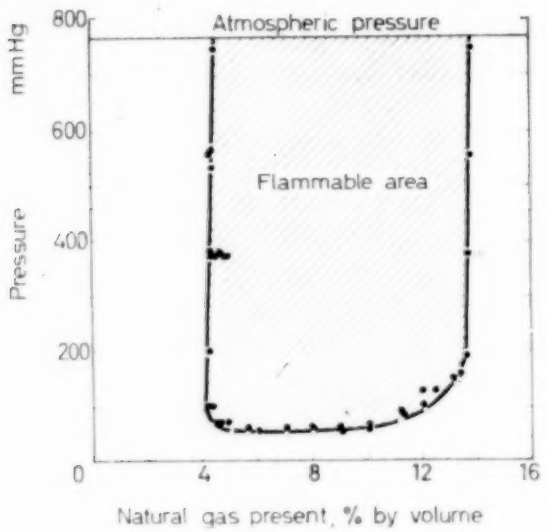

Figure 1. Flame propagation limits in a pressure / composition plane[1] (Burner diameter, 5 cm)

the limiting conditions the flame speeds are observed to be finite, being of the order of several cm/s. No such limits are predicted by theoretical treatments describing the steady-state combustion wave based on the analysis of adiabatic flame models[2]. In regard to the low pressure limit satisfactory interpretation of the observed data can be made by taking into account, within the framework of steady-state relations, heat loss or diffusion loss of active chemical species from the flame front to the neighbouring walls[3–7]. Theoretical interpretation of the composition limits in

*Technical Note No. 4555-6, June 1957. †Present address: Rocketdyne, Canoga Park, Calif.

flame models obeying conservation laws is generally sought in possible intrinsic instability of the steady-state solutions when subjected to temperature perturbations[8–10], but up to the present time the results of the intrinsic instability studies appear to have no immediate applicability to the observed composition limits.

In this note we consider, within the scope of elementary thermal flame relations, the effect of heat loss from the flame front upon the steady-state propagation of a one-dimensional combustion wave. The underlying physicochemical principles which lead to propagation limits may be qualitatively expressed as follows. The temperature levels attained in the flame front (characterized by a peak temperature, T_f) govern the chemical reaction rates and hence the heat generation rates in accordance with an exponential law of the Arrhenius type

$$\text{generation rate} \sim \exp(-E/RT_f)$$

where E cal/mol is the activation energy, R cal/mole °K is the universal gas constant and T_f °K is the peak flame temperature. The heat loss rates depend, in general, on the difference between T_f and the environment temperature T_u °K; or on some appropriate power of the temperature difference, dependent on the mechanism of heat loss. Subscripts f and u denote final (or burnt) and initial (or unburnt) states respectively. If now T_f is reduced because of heat losses, the exponentially dependent heat generation rates diminish more rapidly than the corresponding heat loss rates, and, therefore, energy balance requirements will limit the possible level to which T_f may be reduced by heat loss. In this note we determine the limiting flame propagation conditions from an energy balance equation and deduce limit criteria for the special cases of: (*1*) convective heat loss applicable to flame-quenching in a circular tube, and (*2*) radiative heat loss applicable to free flames near the composition limit.

EFFECTS OF HEAT LOSS ON LAMINAR FLAME PROPAGATION

The effects of heat loss on a stationary one-dimensional premixed flame are conveniently discussed with reference to conditions in an adiabatic flame front. A comparison of temperature profiles in the flame front with and

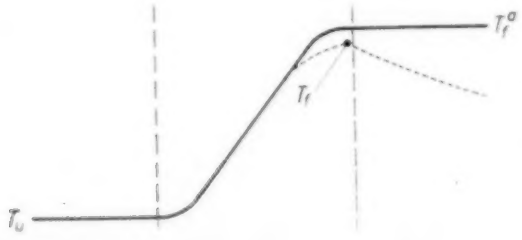

Figure 2. Schematic comparison of temperature profiles in flame front with and without heat loss

without heat loss is shown schematically in *Figure 2*. The solid curve represents the adiabatic flame with temperature rise from T_u in the unburnt mixture to T_f^a, the theoretical adiabatic flame temperature in the burnt mixture. The dotted curve represents the temperature profile in a flame front with possible heat losses both in the reaction zone and the post-reaction

zone where the mixture temperature is above that of the environment. Energy balance equations may be stated with respect to the reference surfaces enclosing the flame front, as sketched in *Figure 2*. For the adiabatic flame the energy equation is

$$\rho_u S_u^a [c_p T_u + H^a] - \rho_u S_u^a c_p T_f^a = 0 \qquad \ldots . [1]$$

where $\rho_u S_u^a$ is the adiabatic mass flux (ρ denoting density and S laminar flame speed), c_p cal/g °K is the gas specific heat, and H^a cal/g is the energy released per unit mass of the mixture. (The superscript a refers to adiabatic values of magnitude primarily dependent on chemical composition.) Changes in the specific heat are assumed to be negligible. In view of equation 1, we may regard $T_f^a = T_u + H^a/c_p$ as a datum which specifies the chemical energy content in the unburnt mixture. If heat loss is taken into account, the peak temperature T_f, assumed to occur near the end of the reaction zone, satisfies a more general energy-balance equation

$$\rho_u S_u [c_p T_u + H^a] - \rho_u S_u c_p T_f - q(\lambda, T_f) = 0 \qquad \ldots . [2]$$

where $\rho_u S_u$ is the mass flux and q cal/s cm^2 is the heat loss rate per unit area of the flame front contained between the reference surfaces sketched in *Figure 2*. The actual flame speed S_u cm/s is primarily a function of the peak temperature T_f in accordance with thermal flame theories, and in agreement with experimental data obtained with flames stabilized on cooled porous plugs[11]. Furthermore, the heat loss rate, q, introduced in equation 2, is dependent primarily on T_f and on a heat loss parameter* λ independent of T_f, as illustrated below in detail. Thus, for a variety of heat loss mechanisms, it is possible to write the energy equation relating the actual flame temperature T_f to a thermochemical property H^a (or T_f^a) and a suitably defined heat loss parameter λ

$$F(T_f^a, \lambda, T_f) = 0 \qquad \ldots . [2']$$

In this form the energy equation represents a surface of propagation in the coordinate system defined by the T_f^a, λ, T_f axes. Propagation limits may occur for a given mixture composition (T_f^a) if the heat loss parameter λ attains a critical value λ_c, and for a given heat loss mechanism (λ) if the composition parameter attains a critical limiting value $T_{f,L}^a$ (subscript L denoting flammability limit). By formal procedure, these limits may be found from the partial derivatives

$$(dT_f/d\lambda)_{T_f^a} = \infty \qquad \ldots . [3]$$

$$(dT_f/dT_f^a)_\lambda = \infty \qquad \ldots . [4]$$

Thus, elimination of T_f between equations 2′ and 3 leads to the limiting heat loss parameter for a given composition

$$\lambda_c = \lambda_c(T_f^a) \qquad \ldots . [5]$$

*The parameter λ may represent variables readily controlled under experimental conditions, e.g. the diameter of a burner tube or the tube temperature in a quenching experiment. In some heat loss systems λ may be less subject to experimental control, e.g. when λ represents a thermal emissivity parameter.

Elimination of T_f between equations 2′ and 4 yields the limit composition temperature for a given heat loss parameter

$$T^u_{f,\,L} = T^u_{f,\,L}(\lambda) \qquad \ldots . [6]$$

An alternative, physically more meaningful procedure for determining propagation limits, equivalent to the use of equations 2′–6, will be developed below in illustrative applications to quenching and composition limit data in hydrocarbon–air mixtures.

HEAT LOSS MECHANISMS

Before applying equation 2′ to the calculation of propagation limits, we specify the relevant mechanisms of heat loss in terms of thermal flame concepts.

Within the scope of thermal flame theories S_u is primarily a function of the actual flame temperature T_f. A particularly useful representation of S_u is the Arrhenius–Semenov form

$$S_u(T) = B \exp(-E/2RT) \qquad \ldots . [7]$$

involving the empirical mixture parameters: B, the rate constant (flame speed parameter, cm/s), and E cal/mol, the apparent activation energy.

The parameters B and E are readily estimated by comparison of equation 7 with experimental data[11] obtained with flat flames stabilized on cooled porous plugs (see *Figure 3*). It follows from equation 7 that the flame

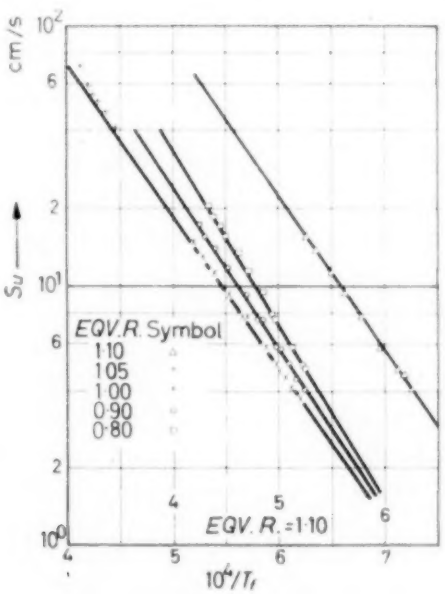

Figure 3. Flame speeds of propane–air mixtures[11]. Abscissae of EQV. R. = 1·10 points displaced as indicated

speed corresponding to the actual flame temperature T_f is related to the adiabatic flame speed S_u^a by

$$S_u(T_f) = S_u^a \exp(E/2R)(1/T_f^a - 1/T_f) \qquad \ldots . [8]$$

Another useful order-of-magnitude expression based on thermal flame theory relates the reaction zone thickness δ (cm) to S_u and the average thermodiffusivity $\bar{\alpha}$ of the mixture in transit through the flame front

$$\delta \simeq \frac{\bar{\alpha}}{S_u} = \frac{\bar{k}/\bar{\rho}c_p}{S_u} \qquad \ldots.[9]$$

Here $\alpha = k/\rho c_p$ cm^2/s, k in cal/s cm °K, and the superior bar denotes a value averaged over the temperature interval from T_u to T_f. From the known temperature dependence of the thermal conductivity $k \sim T^{\frac{1}{2}}$ and $\rho \sim T^{-1}$ we may express $\bar{\alpha}$ as

$$\bar{\alpha} = \alpha_u \left\{ \frac{T_f + T_u}{2T_u} \right\}^{1.75} \qquad \ldots.[10]$$

where $\alpha_u = k_u/\rho_u c_p$ is the thermodiffusivity in the unburnt mixture at the temperature T_u. The combined effect of diminishing $\bar{\alpha}$ and S_u as T_f decreases is to increase the reaction zone thickness δ in equation 9.

The particular heat loss mechanisms of interest in the application of equation 2′ to the quenching and composition limits are, respectively, (*1*) convective heat transfer in laminar flow, and (*2*) thermal radiation from a flame to its environment.

Convective heat transfer

Near quenching conditions, the flame at the exit of a bunsen tube is essentially a flat disc (in contrast to the conical shape of the usual bunsen flame). Although the flame about to be quenched is only roughly represented by the idealized flow conditions in a premixed laminar flame, it will be sufficient to consider heat loss per unit area of the flame by the convective heat loss formula

$$q_{\text{conv.}} = h(T_f - T_u)\pi D\delta / \tfrac{1}{4}\pi D^2 \qquad \ldots.[11]$$

where h cal/s cm^2 °K is the heat transfer coefficient, T_u is the tube wall temperature (assumed equal to the temperature of the unburnt mixture), and $\pi D\delta$ is the heat transfer area between the reaction zone and the tube (D cm being the diameter). In general, the convective heat transfer coefficient in laminar flow through the tube is of the form

$$h = F^2\bar{k}/D \qquad \ldots.[12]$$

where F, the flame configuration factor, is a constant of the order of unity. (Nusselt's theoretical result[12] for a circular tube is $F^2 = 3{\cdot}65$.) Upon substitution for h and δ from equations 12 and 9 respectively, we have from equation 11

$$q_{\text{conv.}} = 4F^2(\bar{k}\bar{\alpha}/D^2S_u)(T_f - T_u) \qquad \ldots.[11']$$

The convection mechanism described here implies, in general, increasing heat loss at lower values of T_f because of thickening of the reaction zone $\delta \simeq \bar{\alpha}/S_u$ as T_f is diminished. The factor F is likely to depend on the detailed configuration of the flame near quenching; its value may be determined by comparison of calculated results with experimental data.

Radiation losses

The effect of radiation heat loss from the flame on reduction may be conveniently described by considering (*1*) conduction of heat into the post-reaction zone which cools by radiative heat loss, and (*2*) radiative heat loss from the reaction zone itself.

In steady-state one-dimensional flame propagation, the temperature in the post-reaction zone is governed by the energy equation

$$\rho_u c_p S_u \frac{dT}{dx} - \frac{d}{dx} k \frac{dT}{dx} = -\mathbf{R}(T) \qquad \ldots . [13]$$

where $\mathbf{R}$ cal/cm^3 s is the volumetric heat loss rate dependent on the concentration of radiating species and on the local temperature distribution in the post-reaction zone. For typical mass flow rates, the transport term on the left of equation 13 is much greater than the diffusion term. If now under the influences of heat losses the peak temperature T_f (near the end of the reaction zone) is attained, equation 13 yields in the first approximation*

$$(dT/dx)_{x=x_f} = -\mathbf{R}(T_f)/\rho_u c_p S_u(T_f) \qquad \ldots . [14]$$

From equation 14 we obtain the heat loss rate from the reaction zone per unit area of the flame front due to conduction into the cooling post-reaction zone

$$q_{\text{rad.,}\,1} = k_f \mathbf{R}(T_f)/\rho_u c_p S_u(T_f) \qquad \ldots . [15]$$

From the reaction zone itself the radiation heat flux is

$$q_{\text{rad.,}\,2} = \int_0^{\delta} \mathbf{R}_r \, dx \qquad \ldots . [16]$$

where $\mathbf{R}_r$ is a rapidly varying function of position in the reaction zone, since here both temperatures and radiative species concentrations rapidly change from generally negligible values at the upstream end to significant levels at the downstream end of this zone. It is interesting to note that, if $\mathbf{R}_r$ is assumed constant at its terminal value $\mathbf{R}(T_f)$, equation 16 yields

$$q_{\text{rad.,}\,2} \to \mathbf{R}(T_f)\delta = \frac{\bar{k}}{\rho c_p} \frac{\mathbf{R}(T_f)}{S_u(T_f)}$$

which is of the same order of magnitude as $q_{\text{rad.,}\,1}$ in equation 15. However, inasmuch as the space-average value of $\mathbf{R}_r$ in the reaction zone is much lower than $\mathbf{R}(T_f)$, in general $q_{\text{rad.,}\,2} \leqslant q_{\text{rad.,}\,1}$. Therefore, only $q_{\text{rad.,}\,1}$ will be considered in the calculation of composition temperature limits.

*The next approximation which includes the effect of the diffusion term on the left of equation 13 is obtained by an iterative procedure leading to

$$\left(\frac{dT}{dx}\right)_{x=x_f} = \frac{-\mathbf{R}(T_f)/\rho_u c_p S_u}{\left[1 + \left\{k_f/(\rho_u c_p S_u)^2\right\}\right]\left[d\mathbf{R}/dT\right]_{T=T_f}} \qquad \ldots . [14']$$

The volumetric radiation rate $\mathbf{R}(T)$ is readily determined from experimental data on gaseous emissivities ε_i for several typical gaseous reaction products i such as carbon dioxide, water, and sulphur dioxide. Curves of ε_i versus 'optical path thickness' $\xi_i = p_i l$ (with p the pressure in atmospheres) and gas temperature[13] T are employed to calculate the radiation rate from a gas layer of infinitesimal thickness Δl

$$\mathbf{R}(T)\Delta l = 2\sigma \Delta \varepsilon_i T^4 \quad \ldots . [17]$$

where σ cal/s cm^2 (°K)^4 is the Stefan–Boltzmann radiation constant and

$$\Delta \varepsilon_i = p_i \Delta l (\mathrm{d}\varepsilon_i / \mathrm{d}\xi_i)_{\xi_i \to 0} \quad \ldots . [18]$$

The empirical curves for ε_i indicate that the derivative in equation 18 varies nearly as T^{-2}. For the combined effect of carbon dioxide and water in the reaction products we thus obtain, upon normalizing with respect to $T = 1400$ °K,

$$(\mathrm{d}\varepsilon / \mathrm{d}\xi)_{\xi \to 0} = (1400/T)^2 \{0{\cdot}0765\, p_{\mathrm{CO_2}} + 0{\cdot}0135\, p_{\mathrm{H_2O}}\} \quad \ldots . [19]$$

Inserting equation 19 into equation 18 and substituting into equation 17 we arrive at

$$\mathbf{R}(T) = C^a T^2 \quad \ldots . [17']$$

where C^a, the effective thermal emissivity, in cal/s cm^3 (°K)^2 is given by

$$C^a = 4{\cdot}1 \times 10^{-7} \{p_{\mathrm{CO_2}} + 0{\cdot}18\, p_{\mathrm{H_2O}}\} \quad \ldots . [20]$$

QUENCHING

Basic experimental data on the dependence of quenching tube diameters on pressure and chemical composition lead to correlations which indicate that the Peclet number

$$P_e = S_u^a D / \alpha_u \quad \ldots . [21]$$

is nearly constant at quenching conditions[14, 15, 7]

$$P_e \sim 30\text{–}50 \quad \ldots . [22]$$

The theoretical limiting Peclet number obtainable by the system equations 2′, 3 and 5 will now be derived by application of the convective heat loss mechanism $q_{\mathrm{conv.}}$ in equation 11′.

Consider the energy equation in the form

$$q_{\mathrm{loss}}(T_f^a, T_f) = q_{\mathrm{conv.}}(D, T_f) \quad \ldots . [23]$$

where

$$q_{\mathrm{loss}} = \rho_u S_u [c_p T_u + H^a] - \rho_w S_u c_p T_f$$
$$= \rho_u c_p S_u (T_f) [T_f^a - T_f] \quad \ldots . [24]$$

represents, by definition, the heat loss rate per unit area of the flame front independent of the loss mechanism. The solutions of equation 23 are graphically illustrated in *Figure 4* showing curves of q_{loss} and $q_{\mathrm{conv.}}$ versus T_f for a particular combustible mixture with adiabatic flame temperature T_f^a. The q_{loss}/T_f curve has a maximum determined by the combined

effect of increasing flame speed S_u and diminishing temperature defect $T_f^a - T_f$, as the actual flame temperature, T_f, increases. The convective heat loss is shown by dotted curves corresponding to several burner tube diameters. For sufficiently large diameter D_1 two intersections* of q_{loss}

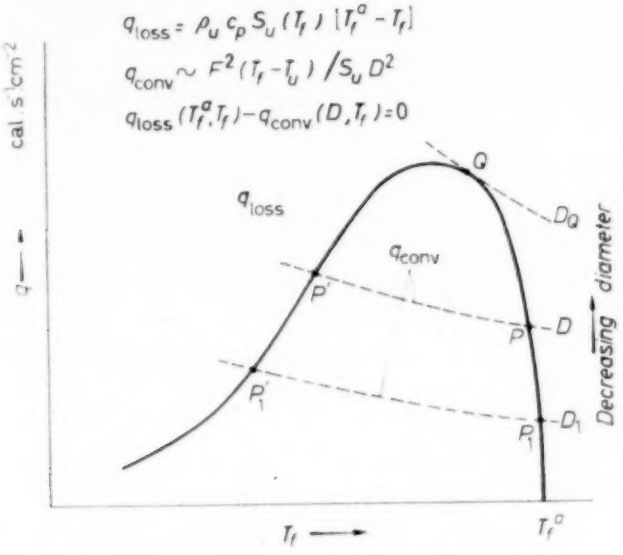

Figure 4. Heat loss rate versus actual flame temperature, T_f, illustrating quenching

with $q_{conv.}$ are possible (designated by P_1, P_1' in *Figure 4*). As D is decreased the intersections P, P' approach a limiting point, Q, interpreted as the quenching limit. This limit is attained if $D = D_Q$ and no intersections are obtained for $D < D_Q$; i.e. no real value of T_f satisfies equations 23, 24, 11′ if $D < D_Q$. (The possible propagation points P, P' along the q_{loss}/T_f

*Although two possible propagation points, P, P' at temperatures T_f, T_f' are obtained from the solution of equation 23 for sufficiently large D, only the point P can represent stable propagation. This is readily shown by a 'static stability' analysis illustrated in *Figure 5*. If the flame at P_1, i.e. $T_{f,1}$ is

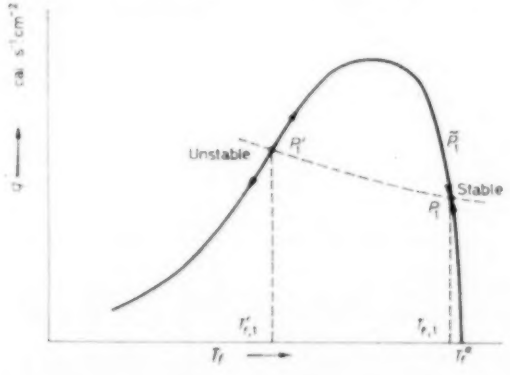

Figure 5. Static stability of propagation points in q/T_f plane

displaced along the propagation curve q_{loss}/T_f to the point $\tilde{P}_1$ at a lower temperature, $\tilde{T}_{f,1} < T_{f,1}$, the mechanism cannot remove sufficient heat and the temperature will rise towards the equilibrium value $T_{f,1}$, as indicated by an arrow along the propagation curve in *Figure 5*. Similarly, other conceivable displacements from P_1, P_1' will lead to flame temperature changes as shown by arrows on the propagation curve. Thus, an increase in the temperature of a flame at P_1' results in continuously increasing temperature from $T_{f,1}'$ to $T_{f,1}$ while a temperature decrease at this propagation point leads to extinction of the flame.

curve of *Figure 4* correspond to an arc on the general propagation surface $F(T_f^a, \lambda, T_f)=0$ of equation 2′ contained in the $T_f^a=$const. plane, with the heat loss parameter λ representing the burner diameter.)

It is clear from the graphical illustration in *Figure 4* that the quenching diameter must satisfy a tangency condition at Q

$$dq_{loss}(T_f^a, T_f)/dT_f = dq_{conv.}(D, T_f)/dT_f \quad \ldots [25]$$

(This condition may be formally deduced from the general system equations 2′ and 3 if $F=q_{loss}-q_{conv.}$)

The analytical form of the quenching condition based on the energy equation 23 with the convective heat loss mechanism equation 11′ is now obtained as follows. Introducing into the energy equation the temperature dependence of S_u and $\bar{\alpha}$ from equations 8 and 10, respectively, we obtain upon rearrangement with dimensionless notation

$$\psi \exp[-G\psi/(1-\psi)] = 4(F/P_e)^2(T_f^a/2T_u)^{2\cdot5}(\phi_1-\psi)^{2\cdot5}(\phi_2-\psi)\exp[G\psi/(1-\psi)] \quad \ldots [23']$$

where the temperature defect ψ is given by

$$\psi=(T_f^a-T_f)/T_f^a; \text{ and } G=E/2RT_f^a$$

also

$$\phi_1=(T_f^a+T_u)/T_f^a; \text{ and } \phi_2=(T_f^a-T_u)/T_f^a$$

The tangency condition 25, obtained by differentiation of both sides in equation 23′ with respect to ψ, may be combined with equation 23′ to eliminate factors independent of ψ. We thus arrive at an equation for the value of ψ at quenching

$$\frac{1}{\psi}+\frac{2\cdot5}{\phi_1-\psi}+\frac{1}{\phi_2-\psi}-\frac{2G}{(1-\psi)^2}=0 \quad \ldots [26]$$

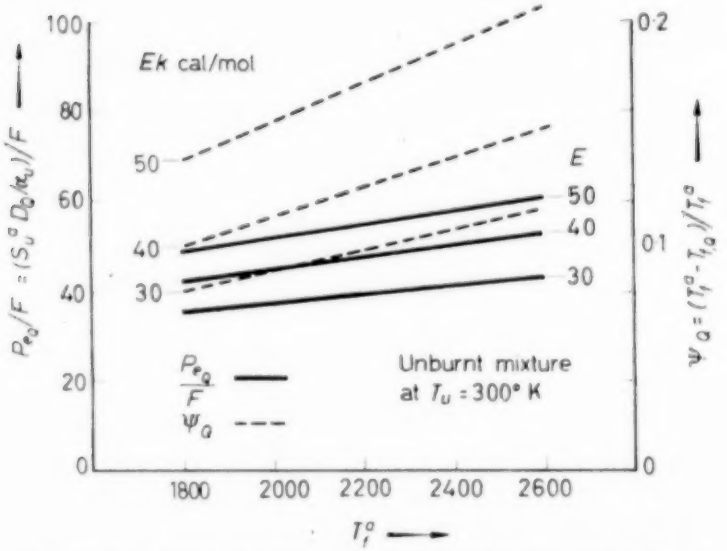

Figure 6. Quenching Peclet numbers and temperature defects versus adiabatic flame temperature

The temperature defect $\psi=\psi_Q$ obtained from equation 26 is shown in *Figure 6* as a function of the adiabatic flame temperature T_f^a and activation energy E for initial mixture temperature $T_u=300\,^\circ$K. This figure also shows the quenching Peclet number calculated from equation 23′ with $\psi=\psi_Q$; i.e. from

$$\frac{P_{e_Q}}{F}=2\exp\left(\frac{G\psi_Q}{1-\psi_Q}\right)\left\{\left(\frac{T_f^a}{2T_u}\right)^{2\cdot5}\frac{(\phi_1-\psi_Q)^{2\cdot5}(\phi_2-\psi_Q)}{\psi_Q}\right\}^{0\cdot5} \quad \ldots.[23'']$$

With the configuration factor assumed equal to unity, $F=1$, the calculated results are in satisfactory order-of-magnitude agreement with the experimental correlations summarized in equation 22. Furthermore, quenching correlations for hydrocarbon–air flames[16] indicate heat loss factors at quenching in agreement with the temperature defect $\psi_Q\sim0{\cdot}15$. Finally, the theoretical result equation 23″ expresses the variation of the quenching Peclet number with activation energy and temperature-dependent thermodiffusivity (implicit in T_f^a/T_u).

COMPOSITION LIMITS

The composition limits obtainable from the energy balance equation will now be derived by application of the heat loss mechanism $q_{\text{rad.,1}}$ in equation 15.

Consider the energy equation in the form

$$q_{\text{loss}}(T_f^a, T_f)=q_{\text{rad.,1}}(C^a, T_f) \quad \ldots.[27]$$

where q_{loss} is given by equation 24. The solutions of equation 27 for real T_f are graphically represented in *Figure 7* by intersections of q_{loss} and $q_{\text{rad.,1}}$ curves in a q/T_f plane. The solid curves correspond to a set of near-limit mixtures with $T_{f,1}^a>T_{f,2}^a>T_{f,3}^a$ . . . in a sequence of

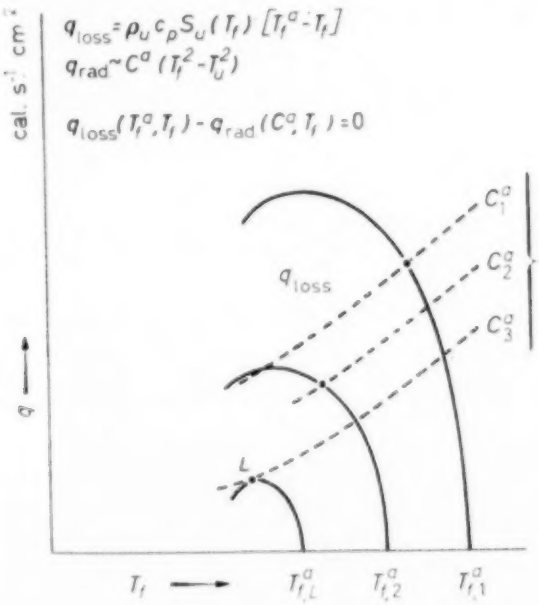

Figure 7. Heat loss curves versus actual flame temperature T_f, in near-limit mixtures illustrating composition limit

increasingly leaner (or richer) mixtures. Dotted curves show the associated radiation losses $q_{rad.,1}$, which depend somewhat on the concentration of radiating molecules in the reaction products implicit in C^a. As the composition is varied, a limit propagation point is reached at L.

An analytical procedure for determining the limit point L now consists of solving equation 27 together with the tangency condition

$$\frac{dq_{loss}(T_f^a, T_f)}{dT_f} = \frac{dq_{rad.,1}(C^a, T_f)}{dT_f} \quad \ldots . [28]$$

Introducing the temperature dependence of S and $\varkappa$ into equation 24 for q_{loss} and equation 15 for $q_{rad.,1}$, we express the energy equation in dimensionless notation

$$\psi \exp\left(-\frac{G}{1-\psi}\right) = \Lambda \frac{(1-\psi)^{2.75} \exp[G/(1-\psi)]}{(2G)^{1.75}} \quad \ldots . [27']$$

where, in addition to previously defined terms, we have the radiation heat loss parameter Λ, given by

$$\Lambda = \varkappa_u (E/RT_u)^{0.75} (E/R) C^a / \rho_u c_p B^2 \quad \ldots . [29]$$

The tangency condition 28, obtained by differentiation of both sides in equation 27′ with respect to ψ, may be combined with equation 27′ to eliminate factors independent of ψ. We thus arrive at an equation for the value of ψ at the propagation limit

$$\frac{1}{\psi} + \frac{2.75}{1-\psi} - \frac{2G}{(1-\psi)^2} = 0 \quad \ldots . [30]$$

With ψ_L/G determined from equation 30, the limiting heat loss parameter from equation 27′ becomes

$$\Lambda = \frac{\psi_L}{1-\psi_L}\left(\frac{1}{\psi_L} + 1.75\right)^{1.75} \exp(-1/\psi_L - 1.75) \quad \ldots . [27'']$$

The relation between G and Λ at the propagation limit thus determined is shown graphically in *Figure 8*. The region under the $2G = E/RT_f^a$ versus Λ

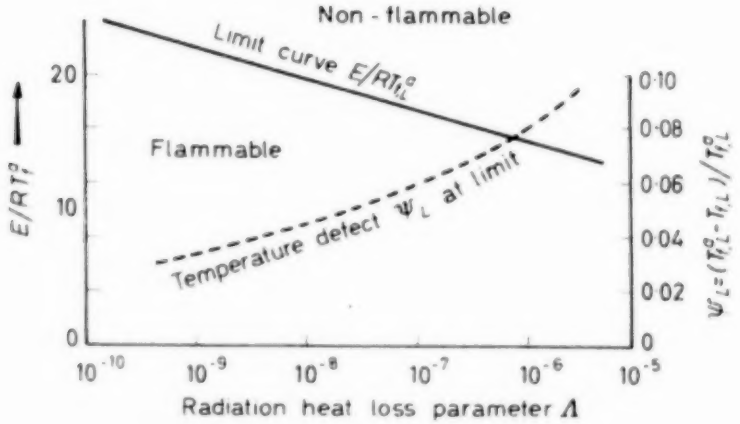

Figure 8. Propagation limit curve

curve shown here represents the 'flammable area' in the $(E/RT_f^a)/\Lambda$ plane. Every point in this plane corresponds to a mixture with presumably known thermochemical and physical data relating to both the unreacted mixture and its reaction products. The reaction rate parameters B and E can, of course, be obtained empirically only for flammable mixtures, but may, in principle, be estimated from adiabatic theories for non-flammable mixtures also.

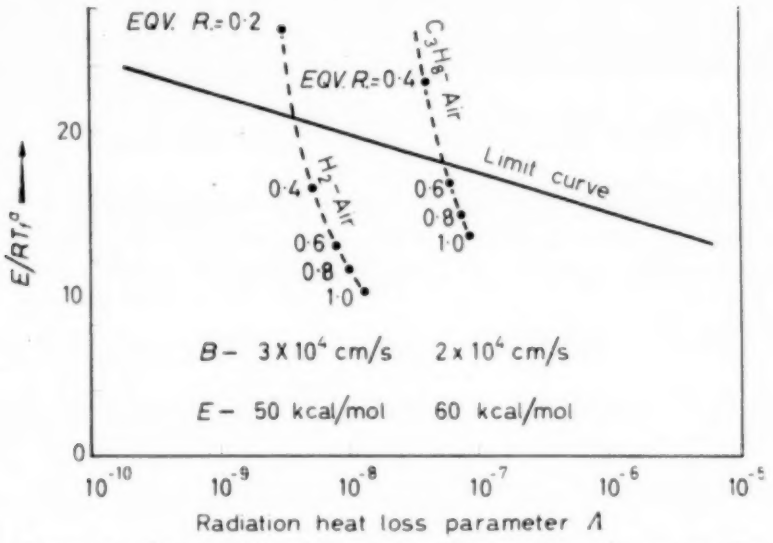

Figure 9. Flammability limits of hydrogen–air and propane–air mixtures

Illustrative numerical applications are shown in *Figure 9* for hydrogen–air and propane–air data listed in the *Tables 1* and *2*. Order-of-magnitude values of E and B were taken[11] for near-limit compositions. With these parameters held fixed, Λ and E/RT_f were calculated over a range of equivalence ratios $EQV.R.$ from 0·2 to unity. The intersection of the E/RT_f^a versus Λ curves for the mixtures considered with the theoretical limit curve indicates composition limits at $EQV.R.=0{\cdot}30$ and 0·55 for hydrogen–air and propane–air mixtures, respectively. The observed composition limits in these mixtures are at equivalence ratios of 0·25 and 0·50, respectively. The agreement is considered reasonable in view of uncertainties in the E and B data.

Table 1. Hydrogen–air data

$E=50$ kcal/mol $B=3\times10^4$ cm/s

Equivalence ratio	T_f^a °K	p_{H_2O}	$10^8\,\Lambda$	E/RT_f^a
0·2	940	0·081	0·29	26·6
0·4	1500	0·145	0·51	16·7
0·6	1910	0·225	0·82	13·1
0·8	2160	0·290	1·01	11·5
1·0	2340	0·350	1·25	10·7

Table 2. Propane–air data

$E=60$ kcal/mol $\quad B=2\times10^{4}$ cm/s

Equivalence ratio	T_f^a °K	$p_{CO_2}=\frac{3}{4}\,p_{H_2O}$	$10^8\,\Lambda$	E/RT_f^a
0·2	820	0·025	1·9	36·6
0·4	1300	0·051	3·8	23·0
0·6	1725	0·072	5·6	17·4
0·8	2030	0·095	7·0	14·8
1·0	2250	0·116	8·6	13·3

DISCUSSION

The propagation limits observed in quenching experiments have been the subject of several theoretical treatments based on heat loss considerations. Previous treatments generally involve the concept of a somewhat arbitrary critical temperature (T_i = ignition temperature[3, 4]) or critical heat loss-to-generation ratio[6, 16] below which flame propagation is assumed to be impossible. In regard to composition limits due to thermal loss from the flame, D. B. SPALDING[17] has suggested that laminar flames, in analogy with space-homogeneous reaction zones, will fail to support combustion when radiation loss rates become sufficiently large compared with heat liberation rates. In a recent treatment of one-dimensional, non-adiabatic flame propagation as an eigenvalue problem, D. B. SPALDING[18] shows that propagation limits occur at finite flame speeds dependent on the temperature characteristics of the heat loss and generation mechanisms. For heat loss rates less than that corresponding to the propagation limit, Spalding finds two possible eigenvalues, i.e. two flame speeds for each value of the heat loss parameter, the higher speed being normally stable. Similar conclusions were reached in the flame-quenching analysis[7] and are confirmed by the energy balance method presented in this paper. It is to be noted that the possibility of two flame speeds for a given mixture with heat loss is implicit in the quenching theory of von Elbe and Lewis (Ref. 3, Fig. 7). In the two-dimensional flame front model considered by these authors, the flame may propagate in a duct of given dimension in one of two modes: in one mode the combustion core is relatively large and considerable heat loss may occur across a small 'dead space' adjacent to the duct wall; in the second mode, the combustion core is small, and the correspondingly thicker 'dead space' insulates the core against excessive heat loss. Lewis and von Elbe remark that the latter mode is of no physical significance.

While the energy balance method yields limit criteria free from the special assumptions of ignition temperature or critical heat loss-to-generation ratio introduced in previous theories, in application to quenching phenomena, this method, as well as previous treatments, can yield little better than order-of-magnitude relations among the flame parameters at quenching. Further refinement in quenching theory must take into account more realistically, not only the two-dimensional character of the gas flow, but also the role of preferential diffusion under quenching conditions[19].

In regard to the fundamental question of the influence of heat loss on composition limits, direct experimental checks may be made by insulation of near-limit flames against heat loss from the post-reaction zone. For example, in flat flames stabilized on porous plugs, the insertion of a ceramic grid maintained at about 1500°K in the post-reaction zone should serve to reduce the temperature gradients primarily responsible for heat loss from the flame front; the reduced heat loss should then permit combustion at mixture ratios weaker than those of the free flame limit mixtures.

The quantitative determination of composition limits by the energy balance method is not restricted to the use of the Arrhenius–Semenov form[7] for the dependence of flame speed on temperature. Within the restriction of this form, further check of the theoretical results against experimental data requires more definitive data on B and E than is presently available for near-limit compositions. In view of the present uncertainties regarding these reaction rate parameters, the agreement between theory and experimental results in the illustrative example is considered satisfactory.

CONCLUSIONS

An energy balance equation for steady-state one-dimensional laminar flames with heat loss leads to the following conclusion:

(*1*) The flame speed in general depends both on the chemical mixture and the heat loss mechanism

(*2*) For every combustible mixture flame propagation limits occur dependent on the heat loss mechanism

(*3*) With convective heat loss to the cold walls of a burner, the limit criterion (quenching) may be expressed as a Peclet number which depends on the theoretical adiabatic temperature and apparent activation energy

(*4*) With radiative heat loss from the reaction products to the 'cold' environment, flammability limits occur at mixtures which possess relatively low reaction or heat generation rates. The flammability limit criterion relates the intrinsic thermal emissivity of the reaction products to simplified reaction rate parameters, activation energy and theoretical flame temperature of the mixture

(*5*) Comparison of theoretical results with experimental data on hydrocarbon–air mixtures leads to satisfactory order-of-magnitude agreement in regard to both quenching and flammability limits.

This research was supported by the United States Air Force through the Air Force Office of Scientific Research of the Air Research and Development Command under Contract No. 18(600)–1560.

Report Control Nos. AFOSR TN 57–296; AD 132 367.

ARDE Associates,
Newark, New Jersey

(Received June 1957)

REFERENCES

[1] JONES, G. W. and KENNEDY, R. E. *Rep. Invest. U.S. Bur. Min. No. 3798* (1945)
[2] EVANS, M. W. *Project Squid, Tech. Rep. No. 27* Princeton University, New Jersey
[3] VON ELBE, G. and LEWIS, B. *Third Symposium (International) on Combustion*, p 68. Williams and Wilkins : Baltimore, 1949
[4] WOHL, K. *Fourth Symposium (International) on Combustion*, p 68. Williams and Wilkins : Baltimore, 1953
[5] SIMON, D. M., BELLES, F. E. and SPAKOWSKI, A. E. *Fourth Symposium (International) on Combustion*, p 126. Williams and Wilkins: Baltimore, 1953
[6] POTTER, A. E., Jr and BERLAD, A. L. *Tech. Note Nat. Adv. Comm. Aero., Wash. No. 3398* (1955)
[7] MAYER, E. *Tech. Note Air Force Off. Sci. Res. No. 56-478 (AD 97 362)*
[8] LEWIS, B. and VON ELBE, G. *Selected Combustion Problems*, Vol. II, p 63. AGARD Butterworths : London, 1956
[9] ROSEN, J. B. *J. chem. Phys.* 22 (1954) 733
[10] WEHNER, J. F. *Tech. Note Air Force Off. Sci. Res. No. 55-426*
[11] KASKAN, W. E. *G. E. (N.Y.) Res. Lab. Rep. No. 56-RL1544*
[12] ECKERT, E. R. G. *Introduction to the Transfer of Heat and Mass*, p 100. McGraw-Hill : New York, 1950
[13] MCADAMS, W. H. *Heat Transmission*, 3rd ed. McGraw-Hill: New York, 1954
[14] PUTNAM, A. A. and JENSEN, R. A. *Third Symposium (International) on Combustion*, p 89. Williams and Wilkins: Baltimore, 1949
[15] CULLEN, R. E. *Trans. Amer. Soc. mech. Engrs* 75 (1953) 43
[16] POTTER, A. E., Jr and BERLAD, A. L. *Tech. Note Nat. Adv. Comm. Aero., Wash. No. 3882* (1956)
[17] SPALDING, D. B. *Some Fundamentals of Combustion* Academic Press: New York, 1955
[18] SPALDING, D. B. *Proc. Roy. Soc. A*240 (1957) 83
[19] FRIEDMAN, R. and JOHNSTON, W. *J. chem. Phys.* 20 (1952) 919

Extinction of Fires in Liquids by Cooling with Water Sprays

D. J. RASBASH and Z. W. ROGOWSKI

Extinctions which occurred when liquids burning in open vessels were cooled by water sprays projected downwards on to the liquid surface have been correlated in one equation relating the extinction time with the spray and the fire properties. The extinction time was directly proportional to the drop size of the spray and the preburn time and inversely proportional to the rate of flow of water per unit of fire area, and also to the difference in temperature between the fire point and ambient temperature raised to the power 1·75. The equation does not cover conditions in which splash fires were developed. It is inferred that in the tests on which the equation is based cooling took place as a result of heat transfer between the oil and the water drops.

ALTHOUGH water sprays can extinguish fires in burning liquids in a number of ways, the most reliable ways are those which depend on a reduction of the rate of evolution of vapour from the burning liquid to a value lower than that required to sustain flame[1]. One of the mechanisms of extinction which fall into this category is the cooling of the burning liquid to the fire point. In order to extinguish a liquid fire by cooling, the flow rate must be above a certain critical value; at lower flow rates cooling takes place to a temperature which is higher than the fire point. Information on this critical value for two kerosene fires has been given elsewhere[2]. However, from a practical point of view, particularly in the design of protective installations where rapid extinction is essential, it is often more important to predict the extinction time of the fire. In this paper, tests with water sprays on burning liquid fires in which there was evidence that the sprays extinguished the fire by cooling the liquid have been brought together into the form of a single correlation between the extinction time on the one hand, and the properties of the sprays and the fires on the other. The experiments all refer to conditions in which sprays were projected downwards from fixed nozzles to a horizontal surface of the burning liquid.

EXPERIMENTAL

The information was obtained from a series of investigations carried out on liquid fires burning in circular open vessels of various diameters. The experimental details of these investigations have been summarized in *Table 1*. Series 1, 3 and 4 were part of an investigation on the effect of water sprays of various properties on the extinction of liquid fires burning in a vessel of 30 cm diameter. The sprays were produced by means of batteries of impinging jets[1]. Series 2 and 6 were part of an investigation to determine the best types of spray for the protection of plant containing high boiling oils, particularly in electricity generating stations. A wide range of single nozzles was used to produce the sprays in these tests; the sprays were produced from impinging jet nozzles and from swirl nozzles

and some were non-directional and others directional in type. Some of the sprays used in these series are shown in *Figure 1*, which shows the difference between directional and non-directional sprays. Series 5 was an investigation on the control and extinction of a small kerosene fire by sprays of a uniform drop size.

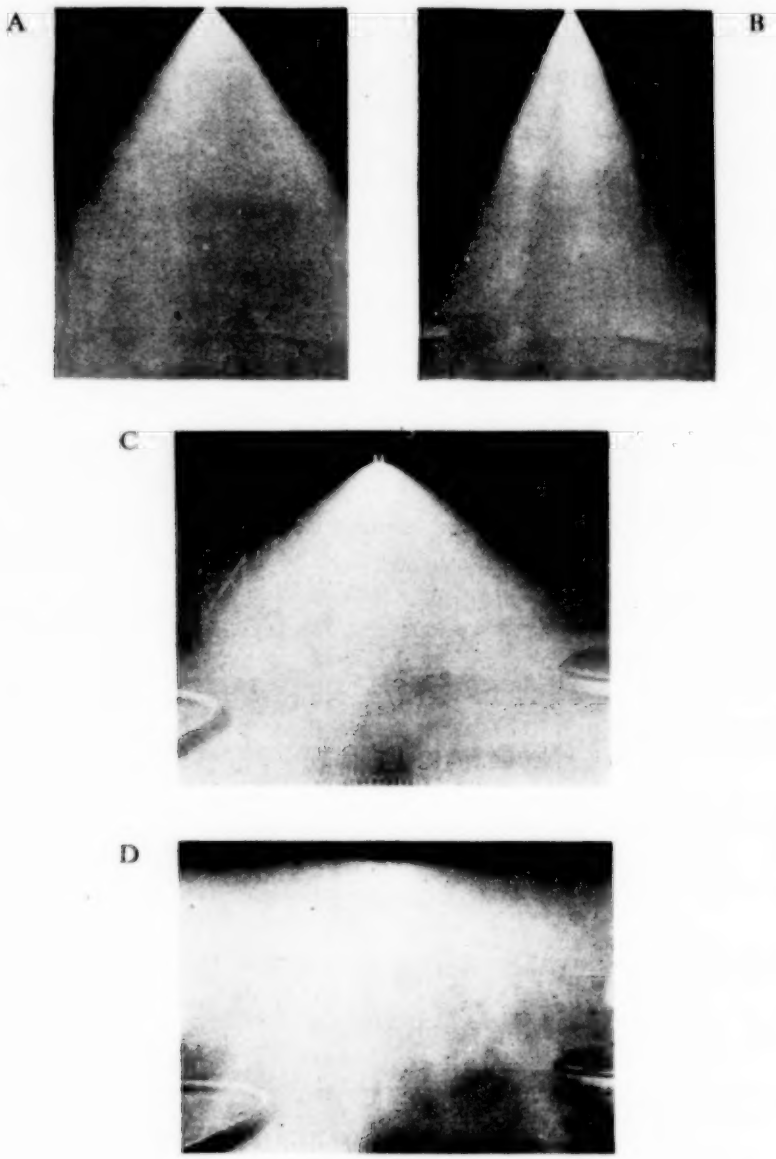

Figure 1. Examples of sprays used in series 2 and 6
A, B. Swirl nozzle. Directional spray
C. Multi-impinging jet. Directional spray
D. Multi-impinging jet. Non-directional spray

The properties of the sprays given in *Table 1* cover those parts of the ranges of sprays tested in which extinctions by cooling the liquid were obtained. In series 1, 3 and 4, frequent extinctions, more rapid than those

Table 1. Details of investigations in which extinction by cooling occurred

Test series No.	Site of tests	Properties of fire						Properties of sprays					
		Diameter of vessel	Ullage	Liquid used	Fire point of liquid	Preburn time	Depth of thermocouple below surface	Method of production	Height of nozzle above burning surfaces	Mean flow rates of spray to combustion vessels	Drop size of spray*	Entrained air velocity of spray	Pressure at nozzle
		cm	cm		°C	s	mm		cm	g cm^{-2} min^{-1}†	mm	cm s^{-1}	Lb in^{-2}
1	Laboratory	30	2·0	Transformer oil	180	120 300	1	Battery of impinging jets	175	1·6	0·39 0·49	350	85
2	Laboratory	30	2·0	Transformer oil	180	300	1	Single nozzles of various types	243	0·3 to 5·0	0·30 to 1·15	100 to 700	25 to 100
3	Laboratory	30	2·0	Kerosene	58	30 to 480	1 and 3	Battery of impinging jets	175	0·6 to 1·6	0·33 to 0·51	200 to 350	10 to 85
4	Laboratory	30	2·0	Gas oil	104	120	1	Battery of impinging jets	175	1·6	0·39 0·49	350	85
5	Laboratory	11	2·0	Kerosene	61	480	5	Battery of hypodermic needles	145	1·2 to 2·0	0·62 to 1·19	N.D.	Air atomization
6	Roofless structure in open air	90 120	4·0 to 5·0	Transformer oil	180	300	1 to 9	Single nozzles of various types	243 456	0·4 to 7·0	0·4 to 3·0	0 to 700	50 to 100

*All drop sizes referred to in this paper are mass median drop sizes.

†Divide by 5 to give gal ft^{-2} min^{-1}.

obtained by cooling, also occurred within the range of conditions given in *Table 1*: these have been discussed in detail elsewhere[1]. With series 3 and 5, a large number of tests were also carried out with sprays of lower flow rate[2] and in general coarser drop size than those listed for these series in *Table 1*; these tests did not give extinction. The methods of measuring the spray properties and the design of the thermocouples used have been described elsewhere[3, 4].

In all tests, the oil and the water used to produce the spray were initially approximately at atmospheric temperature, which varied from 10 to 25°C. With all the tests carried out in the laboratory a fresh sample of oil was used for each test and the depth of the oil before the test was 6·0 cm. In test series 6, however, oil in 'make up' quantities was added before each test, and the depth of the oil layer varied between 5 and 6 cm.

RESULTS

Criteria for extinction by cooling

The main evidence used to decide whether an extinction was by cooling was that the temperature shown by the thermocouple placed near the liquid surface should be reduced to the fire point of the liquid prior to the extinction. In a number of tests, particularly in series 6, the fire continued

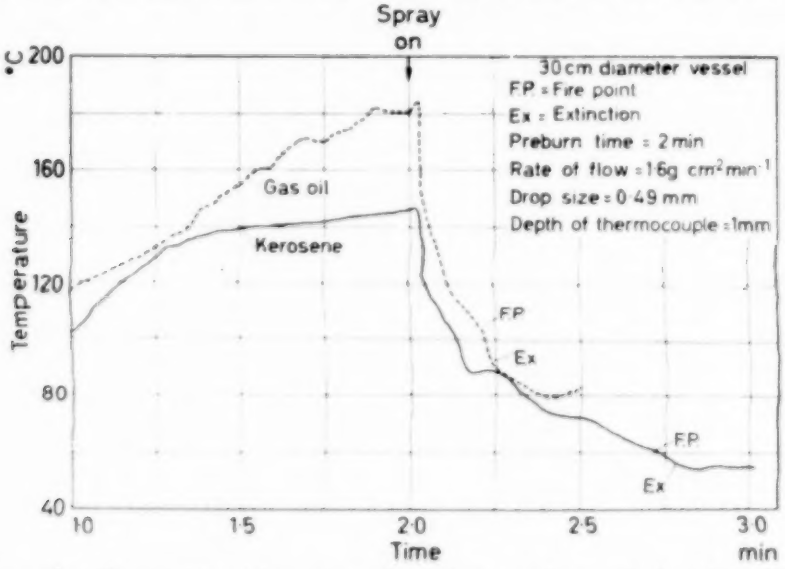

Figure 2. Temperature/time records below surface of burning liquid extinguished by water sprays

to burn for some time after the indicated temperature was reduced to below the fire point. This could be ascribed partly to unevenness in the spray pattern giving rise to different degrees of cooling at various parts of the liquid surface. However, there was also evidence that the flames under these conditions consisted of burning oil drops splashed upwards by the water spray.

It was also characteristic of extinction by cooling that after an initial upsurge, the size of the flames was reduced gradually, until in the last stages

the flames were only a few centimetres high and usually present at the edge of the test vessel only. After extinction, a lighted taper brought up to the liquid surface did not give immediate re-ignition. For these latter two reasons, some extinctions obtained in series 3 were ascribed to cooling even though the temperature indicated by the thermocouple was slightly greater (up to 7°C) than the fire point at the moment of extinction.

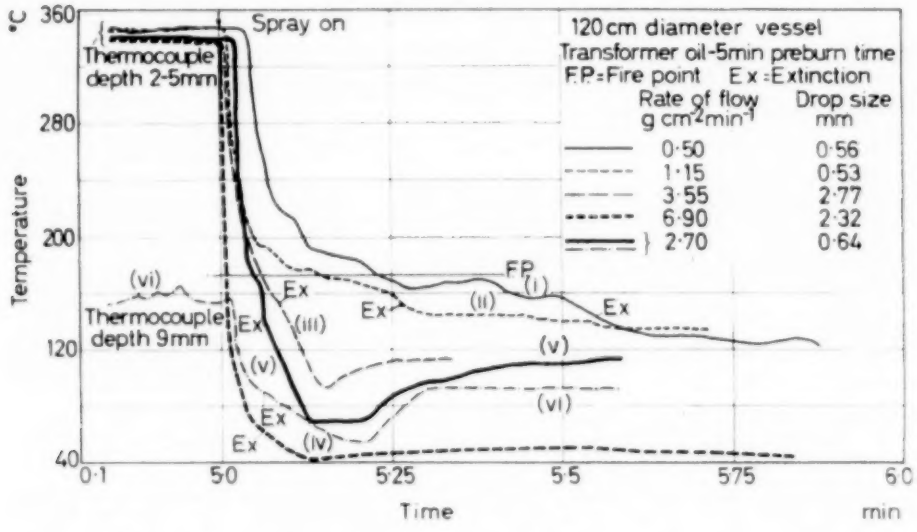

Figure 3. Further temperature/time records below surface of burning liquid extinguished by water sprays

Figures 2 and *3* show examples of temperature records obtained using the 30 and 120 cm diameter combustion vessels respectively, and *Figure 4* the appearance of the flames at different stages of a test in series 6, shown in conjunction with the temperature record. In all cases the spray was turned off within 1 to 2 seconds of extinction but cooling of the liquid continued to take place for a considerable time after the spray was turned off. In *Figure 3* curves v and vi represent replicate tests in which the thermocouple was placed 2 and 9 mm below the surface respectively. Although a very large difference in temperature between the two points existed before the spray was turned on this difference was considerably less when extinction occurred and diminished still further after extinction.

Effect of fire properties

The main properties of the fires that were varied within the series of tests were: (*1*) nature of liquid burning; (*2*) time of preburn; (*3*) diameter of the burning vessel. An estimate of the effect of the burning liquid was obtained from results contained within the series 1, 3 and 4 in which some extinctions took place under conditions in which only the nature of the liquid varied. The extinction times in these tests are plotted in *Figure 5* against the temperature difference, ΔT, between the fire point of the liquid under test and the ambient atmospheric temperature. *Figure 5* shows that there was a rapid decrease in extinction time as ΔT increased such that the

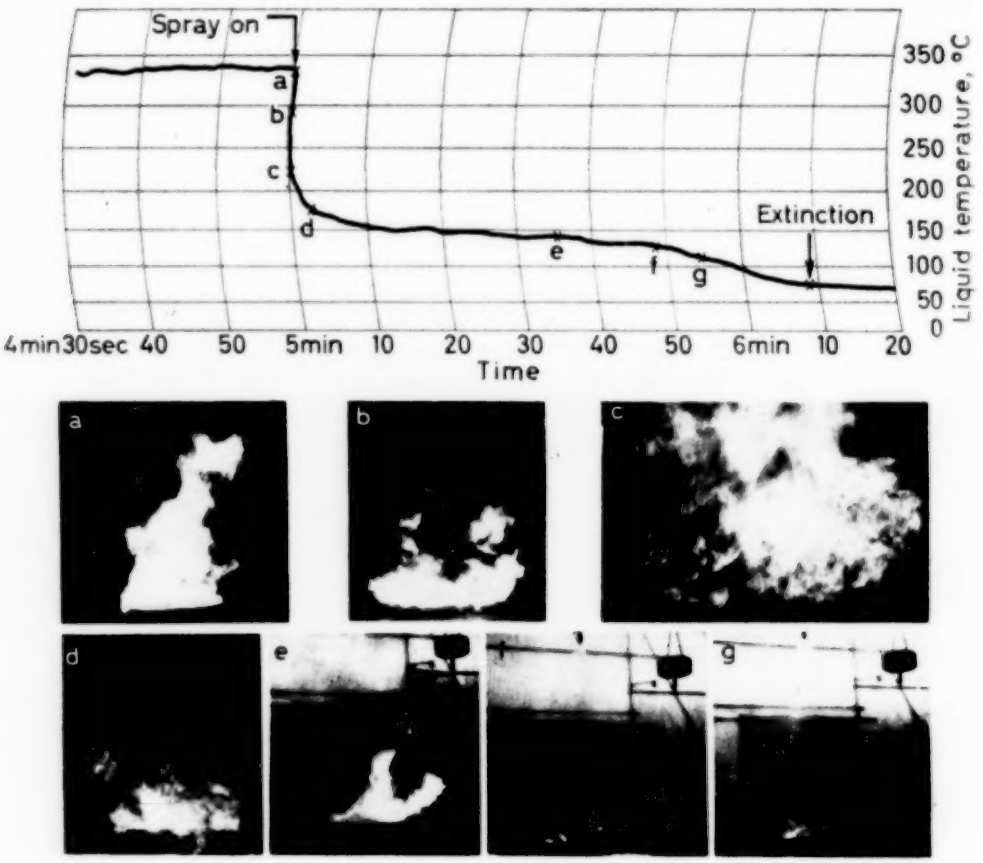

Figure 4. Liquid temperature and photographic record during spray application. Series 6. Pressure 50 lb./in². Rate of flow 1·1 g cm⁻² min⁻¹. Drop size 0·55 mm

(a) *Flame immediately before spray application;* (b) *Flame flattened by downward moving spray;* (c) *Upsurge;* (d) *Flame flattened again and from here not exceeding this size;* (e) *Partial clearance;* (f) *Burning at edges only;* (g) *Small tongue of flame left*

extinction time t was approximately proportional to $\Delta T^{-1\cdot75}$. The effect of the preburn time, mainly from a group of tests with one spray in series 3, is shown in *Figure 6*. Within a fairly wide scatter of the results, the extinction was approximately proportional to the preburn time. The only direct comparison of the effect of the diameter of the burning vessel was obtained within the tests of series 6; there was found to be no significant difference between the extinction times with the 90 cm and the 120 cm vessels used in these tests.

Effect of spray properties

In general it was not possible to ascertain directly from the results the effect of the various spray properties on the extinction time, since over a large part of the range of conditions in which extinctions by cooling occurred, it was not possible to control these properties independently. However,

in a few cases, a direct estimate was possible. Thus, the effect of a drop size difference between two sprays is shown in *Figure 5*. The coarser spray took longer to extinguish the various fires tested than the finer spray. A direct indication of the effect of a difference in the velocity of the entrained air current of two sprays was also obtained from tests in series 2. The two sprays had approximately the same drop size (0·41 and 0·45 mm) and the same rate of flow (1·7 and 1·5 g cm^{-2} min^{-1}) but differed appreciably in the entrained air velocity; the effect of the two sprays on the transformer oil fire in this test is shown in *Figure 7*. When the spray with a low entrained air velocity was applied to the fire, the flames moved upwards against the spray. With a spray of high entrained air current, the spray pushed the flames downwards and there was a smaller extinction time.

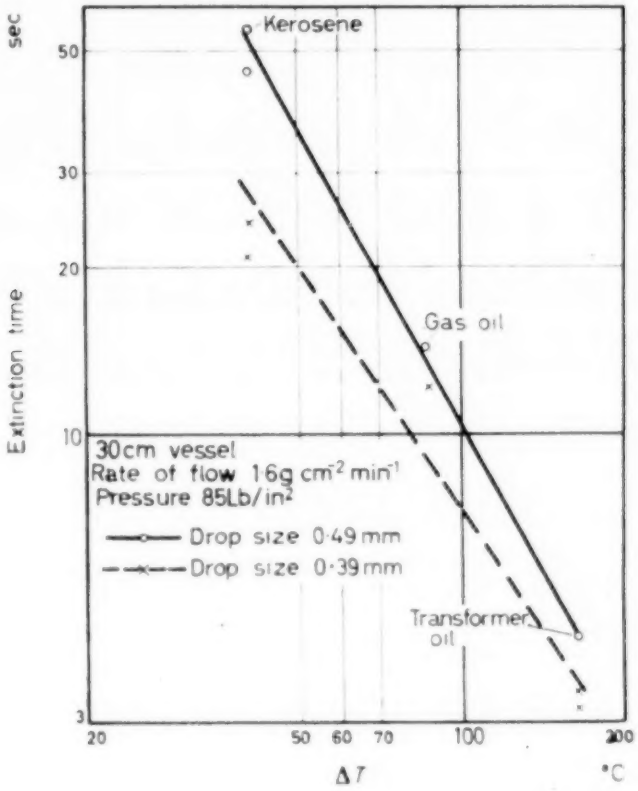

Figure 5. Effect of fire point of liquid on extinction with water spray

Overall estimates of the effect of the spray properties on the extinction time in series 2, 3 and 6 were obtained by carrying out regression analyses. All these analyses showed that within the residual error, the extinction time was directly proportional to the drop size and inversely proportional to the rate of flow of water spray to the fire area. The analyses for the tests in series 2 also showed a significant decrease in the extinction time as the entrained air velocity increased.

General correlation

Following the indications given above of the effect on extinction time of the fire and spray properties, the extinction times in all tests where extinction

was by cooling were plotted against A, where

$$A = (D/M)(Y/\Delta T^{1\cdot 75}) \qquad \ldots . [1]$$

where D mm is the mass median drop size of the spray; M (g cm^{-2} min^{-1}) denotes rate of flow of spray to fire area; ΔT°C is the difference between fire point of liquid and ambient temperature; and Y min is the preburn time.

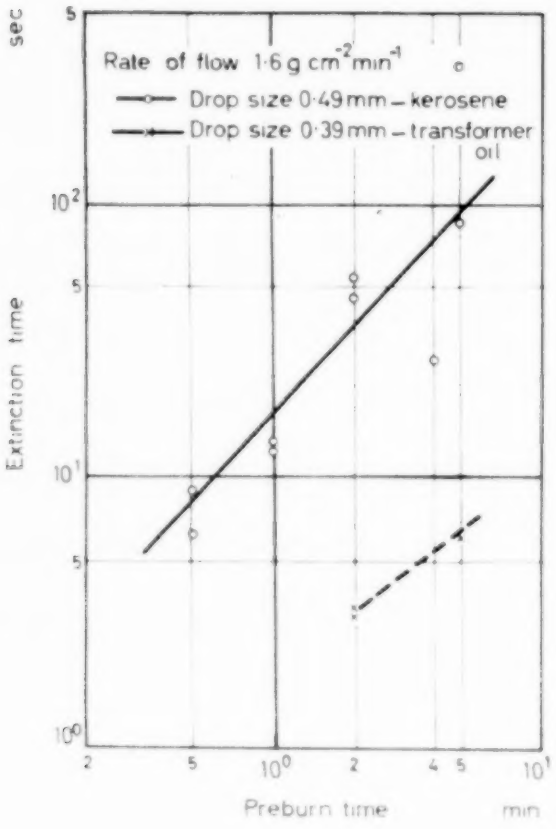

Figure 6. Effect of preburn time on extinction time

Figure 8 shows this plot for the tests within the series 1 to 5. Except for two groups of tests enclosed within the regions a and b the results fall fairly well about a line of unit slope. All the tests represented outside the regions a and b were carried out with sprays in which the velocity of the entrained air current was greater than 8 ft/s; this velocity was approximately equal to the upward velocity of the flame gases. For all the tests within the two regions the entrained air velocity was less than 8 ft/s and it was characteristic of these tests that the flames moved upwards against the sprays. The air velocities appropriate to the points in region a have been shown and it will be noted that in general the deviation from the line increased as the entrained air velocity decreased. It was difficult to introduce a factor to allow for the entrained air current since it was not possible to measure this current for the sprays in test series 5 in a manner which was comparable to those of the other sprays. It was estimated, however, that

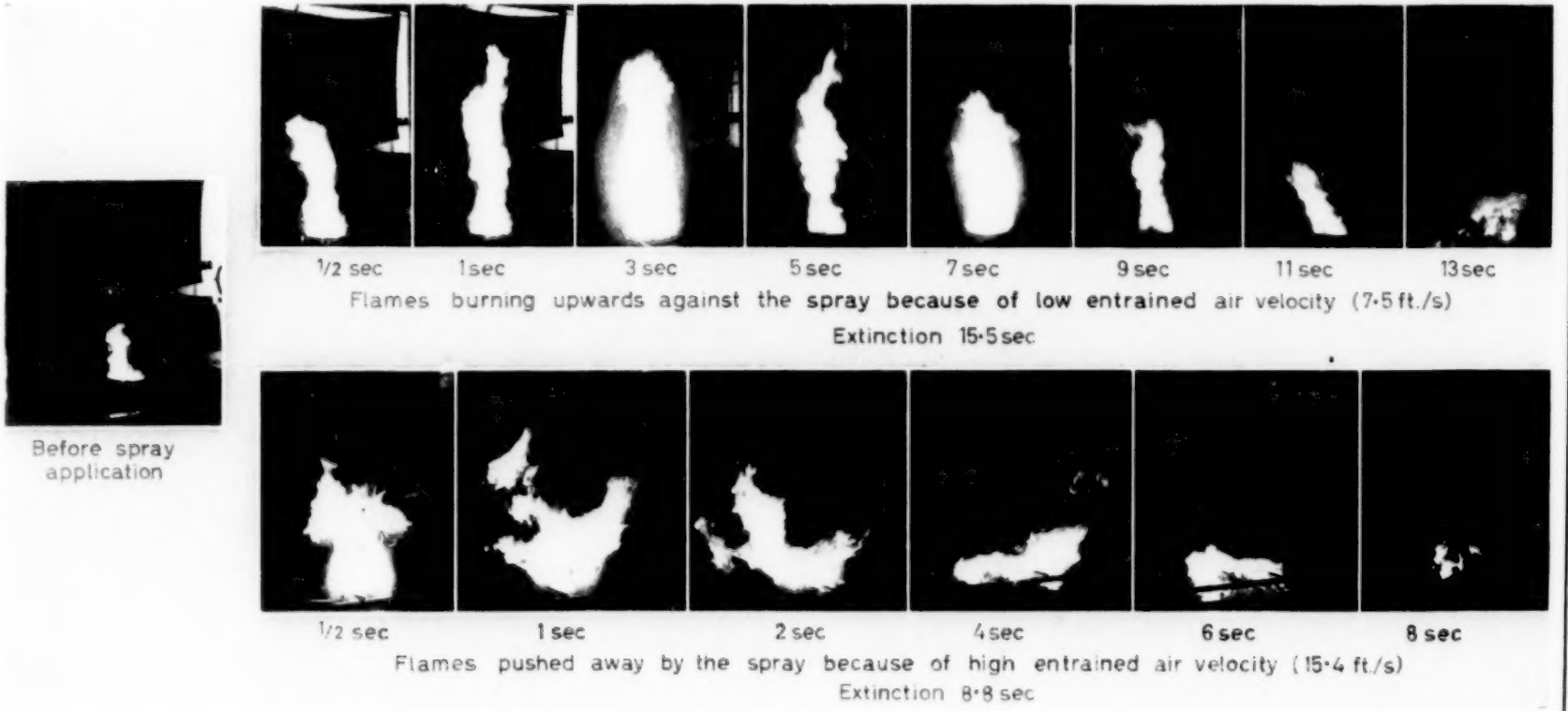

Figure 7. Effect of entrained air velocity in spray on flame movement

the sprays in this series, the results of which appear in region b, had entrained air velocities between 3 and 6 ft/s.

Figure 9 shows the extinction time t plotted against A for the extinctions obtained in series 6. This series was carried out in the open air and the results obtained were very scattered. The scatter is shown in *Figure 9* by the thin vertical lines which join the points for replicate extinctions obtained with given sprays. For given values of A no significant difference can be observed between non-directional or directional sprays or between extinctions with the 90 or 120 cm vessels. In general, however, the non-directional sprays had high values of A because of low flow rates to the fire area, and therefore gave longer extinction times than directional sprays.

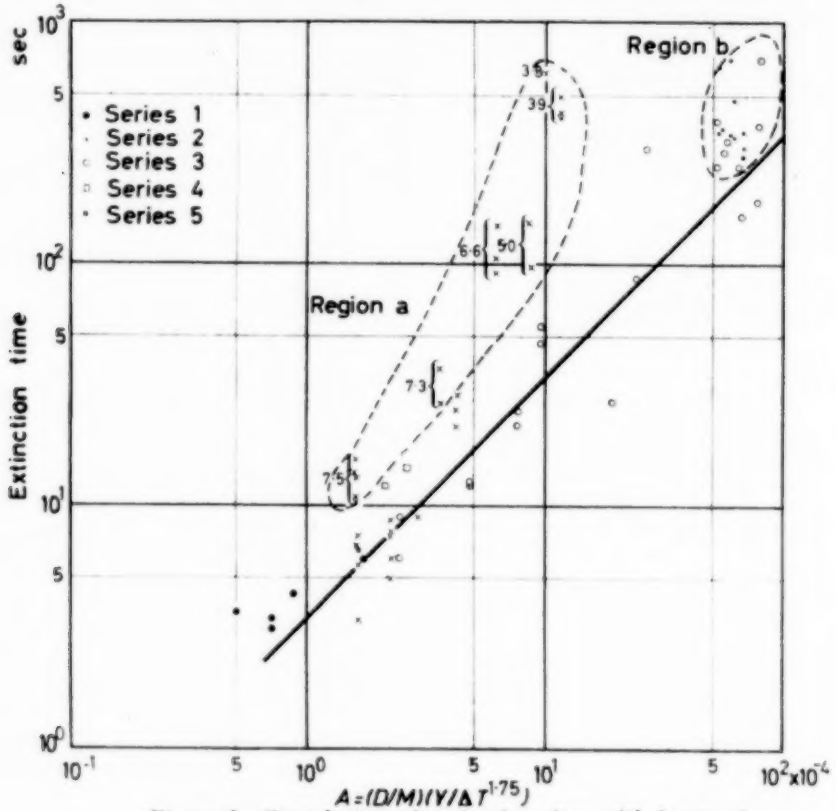

Figure 8. Correlation of extinction time with factor A

Also shown in *Figure 9* is a line of unit slope in the same position as the line in *Figure 8*. Within the error shown by the scatter the points fell about this line fairly well. However, the group of extinctions falling below the line within a region (*c*) all appertained to sprays in which a high flow rate directional spray was used.

DISCUSSION

Factors affecting extinction time

The equation to the straight line of unit slope in *Figures 8* and *9* is

$$t = 34\,000\,A = 34\,000\,(D/M)\,(Y/\Delta T^{1.75}) \qquad \ldots . [2]$$

where t denotes extinction time in seconds.

Except for some extinction times obtained when sprays with low entrained air velocity were used, all extinction times in the various series of tests fell within a distance of this line that was, in general, within the range of reproducibility of the tests.

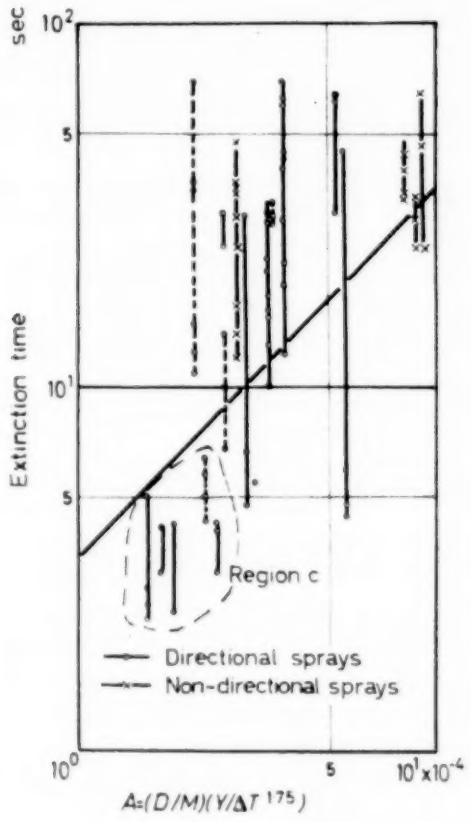

Figure 9. Correlation of extinction time with factor A for tests in series 6. Vertical lines join replicate tests with given spray. Full line for 120 cm vessel; broken line, 90 cm vessel

Equation 2 shows that under given conditions liquids with high fire points are extinguished much more rapidly than those with low fire points and the efficiency of the spray, as measured, for example, by the reciprocal of the extinction time, is proportional to the flow rate of spray to the liquid surface. Equation 2 also shows that the efficiency of the spray increases as the drop size of the spray is reduced. This can be expected to hold only if the spray drops have a momentum sufficiently large to penetrate the flames and reach the burning liquid. Under some conditions a reduction in the drop size of the sprays reduces the ability of the drops to do this. In the results given above this effect of small drop size was implicit in the observed effect of the entrained air current. When this current was greater than the upward velocity of the flames, the flames were pushed flat and most of the spray drops could penetrate to the burning liquid even if the drop size were small. When this current was smaller than the upward velocity of the flames and the spray also had a fine drop size, a large proportion of the drops could not penetrate the flames which moved upwards against the spray. Most of the sprays of low entrained air current

shown within the regions a and b were also of fine drop size (0·3 to 0·5 mm) and the longer extinction times obtained with these sprays may be ascribed to the fact that a large proportion of the drops did not reach the liquid.

It may also be concluded that a number of factors which varied within the tests, but which do not appear in equation 2, did not have a great influence on the extinction time. Thus the size of the fire, which varied from 11 cm diameter in series 5 to 120 cm diameter in series 6, was not an important factor. Also the method of production of the spray, whether it was by impinging jets or swirl nozzles or even air atomization, did not affect the extinction time noticeably. Factors like the pressure at which the spray was produced and the cone angle at which the spray was directed from the nozzles affected the extinction times only in so far as they affected the properties of the spray reaching the fire, i.e. the drop size, the flow rate and the entrained air velocity in the spray.

Mechanism of cooling

Three mechanisms may be suggested to account for the cooling of the burning liquid: (*1*) heat transfer from the hot oil to the water drops; (*2*) mixing of hot oil near the surface with cold oil well below the surface; and (*3*) the formation of an oil-in-water emulsion followed or accompanied by heat transfer from the hot oil drops to the continuous water phase[3].

The manner in which the extinction time depends on the factors in equation 2 is most consistent with the view that the cooling to the fire point of the surface layers of the oil was due to the abstraction of heat from the liquid by water drops within the liquid. Thus, the amount of heat which had to be removed increased as the preburn time increased, and the ability of the spray drops to remove this heat increased as the flow rate of the spray increased, the drop size of the spray decreased and the temperature difference between the fire point and the ambient temperature increased. The latter temperature difference may be regarded as being related to the driving force for heat transfer between the oil and the spray drops when the oil temperature was near the fire point.

In all the tests carried out the temperature distribution in the liquid at the moment of spray application was such that if complete and immediate mixing took place throughout the whole depth of the burning liquid, the temperature of the liquid would have been reduced below the fire point. The observed effect of drop size, however, does not support the view that this mixing effect was the predominant mechanism of cooling, since it would have been expected that the ability of the spray drops to agitate and mix the liquid would increase with increase in drop size and that the efficiency of the sprays should therefore also increase with drop size. It would also be expected that if mixing were the predominant mechanism of cooling the extinguishing power of the spray would have been independent of the initial temperature of the water spray but dependent on the initial oil temperature. The results in general did not provide evidence in this direction, since both the initial water temperature and the initial oil temperature were the same as the ambient temperature. It is quite likely

that the probability for extinction following cooling by mixing was greatest in the first few seconds after the spray application since it was under these conditions that mixing by the formation of steam in the oil was most pronounced. It is thus possible that the rapid extinctions obtained by high flow rate sprays shown in region c of *Figure 9* may have been caused by the intense mixing produced by the spray. However, further evidence, particularly on temperature changes throughout the whole depth of the oil, would be necessary before coming to any conclusion on this point.

In order to obtain information on the contribution of oil-in-water emulsification to the cooling process, separate tests were carried out[6] in which transformer oil was sprayed with some of the coarse sprays used in series 6 and in which the distance between the nozzle and the liquid varied from 2 to 8 ft. These tests did not reveal any definite evidence that oil-in-water emulsification took place when the oil thickness was similar to that used in the above tests (5 to 6 cm), although transient emulsification occurred sometimes with thinner layers of oil floating on water. However, even if in the tests on the fires emulsification did take place, the observed effect of the drop size indicates that it could not have had an important effect on the cooling. It would be expected that the tendency for this emulsification to occur would increase as the drop size increased, because of the extra energy available in the larger drops to shatter the oil. It would follow, therefore, that the extinction time should decrease as the drop size increased; this is not in accord with the observations in these tests.

It should be emphasized that the extinctions correlated in this paper were obtained by cooling the liquid to the fire point, and in examining the contribution that oil-in-water emulsification made to the extinctions it is fitting therefore only to consider its effect in the cooling of the liquid. Oil-in-water emulsification, as a mechanism of extinction in its own right, will be considered in further detail elsewhere[6].

Range of application of the correlation

Equation 2 gives an estimate of the extinction time for a liquid fire burning from a horizontal layer when the spray is projected vertically downwards from a fixed system, subject to the proviso that the water spray drops should be able to reach the liquid surface. The mechanism of extinction is by cooling the liquid, and although more rapid extinction may sometimes be obtained if the mechanism is by extinction of the flames[1] tests carried out so far have indicated that the chance of extinction occurring in this way diminishes as the size of the fire is increased. However, equation 2 does not cover conditions under which splash fires are formed. It is possible for a water spray to cool the whole surface of the burning liquid to below the fire point and yet for a vigorous fire to be maintained in the splashes of the liquid formed by the spray drops. Thus in one experiment[7] in which equation 2 would have led to an expectation of extinction within 20 seconds, the burning of an intense splash fire continued indefinitely, but this fire quickly went out when the spray was turned off. Further work on the conditions under which splash fires form is necessary to ascertain

the conditions under which equation 2 does not apply. From the information available so far it appears that a comparatively high impact energy in the drops is required to cause the splashes but a low entrained air current in the spray is required to allow the establishment of the splash flame. These conditions occur with coarse directional sprays produced at a low pressure. It is also implicit in equation 2 that any flow rate of water spray to the liquid will bring about extinction within a definite time. This is not so since there is a critical rate[2] below which the fire can reach a steady burning state. For kerosene with vertically downward application from fixed nozzles this critical rate is given by equation 3

$$M = 1{\cdot}55\,D \qquad \ldots . [3]$$

For liquids with fire points higher than kerosene the rate is likely to be less although no definite information is available. Finally, in none of the tests was the preburn time longer than 8 minutes. It is unlikely for most liquids that an increase in the preburn times beyond 10 to 20 minutes will give the increase in extinction time predicted by equation 2 since the sensible heat in the liquid above the fire point temperature does not increase significantly after this time[8].

The work described in this paper forms part of the programme of the Joint Fire Research Organization of the Department of Scientific and Industrial Research and Fire Offices' Committee; the paper is published by permission of the Director of Fire Research.

Dept of Scientific and Industrial Research and Fire Offices' Committee
Joint Fire Research Organization
Boreham Wood, Herts

(Received August 1957)

REFERENCES

[1] RASBASH, D. J., ROGOWSKI, Z. W. and STARK, G. W. V. Paper in preparation
[2] RASBASH, D. J. 'Cooling of burning kerosene with water sprays.' *Joint Fire Research Organization. F.R. Note No. 290* (1957)
[3] RASBASH, D. J. and ROGOWSKI, Z. W. 'The extinction of open fires with water spray. Part I. The effect of water spray on a kerosene fire of 30 cm diameter.' *Joint Fire Research Organization. F.R. Note No. 58* (1953)
[4] RASBASH, D. J., ROGOWSKI, Z. W. and STARK, G. W. V. 'Properties of fires of liquids.' *Fuel, Lond.* 35 (1956) 94
[5] BARCLAY, S. F. 'Steam turbine lubrication systems and fire risk.' *Instn mech. Engrs, General Discussion on Lubrication* 2 (1937) 7
[6] RASBASH, D. J. and STARK, G. W. V. Paper in preparation
[7] RASBASH, D. J. and ROGOWSKI, Z. W. 'The design of water sprays for protective installations against high boiling oils. Part II. Tests on transformer oil fires of 3 and 4 ft diameter.' *Joint Fire Research Organization, F.R. Note No. 204* (1955)
[8] BURGOYNE, J. H. and KATAN, L. L. 'Fires in open tanks of petroleum products—some fundamental aspects.' *J. Inst. Petrol.* 33 (1947) 158

Interpretation of the Sample taken by a Probe in a Laminar Concentration Gradient

A. A. WESTENBERG, S. D. RAEZER and R. M. FRISTROM

Current results in the study of laminar flame front structure are being obtained by gas sampling with fine quartz probes. Exclusive of questions of quenching, catalysis, aerodynamic disturbance etc., this technique has raised problems of the significance to be attached to samples withdrawn from regions of large concentration gradients. In the present paper a theoretical study is described in which the situation is approximated by a point sink located in a two-dimensional flow field containing a concentration gradient of a binary mixture. The appropriate diffusion equation is solved by the relaxation technique. The results indicate that the sample entering the sink has a composition which differs only very slightly from that existing at the same point in the unperturbed (no sink) case. A simple experiment is also reported which provides some support for this result, as well as proving conclusively that a probe does not withdraw a sample measuring the total flux (due to diffusion and convection) of each species through a cross section.

THE study of laminar flame structure has recently been considerably advanced by the development of a technique for determining the composition distribution through a flame front[1, 2]. In this method, gas samples are withdrawn at various points through a fine quartz probe and analysed by suitable means. The technique is simple and direct in principle, but presents many subtleties and problems in execution. The experimental details and a consideration of most of the factors entering into such a probe sampling scheme have been discussed[1]. The most important remaining problem was to examine in detail the sampling process itself and its effect on the composition of the sample. In other words, does the sample represent the 'true' (within experimental error of analysis and spatial resolution) composition of the mixture *at* the sampled point, the sum of the fluxes of the various species *through* the sampled cross section, or something appreciably different from either of these? This question is considered in the present paper.

The fundamental reason for the existence of a problem of interpretation is that in a laminar flame front there are large concentration gradients of the reacting species. Obviously, if a non-reacting fluid system is homogeneous in composition and conditions are such that the mean free path is much smaller than the internal diameter of the sampling probe, the sample withdrawn will have the same chemical composition as the original mixture. (The existence of chemical reactions in the gas—as in a flame—is an extraneous complication which we will not consider here, since this brings up the question of rapid quenching which has been discussed elsewhere[1].) If, however, there are gradients in the composition, the flow perturbation

caused by the sampling process itself would be expected to set up different gradients than were originally present, and so alter the composition of the gas entering the probe. Stripped to its essentials then, the problem is reduced to determining the importance of this alteration in composition in a non-reacting binary system containing a concentration gradient. Both theoretical and experimental studies were carried out.

THEORETICAL APPROACH

Two-dimensional model

A steady state, laminar flame front may be considered one-dimensional to a very good approximation[3]. Introduction of a probe through which gas is steadily drawn off perturbs the field so that it becomes a three-dimensional flow with axial (cylindrical) symmetry. In practice, the pressure ratio across the probe is such ($\geqslant 2$) that sonic velocity exists at the throat, i.e. the probe is a 'choking' orifice. Therefore, to be rigorous the flow into the probe should be treated as compressible. With the probe sizes used, however (5 to 50μ i.d.), the sampling rate is such that the flow velocity does not become great enough to cause appreciable compressibility effects until exceedingly close to the tip ($\sim$ one diameter). Thus it is quite adequate to regard the probe as a point sink. The incompressible flow pattern calculated on this basis will be realistic except for the narrow region downstream of the sink which is actually occupied by the probe itself. A previous calculation[4] of the flow into a sampling probe treated the probe as a disc sink, with flow entering only from the upstream face of the disc. It is felt that this is unnecessarily complicated and that the point sink is more realistic.

In view of the axial symmetry possessed by the actual flow into a probe, a further simplification is afforded by use of a two-dimensional model. The point sink is replaced by a line sink and the flow field becomes the well known case of the line sink in a uniform velocity stream[5]. With a constant velocity U (infinitely far from the sink) flowing in the positive z direction, and a line sink perpendicular to the y–z plane, the stream function is given by

$$\psi = Uy - (s/2\pi)\tan^{-1}(y/z) \qquad \ldots.[1]$$

where s is the sink strength defined as the volume flow rate per unit length of sink (cm^2/s). The velocity components are given by

$$v = -\frac{\partial\psi}{\partial z} = -\frac{s}{2\pi}\frac{y}{y^2+z^2}; \quad w = \frac{\partial\psi}{\partial y} = U - \frac{s}{2\pi}\frac{z}{y^2+z^2} \qquad \ldots.[2]$$

where v and w are the y and z components, respectively. It is convenient to define the dimensionless quantities

$$\psi' = \psi/D; \quad v' = v/U; \quad w' = w/U; \quad \alpha = Uy/D; \quad \beta = Uz/D \qquad \ldots.[3]$$

where D is the (constant) binary diffusion coefficient characteristic of the system under consideration. The relations 1 and 2 then become

$$\psi' = \alpha - (s/2\pi D)\tan^{-1}(\alpha/\beta) \qquad \ldots.[4]$$

and

$$v' = -\frac{s}{2\pi D}\frac{\alpha}{\alpha^2+\beta^2}; \quad w' = 1 - \frac{s}{2\pi D}\frac{\beta}{\alpha^2+\beta^2} \qquad \ldots.[5]$$

Lines of constant ψ', i.e. the streamlines, are plotted in *Figure 1* for a sink at the origin. (The flow pattern is symmetrical about the β axis and only half of the field is shown.) The two-dimensional parameter $s/2\pi D$ is chosen to simulate as nearly as possible the actual three-dimensional probe

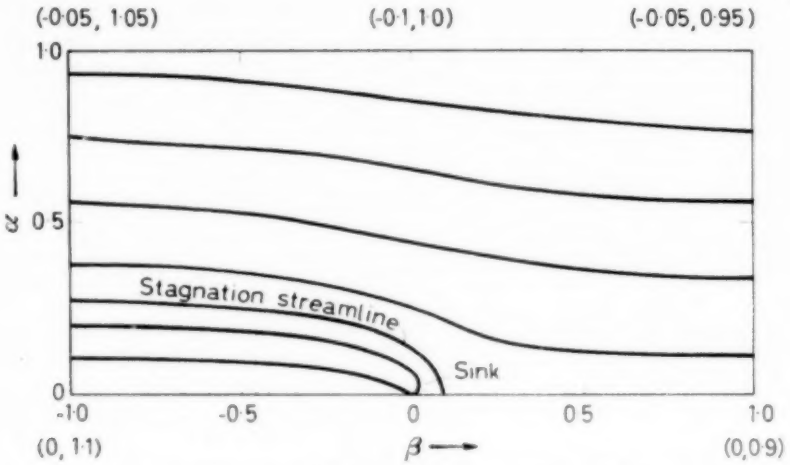

Figure 1. Two-dimensional model of the flow into a sampling probe: dimensionless plot of streamlines for a line sink in a uniform velocity stream. Velocity components at boundary points given in parentheses

(sink). This can be accomplished by noting that in the latter case the quantity $QU/4\pi D^2$ enters, where Q is the volume flow rate into the sink. Thus we equate

$$s/2\pi D = QU/4\pi D^2 = mU/4\pi D^2\rho_0 \quad \ldots . [6]$$

where m is the mass flow rate into the real probe and ρ_0 is the density of the gas infinitely far from the probe. In typical cases dealt with in flame sampling one might have

$$m/\rho_0 = 0{\cdot}005\ \text{cm}^3/\text{s}; \quad U = 100\ \text{cm/s}; \quad D = 10\ \text{cm}^2/\text{s}$$

which would give a sink perturbation parameter of about 0·0004. We have deliberately exaggerated this to $s/2\pi D = 0{\cdot}1$ in calculating the pattern in *Figure 1* and in the subsequent calculation, so that an extreme sampling perturbation is being considered. The numerals in parentheses give the value of the velocity components (v', w') at the designated points. Thus the area shown extends to a velocity perturbation of ± 10 per cent on the β axis. All of the flow bounded by the stagnation streamline enters the sink. Strictly, the sink perturbs the flow to infinity in all directions, and the 'capture radius', i.e. the half-width of the stagnation streamtube at $\beta = -\infty$, is given by

$$z_c = s/2D \quad \ldots . [7]$$

In the present case $z_c = 0{\cdot}1\pi$.

We now superimpose diffusion on this model of the flow into the sampling probe. With the assumptions of steady state, no chemical reactions or

external forces, and constant temperature, pressure, and diffusion coefficient, the rigorous diffusion equation for component 1 of a binary mixture is

$$\nabla^2 f_1 - (1/D)\mathbf{V}\cdot\nabla f_1 - \{(M_1 - M_2)N/\rho\}\nabla f_1\cdot\nabla f_1 = 0 \qquad \ldots.[8]$$

where f_1 is the mole fraction, $\mathbf{V}$ is the mass average velocity vector, M_1 and M_2 are the molecular weights of the two components, N is the total number of moles of gas per unit volume, and ρ is the mass density. It is convenient to make the additional simplifying assumption that the two components have equal masses, i.e. $M_1 = M_2$*. This means that the density is constant as assumed implicitly in the potential flow treatment described earlier. An equation of the same form is obtained with the limiting condition that component 1 is present as a trace. The conclusions to be drawn from this work are not affected in either case. Equation 8 then becomes

$$\frac{\partial^2 f}{\partial y^2} + \frac{\partial^2 f}{\partial z^2} - \frac{1}{D}\left(v\frac{\partial f}{\partial y} + w\frac{\partial f}{\partial z}\right) = 0 \qquad \ldots.[9]$$

in which the subscript 1 has been dropped. In terms of dimensionless variables this may be written

$$\frac{\partial^2 f}{\partial z^2} + \frac{\partial^2 f}{\partial \beta^2} - \left(v'\frac{\partial f}{\partial z} + w'\frac{\partial f}{\partial \beta}\right) = 0 \qquad \ldots.[10]$$

It remains now to apply the general relation 9 to an appropriate system having a concentration gradient similar to those existing in laminar flames. Let us imagine an unperturbed (i.e. without a probe) one-dimensional flow of a binary mixture moving with velocity U in the positive z direction. At the point $z = L$ one component is steadily being quantitatively removed by some unspecified means, so that $f = 0$. At $z = -\infty$ the concentration of this component is f_0. With these boundary conditions the solution of equation 9 for $v = 0$, $w = U$ is simply

$$f = f_0\left\{1 - \exp\left[\frac{U}{D}(z - L)\right]\right\} \qquad \ldots.[11]$$

Such a function is a reasonable approximation to the distribution of some species in flames (e.g. propane in the propane–air flame[2]). Somewhat more generality may be introduced by letting $f/f_0 = F$, $UL/D = \beta_0$, and writing equation 11 as

$$F = 1 - \exp(\beta - \beta_0) \qquad \ldots.[12]$$

Similarly, equation 10 can be written in terms of F and use made of the velocity components given by equation 5 to get

$$\frac{\partial^2 F}{\partial z^2} + \frac{\partial^2 F}{\partial \beta^2} + A\frac{\partial F}{\partial z} - (1 - C)\frac{\partial F}{\partial \beta} = 0 \qquad \ldots.[13]$$

$$A = 0{\cdot}1\,\frac{z}{z^2 + \beta^2}; \quad C = 0{\cdot}1\,\frac{\beta}{z^2 + \beta^2}$$

*It is perhaps not generally recognized that the assumption of equal masses has been made (usually without so stating) when the diffusion equation is given in its more familiar form, i.e. without the third term.

The problem is to solve equation 13 for the value of F at (or very near) the sink location, as it is assumed that this is the concentration of the mixture which the sink will withdraw.

Relaxation solution

Numerical methods must be used to solve equation 13. Since we are interested in a solution within a closed area around the sink, the relaxation method[6] appears well suited to this problem. The coordinate origin is taken to be the position of the sink in *Figure 2*, while the sink position in

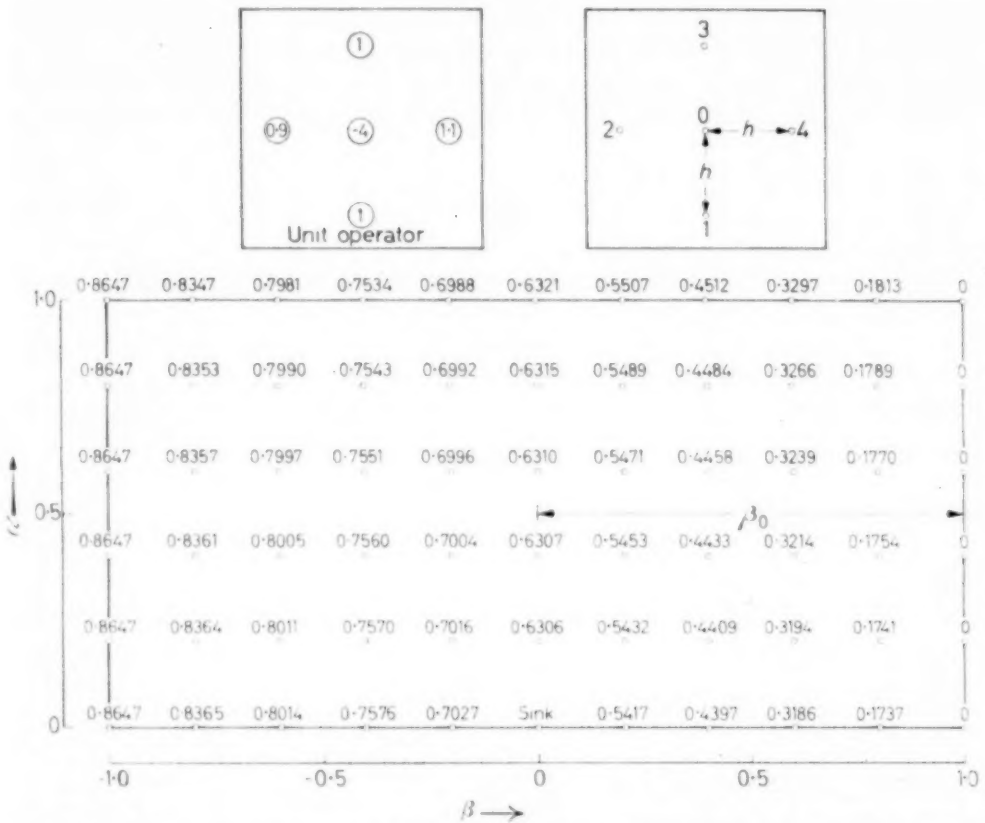

Figure 2. Coarse relaxation results for the concentration distribution around the sink. Values of F given at mesh points

the flow field is indicated by the length parameter β_0, the distance from the $F=0$ boundary. In the present problem we have taken $\beta_0=1$. The relaxation network is set up in the area defined by $-1\leqslant\beta\leqslant1$ and $0\leqslant\alpha\leqslant1$. With the sink strength used ($s/2\pi D=0{\cdot}1$), this region extends about three capture radii in each direction from the sink. At these boundaries the flow field may be regarded as essentially unperturbed, as the parenthetical numerals in *Figure 1* representing the velocity v' and w' show. The boundary conditions obtained from equation 12 are

$$\begin{array}{llll} \beta=1, & F=0 & \alpha=1, & F=1-\exp(\beta-1) \\ \beta=-1, & F=0{\cdot}8647 & \alpha=0, & \partial F/\partial\alpha=0 \end{array} \quad \ldots.[14]$$

The differential equation 13 may be written in finite difference form as

$$\frac{F_1+F_3-2F_0}{h^2}+\frac{F_4+F_2-2F_0}{h^2}+\frac{A}{2h}(F_3-F_1)-\frac{(1-C)}{2h}(F_4-F_2)=0 \quad \ldots.[15]$$

where the subscripts designate the points on a pattern such as is shown on *Figure 2*, and h is the chosen finite difference interval. Since A and C are small compared to unity (except very close to the sink), it is convenient to write equation 15 as

$$F_1+(1+\tfrac{1}{2}h)F_2+F_3+(1-\tfrac{1}{2}h)F_4-4F_0+\tfrac{1}{2}h[A(F_3-F_1)+C(F_4-F_2)]=0 \quad \ldots.[16]$$

The last term in brackets thus represents the perturbation term. In the coarse network used first, the area was covered with a square mesh of 66 points, so that $h=0{\cdot}2$ and the working form of equation 16 was

$$F_1+1{\cdot}1F_2+F_3+0{\cdot}9F_4-4F_0+0{\cdot}1[A(F_3-F_1)+C(F_4-F_2)]=R_0 \quad \ldots.[17]$$

in which R_0 is the residual at any point ($_0$) to be made to vanish everywhere at the final solution. Since the quantities A and C were functions of position according to condition 13, these were computed and written directly on the large relaxation work sheet. For the *relaxation* process, only the first five terms of equation 17 were used, giving the unit point relaxation pattern (coarse) shown in *Figure 2*. After several such relaxation operations at a point the residual would be slightly in error due to the incomplete use of equation 17, so that the exact residual was computed with the full equation. Frequent use of appropriate block relaxation operations greatly facilitated the process in the early stages.

The boundary condition $\partial F/\partial z=0$ at $z=0$ was fulfilled by using a set of fictitious mesh points outside the relaxation area (at $z=-0{\cdot}2$) at which the value of F was kept always equal to that at the equidistant point across the boundary (at $z=0{\cdot}2$). The value of F at the sink was used in calculating the residuals at surrounding mesh points, but the residual at the sink was ignored and allowed to pile up, since the sink represents a singularity in the solution anyway. The concentrations at the points immediately around the sink were the quantities of ultimate interest as these would represent the mixture which the sampling probe takes in. Relaxation was continued until the residual was no greater than ± 2 in the fourth decimal place at every point in the area. The results are shown in *Figure 2* where the value of F is given at each mesh point.

In order to define the concentrations around the sink more closely, a finer net was used locally in the area $-0{\cdot}2\leq\beta\leq 0{\cdot}2$, $0\leq z\leq 0{\cdot}2$, and a second relaxation process carried out. Again 66 points were used with $h=0{\cdot}04$, so that the working form of equation 16 was

$$F_1+1{\cdot}02F_2+F_3+0{\cdot}98F_4-4F_0+0{\cdot}02[A(F_3-F_1)+C(F_4-F_2)]=R_0 \quad \ldots.[18]$$

This equation was only valid for points in the interior of the fine net area. At the junction between coarse and fine nets a special formula had to be derived for each point. This was done by means of a polynomial expansion procedure for 'irregular stars' described by F. S. SHAW[6]. In actual practice,

an initial relaxation was done using fixed boundaries along $\beta = \pm 0{\cdot}2$ and $\alpha = 0{\cdot}2$ obtained by interpolating graphically between the coarse net values. Then the boundaries were included in the relaxation using the special formulae. This affected the fine net interior, of course, so that further relaxation was required. The original coarse net solution was affected only very slightly—negligibly, in fact. The fine net relaxation was carried out using five significant figures in F, with the results rounded off to four figures given in *Figure 3*. The whole relaxation procedure went smoothly and no special difficulties were encountered, even though the authors were inexperienced in this field.

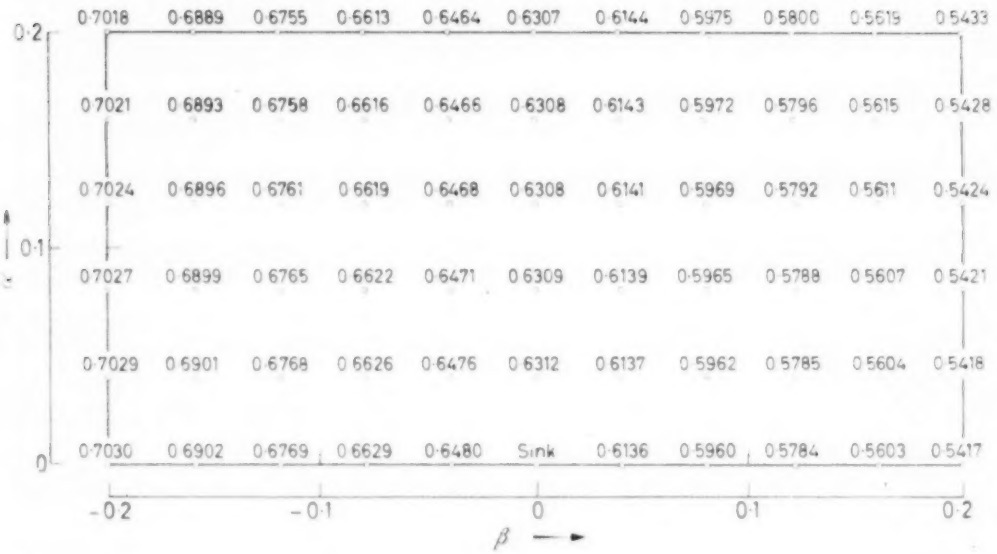

Figure 3. Results of local fine relaxation for the concentration distribution around the sink. Values of F given at mesh points

Discussion

A few remarks about the generality of this solution are in order first of all. No relaxation treatment can be any more general than its boundary conditions, i.e. different boundary conditions would have given a different value of F at each mesh point. The steeper the unperturbed concentration gradient (the $\alpha = 1$ boundary) the more would the concentration at the sink deviate from its unperturbed value. However, the case worked out here was chosen as a fairly typical gradient found in laminar flames. The other aspect in which the solution is unique is the choice of the perturbation parameter $s/2\pi D$. As mentioned previously, this was equated to $mU/4\pi D^2\rho_0$ for an actual three-dimensional probe. The value 0·1 finally used represents an extreme case of perturbation likely to be encountered in practice. Aside from these two factors—boundary conditions and value of $s/2\pi D$— the solution obtained is a general one in terms of the dimensionless variables F, α and β.

It can be seen from *Figures 2* and *3* that the presence of the sink perturbs the concentration distribution surprisingly little. As would be expected, in the region upstream of the sink the iso-concentration lines are ahead (i.e. downstream) of the corresponding lines in the unperturbed case, while downstream of the sink the reverse is true. However, the effect is very small. For example, at the point $\alpha=0$, $\beta=-0{\cdot}2$ the unperturbed concentration is 0·6988, while with the sink present this concentration exists at the point $\alpha=0$, $\beta=-0{\cdot}186$. An interpolation between values at $\alpha=0$, $\beta=0{\cdot}02$ and $\alpha=0$, $\beta=-0{\cdot}02$ for the concentration at the sink mesh point yields $F=0{\cdot}6315$. The unperturbed value is 0·6321. Thus a probe located at the sink point would give a sample reading about 0·1 per cent too low. Another way of interpreting this result is to note that the concentration at the sink is that which would exist approximately at the point $\alpha=0$, $\beta=0{\cdot}002$ in the unperturbed case, i.e. *downstream* of the sink location. Assuming typical values of $U=100\,\text{cm/s}$ and $D=10\,\text{cm}^2/\text{s}$, one would say that the probe takes a sample characteristic of that existing about 2μ downstream. These values should be regarded only as a very rough approximation to an actual probe case, of course.

The fact that the sink perturbs the gradient as little as it does in this simplified treatment is perhaps not unexpected—with the benefit of hindsight. Two factors are responsible for this. Most important is the degree of symmetry about the $\beta=0$ axis, by which the tendency for the sink to 'see' too high a concentration upstream is counteracted by too low a concentration downstream. In the limit of zero flow velocity U, a sink located in an exactly linear concentration gradient would sample precisely the correct concentration. The other factor is the 'self-correcting' property of diffusion. Any new concentration gradients which occur because of the sink perturbation tend to be smoothed out by the diffusion process. The perturbation parameter $QU/4\pi D^2$ shows these effects clearly. The larger this parameter the greater is the perturbation caused by the sink, and this could result from increasing the sink strength Q, the velocity U, or decreasing the diffusion coefficient D. The example worked out here indicates that, under conditions reasonably similar in essential features to those in actual flames, a probe yields samples accurately representative of the mixture at the probe tip for all practical purposes. It is perhaps worth noting that since a condition of constant temperature was assumed in the theoretical model treated in this paper, any possible effects of thermal diffusion on sampling from a flame have been ignored. Thermal diffusion is generally a legitimately negligible effect in laminar flame fronts, although an exception to this rule is mentioned in the footnote on p 224 of ref. 2.

EXPERIMENTAL APPROACH

Background

The ultimate solution to the sampling problem is to set up an experiment in which the concentration gradient is known accurately, and then compare sampled concentrations with the known values. Since flame studies are of primary interest in this connection, the experiment should include as many features similar to laminar flames as possible. As mentioned previously,

the chemical reaction and heat release features of flames are of secondary importance as far as this problem is concerned, but a realistic convection velocity and steady state concentration gradient are required. Unfortunately, a flow system where the concentration distribution is known is difficult to realize experimentally. Several ideas were considered, but all depended ultimately upon measuring the concentration of a binary mixture by some independent means and comparing with the value obtained by sampling, and none of the independent methods appeared accurate enough for the purpose. The compromise system finally used was that of the classic Stefan method[7] for determining the diffusion coefficient of a vapour in a gas. As shown in *Figure 4*, a volatile liquid (acetone) was allowed to

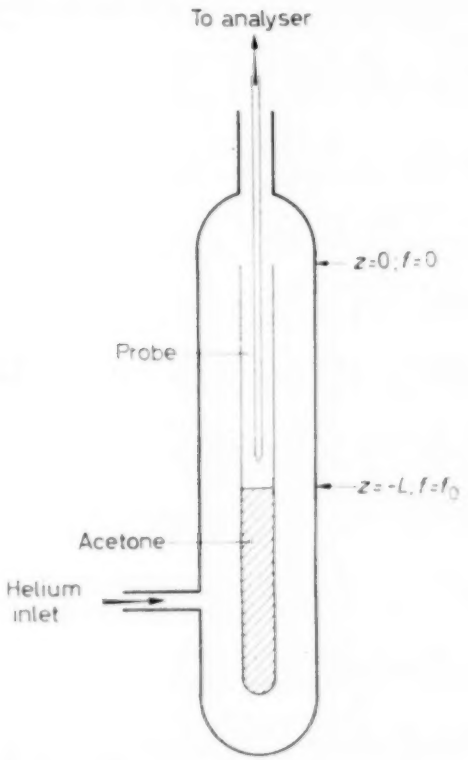

Figure 4. Apparatus and boundary conditions for Stefan diffusion experiment

evaporate from the bottom of a vertical tube of small diameter. The open end of the tube was made to simulate an infinite reservoir by passing a stream of gas (helium) over it. A steady state eventually obtains in which the concentration of acetone is determined by the vapour pressure at the liquid surface and approaches zero at or near the open end of the tube. The distribution along the tube is given by the solution of the diffusion equation.

In this case the one-dimensional form of equation 8 applicable to the Stefan tube is

$$\frac{d^2 f_1}{dz^2} - \frac{w}{D}\frac{df_1}{dz} - \frac{N(M_1 - M_2)}{\rho}\left(\frac{df_1}{dz}\right)^2 = 0 \qquad \ldots . [19]$$

where the subscript 1 refers to the vapour. It is worth noting that there is a finite mass average velocity w along the tube axis because of the impermeability of the liquid surface to helium. The latter has a definite diffusion velocity downwards and this must be counteracted by an upward convection velocity w, since in the steady state there is no net transfer of helium. Furthermore, the velocity w is a variable and it is much simpler to make use of the number average velocity ω defined[8] by

$$\omega = w + f_1 V_1 + f_2 V_2 \qquad \ldots . [20]$$

where V_1 and V_2 are the diffusion velocities. Equation 19 may be written[9] as (dropping the subscript)

$$\frac{d^2 f}{dz^2} - \frac{\omega}{D}\frac{df}{dz} = 0 \qquad \ldots . [21]$$

with the boundary conditions

$$f = 0 \text{ at } z = 0$$
$$f = f_0 \text{ at } z = -L \qquad \ldots . [22]$$

The assumption is made that the liquid level does not drop appreciably due to evaporation during the experiment, i.e. L is constant. ω is also constant for this system, so that equation 21 has the solution

$$\frac{f}{f_0} = F = \frac{1 - \exp(\omega z/D)}{1 - \exp(-\omega L/D)} \qquad \ldots . [23]$$

From equation 20 and the requirement that $w = -V_2$, it may be shown that

$$\omega = (D/L)\ln\{1/(1 - f_0)\} \qquad \ldots . [24]$$

so that equation 23 becomes

$$F = \{(1 - f_0)^{z/L} - 1\}/f_0(1 - f_0)^{z/L} \qquad \ldots . [25]$$

This equation is plotted as the solid line of *Figure 5*, for $f_0 = 0{\cdot}324$ (acetone–helium at one atmosphere total pressure and 26·6°C). If ω is neglected —as is sometimes done—the linear solution to equation 21 shown as the dotted line is obtained. As is apparent, the two are appreciably different.

Apparatus

The system is sketched in *Figure 4*. The glass diffusion tube was 1·3 cm in diameter and filled to within about 15 cm of the open end with CP acetone. It was surrounded by a glass jacket through which helium was passed at a rate (not critical) of about 10 cm^3/s. The current of helium caused the zero acetone concentration boundary at the open end of the diffusion tube and also thermostatted the tube against stray convection currents. The glass sampling probe was similar to the quartz probes used in flame sampling[1]. Its throat was about 6μ i.d. Samples were withdrawn to a simple freeze-out analysis system in which the pressure and volume of the mixture were measured, the acetone trapped quantitatively in a capillary immersed in liquid nitrogen, and the residual helium pressure and volume read. From these data the mole fraction of the sample was determined.

Results and discussion

The data obtained by sampling are plotted in dimensionless form in *Figure 5*. The mole fraction measured close to the liquid surface approached (within 1 per cent) the value expected from the vapour pressure, while the apparent open end of the tube (point where the acetone concentration was extrapolated to zero) was about 1 cm beyond the actual end. It will be noted that the data are very nearly linear. This is more characteristic of the approximate solution neglecting convection than the rigorous

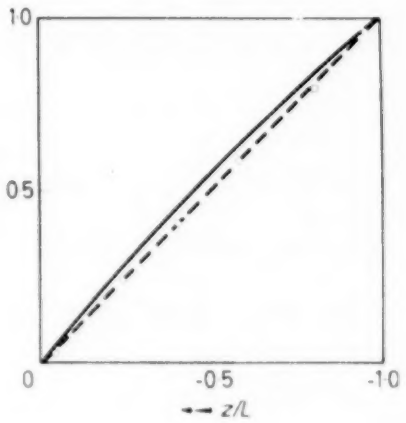

Figure 5. Theoretical (solid line) and experimental (circles) results for dimensionless acetone concentration (F) as function of dimensionless distance (z/L) from end of tube

solution given by equation 25 and the curved (solid) line. The reason for this is that the total sample flow rate was of the same order as the flow rate up the tube due to convection. Thus the sampling process tended to pull helium into the tube at such a rate as to counteract the effects of convection, or in other words, sampling tended to offset the impermeability of the liquid surface to helium. Otherwise, the analyses were precise enough to detect the predicted deviation from linearity.

Two aspects of this experiment, unfortunately but unavoidably, are responsible for the fact that the close check between measured and predicted concentrations does not provide a very convincing proof of the reliability of the sampling process. First, the concentration gradient attainable was not particularly steep—certainly not nearly as steep as those in laminar flames, for example. The parameter $wz/D\,(=\beta)$, however, was of a magnitude comparable to those existing in flames. Secondly, as mentioned previously, it would be expected that a sink located in a linear concentration gradient with no convection would withdraw a sample of the correct concentration. The present experiment nearly falls into this category so that the sink perturbation might be expected to be small.

These experimental results do settle conclusively the argument as to whether a probe samples the total flux (due to convection plus diffusion) of a species through a cross section. If this were so, the sampling data would show a constant acetone concentration everywhere along the tube, since by conservation of species the total acetone flux would have to be constant. This is obviously not the case.

It is a pleasure to note the very great contributions to this work of Professors Howard Emmons and George Carrier of Harvard University who originally suggested application of the relaxation method to this problem, patiently initiated the authors in the details of the technique, and criticized this manuscript. We are also indebted to Dr W. H. Avery of our Laboratory for helpful discussions, and to Mr S. Favin for assistance with the numerical work and preparation of the figures.

This work was supported by the Bureau of Ordnance, U.S. Navy.

Applied Physics Laboratory,

The Johns Hopkins University,

Silver Spring, Maryland

(Received August 1957)

REFERENCES

[1] FRISTROM, R. M., PRESCOTT, R. and GRUNFELDER, C. *Combustion & Flame* 1 (1957) 102
[2] FRISTROM, R. M. and WESTENBERG, A. A. *Combustion & Flame* 1 (1957) 217
[3] FRISTROM, R. M. *J. chem. Phys.* 24 (1956) 888
[4] ROSEN, P. *Applied Physics Laboratory Report No. CF-2248* (1954)
[5] See, for example, MILNE-THOMSON, L. M. *Theoretical Hydrodynamics*, p 196. Macmillan: New York, 1950
[6] For a discussion of this technique see SHAW, F. S. *Relaxation Methods*. Dover: New York, 1953
[7] STEFAN, J. *S. B. Akad. Wiss. Wien* 68 (1874) 385
[8] HIRSCHFELDER, J. O., CURTISS, C. F. and BIRD, R. B. *The Molecular Theory of Gases and Liquids*, p 719. Wiley: New York, 1954
[9] See equation 51 in the chapter by R. B. BIRD in *Advances in Chemical Engineering*, Vol. I, p 175. Academic Press: New York, 1956

Recent Developments and Notes

SPECTRA PRODUCED IN GASES BY SHOCK WAVES

An interesting example of the use of the shock tube for the study of flame-type spectra is provided by the recent work of A. R. FAIRBAIRN and A. G. GAYDON, of the Chemical Engineering Department of the Imperial College of Science and Technology [*Proc. Roy. Soc. A* 239 (1957) 464].

In a fast-burning flame the mixture is raised very quickly, in perhaps 100 μsec, from room temperature to around 3000°K. The flame front, or inner cone, shows certain features, such as bands of C_2 and CH which are associated with the chemical reactions, while the gases beyond the flame front show thermal radiation of OH, H_2O, etc., from the hot products. Reaction processes leading to the C_2 and CH emission are still not completely understood. The new technique here described, that of sudden heating of the gas by an intense shock wave produced by a bursting diaphragm, provides a means of heating pure fuel gases in the absence of oxygen, with the possibility of distinguishing between those radiation processes associated with the pyrolysis of the fuel and those due to its oxidation.

Shocks through hydrocarbon or hydrocarbon plus argon mixtures, without oxygen, give carbon formation and C_2 emission but not CH which is one of the characteristic features of nearly all organic flames. The absence of CH is consistent with the view previously put forward by Gaydon and his colleagues, that electronically excited CH may be formed in flames by the reaction

$$C_2 + OH = CO + CH^*$$

Carbon monoxide plus argon mixtures give strong C_2 but no CO bands; hydrogen or oxygen only slightly quench this C_2, but mixed hydrogen and oxygen quench it strongly. In detonations, OH is very strong, and C_2 and CH are weak compared with burner flames. Time records, using a photomultiplier and oscillograph, indicate that C_2 emission comes from the reaction zones of the detonation, but OH and the continuous spectrum are emitted mainly by the hot gases behind the flame front.

CARBON FORMATION IN DIFFUSION FLAMES

Flat diffusion flames of hydrocarbons, stabilized on a burner similar to that devised by H. G. WOLFHARD and W. G. PARKER [*Proc. phys. Soc. Lond. A* 62 (1949) 722; *A* 65 (1952) 13], have been examined by D. J. COLE and G. J. MINKOFF with a view to obtaining information concerning the processes by which solid carbon particles are formed in such flames [*Proc. Roy. Soc. A* 239 (1957) 280]. For this purpose they used a narrow-beam, recording i.r. spectrometer. The fuels used were methane, ethane, ethylene, propane and butane.

A band at 729 cm^{-1} was observed in both absorption and emission in the spectra obtained and was present in absorption for all the flames studied. This band has been assigned to acetylene. Whilst its position in the flame would be consistent with acetylene being an intermediate in the formation of carbon, the authors put forward evidence as to the relative intensity of this band in the flames of the various fuels, and the effect of additions of acetylene to these flames, which they consider makes it unlikely that acetylene fulfils the role of intermediate in carbon formation.

RUSSIAN EXPERIMENTS ON OPEN-HEARTH COMBUSTION

An account has been given by S. N. BYSTROV and A. A. DOBROKHOTOV of the results of experiments on air-assisted open-hearth combustion [*Stal* 7 (1956); *Iron Coal Tr. Rev.* 174 (1957) 1028]. These experiments were carried out on the plant of the Chelyabinsk Metallurgical Works and were designed to increase the velocity of gas inflow from the port. To do this a method was adopted of feeding additional air into the gas port of an open-hearth furnace using a mixture of blast furnace and coke-oven gas. This air, which is blown into the port at high velocity, is used for the combustion of part of the gas; this raises the temperature and speeds up the inflow of the gas–air mixture. In order to feed the additional air into the port, a water-cooled tuyère, of 6 in. diameter, open at both ends, is placed in the middle of the back wall of the gas port, its end protruding through the brickwork into the port about 16 to 18 in. Along the axis of the tuyère a nozzle is inserted which passes compressed air at 2 to 2·5 atm. The reversing of the additional air feed proceeds automatically and simultaneously with the furnace reversing. The velocity of gas inflow increases from about 38 to 50 or 52 m/s without adversely affecting the distribution of the combustion products in the regenerators. As a result the temperature of the flame at the entry of the bath, near the first door, is increased on an average to between 1860° and 1910°C. Further, the increase obtained in the calorific value of the gas mixture, up to 310 B.Th.U./ft^3, while reducing the consumption of blast-furnace gas, apparently improves the heat transfer from the burner to the bath and thereby increases the efficiency of the furnace. The application of additional air is particularly effective in open-hearth furnaces with basic roofs.

DUST EXPLOSIONS

Recent findings on dust explosions are discussed in a paper by I. HARTMANN, Chief of the Branch of Dust Explosions, Division of Explosives Technology, U.S. Bureau of Mines [*Chem. Engng Progr.* 53 (1957) 107]. An increasing amount of research has been in progress in the past few years at the Bureau's Central Experiment Station in Pittsburgh, in connection with industrial dust explosions.

One of these studies has been concerned with the effect of moisture on the explosibility of dusts. In general the effect of moisture is palliative, because it is inhibiting and cooling, and water vapour acts as an inert gas, diluting the atmosphere and reducing the percentage of oxygen in it. The most important effect of moisture arises from its ability to agglomerate

fine particles of dusts and thereby reduce their dispersibility. Pronounced reduction in inflammability of coal dust is achieved by increasing the moisture content above 5 per cent. The inhibiting effect of moisture is considerably greater than that of added limestone; with a high-volatile bituminous Pittsburgh coal it was more than three times as effective.

Experiments have been carried out on the simultaneous release of explosion pressure and flame quenching in vents, to reduce damage from dust explosions which might occur within improperly designed equipment. The results of these investigations show that it is possible by the aid of wire-screen devices to arrest the flames of many industrial dust explosions within a short distance of their point of origin.

The quenching of dust explosions in the incipient stage is a highly desirable objective in order to prevent secondary explosions due to dust in adjacent regions being raised up by the primary disturbance as a cloud and providing fresh fuel for the flame, thereby extending the region of explosion. It is found possible to prevent some such secondary explosions by dispersing water, limestone, or salt from polyethylene bags or other suspended containers. The quenching agents can be released by firing detonators within the bags, the firing circuit being actuated by a mechanism using the pressure wave preceding the flame in the early stages of explosion.

MIST AND SPRAY EXPLOSIONS

J. H. BURGOYNE has written a short review of work that has been carried out since 1949 at the Imperial College of Science and Technology on mist and spray explosions, incorporating in his paper some new material [*Chem. Engng Progr.* 53 (1957) 121]. He describes suspensions of finely divided liquids as being of two kinds, *condensed mists*, which are the more finely divided and are formed by condensation of saturated vapour, and *mechanical sprays*, which are formed by the atomization of liquid. In the first type of suspension most of the drops are of a diameter less than 0·01 mm and few are larger than 0·02 mm, while in the second type the majority of drops are over 0·1 mm in diameter.

Condensed mists, in which the drop diameters are mostly 0·01 mm or less, propagate flame near the same lower limit of inflammability as the corresponding vapour, as there is time for the drops to vaporize completely in the path of the advancing flame front. If the condensed mist, however, is formed from the saturated vapour of a liquid hydrocarbon of high boiling point, prolonged contact with the source of heat for vaporization may cause pyrolysis with the formation of gaseous products which have combustion properties different from those of the saturated hydrocarbon. Thus the presence of hydrogen or acetylene in the condensed mist will reduce its lower limit of inflammability, raise the requirement of inert gas for suppression of inflammability, and increase the burning velocity.

For drop diameters above about 0·01 mm the mechanism of flame propagation appears to change in that it is no longer possible for the drops to vaporize completely in advance of the flame front. Liquid drops therefore enter the flame and diffusion burning takes place. It appears, moreover, that if the concentration at the lower limit of inflammability is

expressed as the flame-front concentration and not as the volume concentration, drop size has less effect upon the limit value. Work is in progress to elucidate this.

INFRA-RED SPECTROMETRY AND HIGH TEMPERATURE KINETICS

R. BURT and G. J. MINKOFF, of the Imperial College of Science and Technology, London, presented a paper at the XVth International Congress on Analytical Chemistry, held in Lisbon in 1956, on the use of i.r. spectrometry for following high temperature kinetics [*Analyt. chim. Acta* 16 (1957) 259].

It is pointed out that for the detailed elucidation of reaction mechanisms it is not adequate merely to stop a reaction at various times and to analyse the resulting products as a function of time, since many side reactions may occur during chilling. More reliable deductions can be made if the variation with time of the concentration of individual reactants could be determined with the reaction vessel at the reaction temperature. The potentialities and the problems of the use of i.r. spectrometry for this purpose are discussed in the paper. As is well known, the i.r. spectra of aliphatic hydrocarbons are sufficiently distinctive for this technique to be considered of value for following the kinetics of pyrolytic and high-temperature oxidation reactions. Most of these reactions are concerned with aliphatic hydrocarbons and their derivatives.

A sensitive method is described for following the formation, *in situ*, of carbon monoxide and other compounds in the slow oxidation of propane.

EFFECT OF IRRADIATION ON FLAMES

S. W. CHURCHILL, A. WEIR and their colleagues at the University of Michigan, Ann Arbor, have studied the effect of nuclear radiation on the rate of propagation of propane–air flames and on their emission spectra [*Industr. Engng Chem. (Industr.)* 49 (1957) 1419 and 1423].

Using a gold source of radiation with an initial strength of about 10 000 curies, the rate of propagation of bunsen flames of propane–air mixtures at pressures from 4 to 10 in. of mercury was increased up to 50 per cent by the radiation. The effect is attributed to beta radiation, as the estimated number of ion pairs produced by such radiation greatly exceeds the number produced by gamma radiation.

The emission spectra of low-pressure propane–air flames irradiated with a 1000 curie gold source were also studied. Both the preflame mixture and the flame zone were irradiated intensely. The emission at 4315 Å due to CH was increased up to 30 per cent and the emission at 5165 Å due to C_2 up to 150 per cent by the radiation. The emission at 3063 Å due to OH was not affected significantly.

HYDROGEN CYANIDE–FLUORINE–OXYGEN FLAME

Temperatures in excess of 4500°K have been produced by various flames, including those of hydrogen and fluorine, and cyanogen and oxygen. Cyanogen, however, is not commercially available but since these flames produce carbon monoxide, nitrogen and hydrogen fluoride as stable

combustion products at these high temperatures it would appear that if cheap compounds could be burned to such products an inexpensive source of high intensity heat could be obtained. Hydrogen cyanide, fluorine and oxygen which are available in quantity have been experimented with for this purpose by C. S. STOKES and A. V. GROSSE, Jr who have found that a flame of these constituents produces a temperature of approximately 4000°K. A stream of oxygen–fluorine mixture surrounded by one of hydrogen cyanide was burned in a diffusion torch which was inserted into the bottom of a steel chimney [*Industr. Engng Chem.* (*Industr.*) 49 (1957) 1311].

FIRE RESEARCH

In the Reports of the Fire Research Board and the Director of Fire Research for 1956 (*Fire Research 1956*. Department of Scientific and Industrial Research and Fire Offices' Committee, H.M.S.O., 1957) attention is drawn to the importance of the *operational research* approach in investigations on the origin, growth and extinction of fires. An interesting contribution of this type of work has been the launching of a survey of the hazard through the ignition of clothing. This survey has shown very definitely the importance of obtaining a clear perspective of a problem before attempting to solve it by *ad hoc* methods that may be costly, inconvenient and in the end inadequate. The interim results of this work are being considered by a committee of the British Standards Institution. Experiments with fireguards have recently been carried out and have provided fresh information which will be of value in the improvement of design.

Another survey in which certain fire brigades have taken part has shown that between the years 1948 and 1954 the number of chimney fires which were not confined to the chimney but damaged the house has increased more than tenfold. No adequate explanation has yet been found. There is evidence, however, that regular and frequent cleaning of the lower part of the chimney with a flue brush is of importance in addition to the usual major sweeping.

In connection with the vital importance of early detection of outbreaks of fire, the need for a standard test for fire detectors has become increasingly apparent. An apparatus has been designed in which the performance of detectors can be assessed over a range of conditions representative of those which occur during the development of a fire. The apparatus and method of test are to be submitted as the basis of a British Standard.

COMBUSTION OF GASEOUS FUELS

Under the sponsorship of the General Research Planning Committee of the American Gas Association, the Institute of Gas Technology, affiliated with the Illinois Institute of Technology, has conducted over a period of nearly two years an exhaustive search of the literature on the theory of combustion, combustion phenomena, experimental investigations of various phases of combustion and certain fundamentals important to burner design. This information was critically reviewed to determine the deficiencies in

present knowledge and fields in which further work should be done, particularly in relation to the problems of the gas industry. The results of this study have now been published as a monograph entitled *Fundamentals of Combustion of Gaseous Fuels*, by S. A. WEIL, R. T. ELLINGTON, E. F. SEARIGHT and S. HU (Institute of Gas Technology, Chicago, *Research Bulletin No. 15*, 1957, 63 pp.).

NEW TYPE BOILER FOR OIL REFINERY

During a recent routine shutdown of the catalytic cracking unit at Shell's Stanlow refinery, Ellesmere Port, Cheshire, a special boiler was installed for raising steam, the first of its kind in the United Kingdom. The development of this type of boiler, referred to as a carbon monoxide-fired boiler, has recently been reported from America and Canada.

Instead of conventional fuel, this boiler uses mainly gases from the catalytic cracking unit which formerly were discharged to atmosphere. Resulting from regeneration of the catalyst used in the catalytic cracking process, these gases, in addition to being at an already high temperature, undergo combustion in a suitably designed burner to raise steam in the new boiler. Designed by Shell technologists, the boiler was constructed by John Thompson of Wolverhampton.

The gases are led from the top of the catalytic cracking unit, which is over 200 feet high, by a duct 5 feet in diameter specially designed to withstand high temperatures and erosion resulting from small catalyst particles in the gas stream. The operation of the new unit will result in an estimated saving of the equivalent of 30–40 000 tons of heavy fuel oil per annum.

INDUSTRIAL JET-BURNER

An important advance has been made recently by the Research and Development Section, North Eastern Gas Board, in the application of high-pressure gas jet-burners to industrial processes requiring intense local heating. A burner has been developed from which the gases are discharged at temperatures about 1750°C, and at supersonic velocities from 1000 to 1500 ft/s. The high velocities and temperatures available give rapid heat transfer and reduce heat losses, so that fuel costs may be only half those with conventional flames, burning in air. Further, there is no need for a refractory jacket round the material being heated, since radiant heat losses are negligible. Control of the flame and absorption of the noise have been effected by shields of refractory material fixed round the burner, and the heat release is of the order of 250 mil. B.Th.U./ft^3 of flame volume [*Gas World* 146 (1957); *Industrial and Commercial Gas* 36 (20 July 1957) 12].

PROVISIONAL WESTERN STATES SECTION OF THE COMBUSTION INSTITUTE

Following the announcement in this Journal (September, p 384) of the provisional organization of the Western States Section of the Combustion Institute, it is learned that the winter meeting of this Section has been re-scheduled for Monday, 20 January 1958, at the California Institute of

Technology. The tentative selection of papers on flame stabilization and on diffusion flames includes the following:

(1) Stanford Research Institute—Experimental Study of Reverse Jet Flame-Holders
(2) Marquardt Aircraft Co.—Can Burner Combustion
(3) North American Aviation, Inc.—Rocket Combustion Study
(4) Jet Propulsion Laboratory, Calif. Inst. of Technology—Flame Theory of Halogen Flames
(5) Naval Ordnance Test Station—Diffusion Flame Study
(6) California Institute of Technology—Monopropellant Droplet Burning.

The meeting will last the full day. Adequate time for both formal and informal discussions will be provided in the overall schedule. For further information, contact the *Secretary*—G. S. BAHN, Marquardt Aircraft Co., or Dr. E. ZUKOSKI (*Paper Committee*), California Institute of Technology.

FLAMES AND INDUSTRY

A one-day symposium on *Flames and Industry*, organized by the Institute of Fuel was held in London on 9 October. It was arranged in conjunction with the British Flame Research Committee of the International Flame Radiation Research Foundation.

Papers were presented on the characteristics of turbulent jet diffusion flames, by M. W. THRING and E. H. HUBBARD, on the application in industry of experimental techniques used by the International Flame Research Foundation, by E. H. HUBBARD and A. E. PENGELLY, on heat transfer from flames in the steel industry, by J. H. CHESTERS and R. MAYORCAS, in the glass industry, by S. KRUSZEWSKI, in boilers, by W. B. CARLSON, in the cement industry, by E. BURKE and G. FIELD, in gas turbine combustion chambers, by O. A. SAUNDERS, and on radiant heat exchange in a gas-filled enclosure, by H. C. HOTTEL and E. S. COHEN.

The following conclusions may be noted. Compressed-air atomized oil flames of fairly narrow angle are the optimum for high temperature melting furnaces. The compressed air should be preheated after compression and before it is used for atomization, say to 200–300°C, since this increases the jet momentum for a given mass flow of air and a given air pressure. The optimum fuel is that which gives a high flame emissivity without delayed combustion, e.g. heavy liquid fuel with carbon black, tar or pitch creosote.

A useful relation between emissivity and C/H ratio has been shown to exist and the gain from using fuels with a ratio as high as 14 has been clearly demonstrated. The means for producing fuels for use in steel-making furnaces having this high value are being investigated.

Examination of fuel consumption data and heat balances on dual-fired furnaces in the glass industry shows that one ton of heavy fuel oil is equivalent to 1·85 ton of coal, which is about 17 per cent above the calorific value ratio. No significant difference in heat transfer efficiency has been found between heavy fuel oil and coal tar fuel.

A number of new instruments, or modifications of existing ones, have been designed to collect aerodynamic, combustion, and heat transfer data

from flames. Most of these instruments are in use, or are capable of being used, in industry. Descriptions are given of the use of the paramagnetic oxygen meter, the suction pyrometer for measurement of waste gas temperature, the orifice meter connected to pneumatic recorder controllers for measuring air, gaseous and liquid fuels, the soap film apparatus and the Lomchakov modification of the Orsat apparatus for analysing fuel and waste gases, the total radiation pyrometer, the conductivity plug heat flow meter, the calorimeter heat flow meter, and improved forms of pitot tubes and probes for gas and solid particle sampling.

W. A. KIRKBY

FUEL

Readers of *Combustion and Flame* may like to know that *Notes* in the October 1957 issue of *Fuel* included:

Research on thermophysical properties
Continuous analysis of oxygen in flue gas
High energy fuels

Publications

RESEARCH ON FIRE

Edited by HORATIO BOND. Boston, Mass.: National Fire Protection Association, 1957. 184 *pp.* $5.00.

FOR over sixty years the National Fire Protection Association has been the clearing house for activities in connection with the study of fire. This book is a report to the Association's Committee on Research describing the facilities, personnel and management of some of the agencies engaged in research on fire.

The report does not attempt to cover all agencies doing fire research, but representative information is given covering most of the principal agencies, and an adequate picture of the kinds of work going on is presented.

The agencies include laboratories sponsored by various trade associations, by industries maintaining facilities for research and product development, private consultants, universities, research institutes, agencies of the several states of the United States of America, the U.S. Federal Government and the governments of other countries.

While not put together as specifically as history, the reports on the various agencies indicate some of the important dates and developments of research on fire. The history can be traced through the early work on automatic sprinklers out of which came not only the origin of the National Fire Protection Association but the establishment of the Factory Mutual Laboratories, Underwriters' Laboratories and the Laboratories of the British Fire Offices' Committee.

The reports cover fire testing of structural assemblies, measurements of the rate of flame spread over wall finishes, tests of flame-proofing treatments for wood and for fabrics and making determinations with respect to the combustibility, flammability and explosiveness of materials.

ANON

THE SPECTROSCOPY OF FLAMES

A. G. GAYDON. London: Chapman and Hall, 1957. *ix* + 279 *pp.* 6 *plates.* 50*s.*

FOR 15 years, *Spectroscopy and Combustion Theory*, first published by Dr Gaydon in 1942 and revised in 1948, has served as a summary for previous work in the active research area indicated by the title. Even more importantly, the book has served as a guide and a source of stimulation to new workers in the field. New problems and new techniques have come so rapidly that the present revision covering additional material is indeed welcome. The growth of interest in *The Spectroscopy of Flames* is perhaps best illustrated by the size of the bibliographies—258 references in 1942, 301 in 1948, and 495 in the present volume. This increase is even larger than these numbers indicate since some sections of the original volumes have been covered by other books by the same author and are not repeated in the present edition.

This book will be useful to the expert as well as to the novice. The first four chapters give an introduction to the type and the theory of flame spectra as well as to the experimental methods and techniques. Flames of hydrogen, of carbon monoxide, and of organic materials are treated in separate chapters. Flames containing other substances—nitrogen, halogens, sulphur, metals—are described. A short chapter on 'Explosions, engines and industrial flames' is included. Separate chapters are devoted to temperature measurements, to the i.r. region, and to flame spectrophotometry. In one of the longest chapters of the book, Dr Gaydon gives his 'opinions on the interpretations of the [spectral] observations and upon their bearing on theories of chemical reaction processes in flames'. An extensive and very useful appendix contains wavelength tables of band spectra emitted and absorbed by flames. Relative intensities of the bands also are included. Six plates show 35 good reproductions of flame spectra. The book is well arranged with useful author and subject indexes.

Dr Gaydon has given an important criticism of his book in the preface where he states that the book 'is essentially a personal monograph, based largely on experimental work at the Imperial College [of Science and Technology, London]. It gives my own criticism and conclusions on the present state and trend of the subject'. Since such a large share of the recent work on flame spectroscopy has been done by or under the guidance or stimulation of Dr Gaydon, very little is lost by this personal flavour. In fact, it is just this personal approach which allows the author the opportunity of using a very lively and an easily readable style of writing. The book is extremely stimulating and very thought provoking.

H. P. BROIDA

Classified Contents

Behaviour of inverted propane–hydrogen sulphide flames at the blow-off limits, 257
Burning velocities of hydrogen cyanide in air and in oxygen, 60

Cool flame phenomenon in the combustion of acetylene, 99

Determination of composition profiles of flame fronts, techniques for, 102
Determination of flame speed of pentaborane–oxygen–nitrogen mixtures, 420
Determination of minimum ignition energies: results for a neopentane–air mixture, 330
Detonations in gaseous fuming nitric acid–hydrocarbon mixtures, 321
Diffusion flames, in air diluted with nitrogen, some limiting oxygen concentrations for, 155
— turbulent jet, mixing and combustion in free and enclosed, 179
— on positive and negative ions in, 199

Effect of oxygen and ethylene oxide on self combustion of acetylene, 94
Experimental techniques for the study of flat flames by spectroscopy, 241
Explosibility characteristics of coal dust clouds using electric spark ignition, 63
Extinction of fires in liquids by cooling with water sprays, 453
Extraction of ions from a flame, 281

Flame decomposition of the propyl nitrates, 308
Flame zone studies, III. Techniques for the determination of composition profiles of flame fronts, 102
— IV. Microstructure and material transport in a laminar propane–air flame front, 217

Gas turbine combustion chamber, fitted with a swirl atomizer, scale effect in, Part I, 360
— *see also*, 229
Generalized scaling procedures for liquid-fuel rocket engines, 229

Ignition of dust layers on a hot surface, 14
Influence of diborane on blow-off limits of hydrocarbon flames, 212
Interpretation of the sample taken by a probe in a laminar concentration gradient, 467
Investigation of the behaviour and reaction mechanisms of nitric acid–hydrocarbon flames, 264
Isotopic tracer study of carbon formation in hydrocarbon flames, 431

Law of similarity for temperatures in enclosed turbulent flames, 194

Mechanisms for the formation of ions in flames, 385
Method for determining minimum ignition energies: results for a neopentane–air mixture, 330
Microstructure and material transport in a laminar propane–air flame front, 217
Mixing and combustion in free and enclosed turbulent jet diffusion flames, 179

One-dimensional laminar flame theory for temperature-explicit reaction rates, 296
Overseas correspondents' notes, 254

Photoelectric study of the light emission from carbon monoxide–oxygen thermal explosions, 19
Positive and negative ions in diffusion flames, 199
Predicting the laminar flame speed in gases with temperature-explicit reaction rates, 287
Present status of information on transport properties applicable to combustion research, 346

Recent developments and notes, 114, 250, 379, 479
Relation of boundary velocity gradient for flash-back to burning velocity and quenching distance, 127
Role of surface on course of oxidation of methane, 25

Scale effect in a gas turbine combustion chamber fitted with a swirl atomizer, Part I, 360
Self combustion of acetylene, III. Effect of oxygen and ethylene oxide, 94
Slow oxidation of methane—the role of surface on the course of oxidation of methane, 25
Smouldering combustion in dusts and fibrous materials, 129
Some factors influencing stability limits of bunsen flames, 162

Some limiting oxygen concentrations for diffusion flames in air diluted with nitrogen, 155
Some properties of formaldehyde flames, 53
Stability limits of flames of ternary hydrocarbon mixtures, 3
Studies on the oxidation of hydrocarbons under extremely clean experimental conditions, 404
Study of flat flames by i.r. spectroscopy, experimental techniques for, 241

Temperature stability of the laminar combustion wave, 339
Temperature-explicit reaction rates, predicting the laminar flame speed in gases with, 287
— one-dimensional laminar flame theory for, 296
Theory of flame propagation limits due to heat loss, 438
Transport of material in a laminar propane–air flame front, microstructure and, 217
Transport properties, applicable to combustion research, present status of information on, 346

Author Index

BAMFORD, J. A.: *See* HERBERT, M. V. and BAMFORD, J. A.
BENNETT, A. L.: *See* GORDON, A. S., BENNETT, A. L. and DAVIDSON, N.
BERL, W. G., GAYHART, E. L., MAIER, E., OLSEN, H. L. and RENICH, W. T.: Determination of flame speed of pentaborane–oxygen–nitrogen mixtures, 420
BERLAD, A. L. and POTTER, A. E.: Relation of boundary velocity gradient for flash-back to burning velocity and quenching distance, 127
BOYER, M. H. and FRIEBERTSHAUSER, P. E.: An investigation of the behaviour and reaction mechanisms of nitric acid–hydrocarbon flames, 264
BROIDA, H. P.: review of *The Spectroscopy of Flames*, 487
BURKETT, V. T.: *See* WOLF, I. W. and BURKETT, V. T.

CALCOTE, H. F.: Mechanisms for the formation of ions in flames, 385
CARPENTER, D. L.: The explosibility characteristics of coal dust clouds using electric spark ignition, 63
CODEGONE, C.: A law of similarity for temperatures in enclosed turbulent flames, 194
COHEN, L. and SIMPSON, P.: Burning velocities of hydrogen cyanide in air and in oxygen, 60
COLE, D. J. and MINKOFF, G. J.: Experimental techniques for the study of flat flames by infra-red spectroscopy, 241

DAVIDSON, N.: *See* GORDON, A. S., BENNETT, A. L. and DAVIDSON, N.
DECKERS, J. and VAN TIGGELEN, A.: Extraction of ions from a flame, 281

EGERTON, A. C., MINKOFF, G. J. and SALOOJA, K. C.: The slow oxidation of methane—the role of the surface on the course of the oxidation of methane, 25
EISENKLAM, P.: review of *Flow of Gases through Porous Media*, 124

FERGUSON, R. E.: An isotopic tracer study of carbon formation in hydrocarbon flames, 431
FRIEBERTSHAUSER, P. E.: *See* BOYER, M. H. and FRIEBERTSHAUSER, P. E.
FRISTROM, R. M. and WESTENBERG, A. A.: Flame zone studies IV—Microstructure and material transport in a laminar propane–air flame front, 217
— PRESCOTT, R. and GRUNFELDER, C.: Flame zone studies III—Techniques for the determination of composition profiles of flame fronts, 102
— *See* WESTENBERG, A. A., RAEZER, S. D. and FRISTROM, R. M.
FUHS, A. E.: *See* PENNER, S. S. and FUHS, A. E.

GÁL, D.: *See* SZABÓ, Z. G. and GÁL, D.
GAYHART, E. L.: *See* BERL, W. G., GAYHART, E. L., MAIER, E., OLSEN, H. L. and RENICH, W. T.
GORDON, A. S., BENNETT, A. L. and DAVIDSON, N.: A photoelectric study of the light emission from carbon monoxide–oxygen thermal explosions, 19
GRUNFELDER, C.: *See* FRISTROM, R. M., PRESCOTT, R. and GRUNFELDER, C.

HALL, A. R., MCCOUBREY, J. C. and WOLFHARD, H. G.: Some properties of formaldehyde flames, 53

HASELDEN, G. G.: review of *Thermodynamic Functions of Gases*, Volumes I and II, 125
HERBERT, M. V. and BAMFORD, J. A.: Scale effect in a gas turbine combustion chamber fitted with a swirl atomizer, Part I, 360
HULSE, C.: *See* SUNAVALA, P. D., HULSE, C. and THRING, M. W.

IKEGAMI, H.: *See* KINBARA, T. and IKEGAMI, H.

KINBARA, T. and IKEGAMI, H.: On the positive and negative ions in diffusion flames, 199
KIRKBY, W. A.: Recent developments and notes, 114, 250, 379, 479
KURZ, P. F.: Stability limits of flames of ternary hydrocarbon mixtures, 3
— Some factors influencing stability limits of bunsen flames, 162
— Influence of diborane on blow-off limits of hydrocarbon flames, 212
— Behaviour of inverted propane–hydrogen sulphide flames at the blow-off limits, 257

LAFFITTE, P.: Overseas correspondents' notes, 255

MCCOUBREY, J. C.: *See* HALL, A. R., MCCOUBREY, J. C. and WOLFHARD, H. G.
MAIER, E.: *See* BERL, W. G., GAYHART, E. L., MAIER, E., OLSEN, H. L. and RENICH, W. T.
MATSEN, F. A.: *See* ROBERTSON, W. W. and MATSEN, F. A.
MAYER, E.: A theory of flame propagation limits due to heat loss, 438
MINKOFF, G. J.: *See* COLE, D. J. and MINKOFF, G. J.
— *See* EGERTON, A. C., MINKOFF, G. J. and SALOOJA, K. C.

OLSEN, H. L.: *See* BERL, W. G., GAYHART, E. L., MAIER, E., OLSEN, H. L. and RENICH, W. T.

PALMER, K. N.: Smouldering combustion in dusts and fibrous materials, 129
— and TONKIN, P. S.: Ignition of dust layers on a hot surface, 14
PENNER, S. S. and FUHS, A. E.: On generalized scaling procedures for liquid-fuel rocket engines, 229
POTTER, A. E.: *See* BERLAD, A. L. and POTTER, A. E.
— *See* WAYMAN, D. L. and POTTER, R. L.
POWLING, J. and SMITH, W. A. W.: Flame decomposition of the propyl nitrates, 308
PRESCOTT, R.: *See* FRISTROM, R. M., PRESCOTT, R. and GRUNFELDER, C.

RAEZER, S. D.: *See* WESTENBERG, A. A., RAEZER, S. D. and FRISTROM, R. M.
RASBASH, D. J. and ROGOWSKI, Z. W.: Extinction of fires in liquids by cooling with water sprays, 453
RENICH, W. T.: *See* BERL, W. G., GAYHART, E. L., MAIER, E., OLSEN, H. L. and RENICH, W. T.
ROBERTSON, W. W. and MATSEN, F. A.: Self combustion of acetylene III—Effect of oxygen and ethylene oxide, 94
— — A cool flame phenomenon in the combustion of acetylene, 99
ROGOWSKI, Z. W.: *See* RASBASH, D. J. and ROGOWSKI, Z. W.
ROSEN, J. B.: *See* WEHNER, J. F. and ROSEN, J. B.

SALOOJA, K. C.: *See* EGERTON, A. C., MINKOFF, G. J. and SALOOJA, K. C.
SIMMONS, R. F. and WOLFHARD, H. G.: Some limiting oxygen concentrations for diffusion flames in air diluted with nitrogen, 155
SIMPSON, P.: *See* COHEN, L. and SIMPSON, P.
SMITH, W. A. W.: *See* POWLING, J. and SMITH, W. A. W.
SPALDING, D. B.: I. Predicting the laminar flame speed in gases with temperature-explicit reaction rates, 287.
— II. One-dimensional laminar flame theory for temperature-explicit reaction rates, 296.
SUNAVALA, P. D., HULSE, C. and THRING, M. W.: Mixing and combustion in free and enclosed turbulent jet diffusion flames, 179
SZABÓ, Z. G. and GÁL, D.: Studies on the oxidation of hydrocarbons under extremely clean experimental conditions, 404

THRING, M. W.: *See* SUNAVALA, P. D., HULSE, C. and THRING, M. W.
TONKIN, P. S.: *See* PALMER, K. N. and TONKIN, P. S.

VAN TIGGELEN, A.: *See* DECKERS, J. and VAN TIGGELEN, A.

WAYMAN, D. H. and POTTER, R. L.: Detonations in gaseous fuming nitric acid–hydrocarbon mixtures, 321
WEHNER, J. F. and ROSEN, J. B.: Temperature stability of the laminar combustion wave, 339
WEINBERG, F. J.: review of *Selected Combustion Problems II*, 123
WESTENBERG, A. A.: Present status of information on transport properties applicable to combustion research, 346
— RAEZER, S. D. and FRISTROM, R. M.: Interpretation of the sample taken by a probe in a laminar concentration gradient, 467
— *See* FRISTROM, R. M. and WESTENBERG, A. A.
WOLF, I. W. and BURKETT, V. T.: A method for determining minimum ignition energies: results for a neopentane–air mixture, 330
WOLFHARD, H. G.: *See* HALL, A. R., MCCOUBREY, J. C. and WOLFHARD, H. G.
— *See* SIMMONS, R. F. and WOLFHARD, H. G.

Name Index

ADAMS, E. N. 304, 307
ADAMS, G. K. 307, 320
ADAMS, J. R. 70, 92
ADRIAN, F. J. 317, 320
AGNEW, W. G. 248, 249
ALBERTSON, M. L. 187, 193
ALELSEEVA, V. G. 397, 403
ALLISON, V. C. 66, 92
ALLUM, R. E. 41, 51
ANDERSEN, W. H. 384
ANDERSON, D. R. 382
ANDERSON, J. W. 430
ANDERSON, R. C. 59, 98, 128
ANDONIEV, S. M. 116
ANDRADE, E. N. DA C. 199, 211
ARDEN, E. A. 320
ASHOUR, Miss G. 228
AUDIBERT, E. 70, 92
AVERY, W. H. 113, 228, 357, 478

BAHN, G. S. 384, 485
BAMFORD, J. A. 360
BANTA, H. E. 199, 211
BARCLAY, S. F. 466
BARRÈRE, M. 230, 240
BARRETT, G. 249
BATEMAN, J. S. 126
BAYLEY, F. J. 362, 378
BECKER, A. 403
BEDSON, P. 69, 92
BEHRENS, H. 386, 402, 437
BELLES, F. E. 128, 452
BELZER, J. 329
BENNET, W. J. 384
BENNETT, A. L. 19
BENNETT, J. A. J. 385, 402
BENNETT, L. A. 355, 358
BERETS, D. J. 327, 329
BERGH, A. 419
BERL, W. G. 113, 216, 228, 420, 430
BERLAD, A. L. 128, 384, 452
BERNATSKII, V. K. 402
BERNSTEIN, H. J. 320
BILLS, K. W. 384
BINNIE, A. M. 186, 193
BIRD, R. B. 113, 224, 228, 345, 346, 357, 478
BOARDMAN, L. E. 358
BODENSTEIN, M. Z. 412, 419
BOELTER, L. K. M. 187, 188, 193
BOND, H. 487
BONE, W. A. 33, 41, 51, 98, 118, 329
BONHOEFFER, K. F. 385, 402
BOSE, P. K. 280
BOTHA, J. P. 452
BOUCHER, P. E. 199, 211
BOUTON, C. M. 64, 92
BOVEY, H. L. 230
BOYD, C. A. 358
BOYER, M. H. 264
BREDT, I. 386, 402
BRINKLEY, S. R., Jr 329, 392, 393, 403
BROIDA, H. P. 252, 488
BROMLEY, L. A. 271, 280, 353, 357–9
BROTHERTON, T. D. 128
BROW, J. E. 228, 358
BROWN, C. R. 70, 92
BROWN, H. H. 67, 70, 92, 93
BROWN, H. R. 92
BROWN, K. C. 153
BROWN, O. A. 403
BRYAN, A. B. 403
BUILDER, C. H. 384
BULLOCK, B. W. 19, 24
BULLOCK, J. L. 327, 329
BUNDE, R. E. 358
BURGESS, D. S. 120, 402
BURGOYNE, J. H. 121, 358, 466, 481
BURKE, E. 294, 295, 302, 307, 358, 485
BURKE, E. J. 113
BURKETT, V. T. 330
BURT, R. 482
BURWASSER, H. 423
BYINGTON, H. W. 329
BYRNE, J. F. 216, 263
BYSTROV, S. N. 480

CALCOTE, H. F. 286, 385, 389
CALDWELL, F. R. 430
CALVIN, M. 437
CAMPBELL, E. S. 346, 358
CAMPBELL, W. G. 153
CARLSON, W. B. 485
CARMAN, P. C. 124, 125, 382
CARPENTER, D. L. 63, 92
CARRIER, G. 478
CARRUTHERS, J. E. 98
CASHMORE, W. P. 116
CHAMBERLAIN, E. A. C. 100, 101
CHAMBERLAIN, G. H. N. 46, 51
CHAPMAN, D. L. 329
CHAPMAN, S. 358
CHARWAT, A. F. 384
CHEANEY, D. E. 26, 51
CHELKO, L. J. 362, 378
CHESTERS, J. H. 116, 193, 253, 254, 485
CHUPKA, W. A. 403
CHURCHILL, S. W. 482
CLEEVES, V. 187, 193
CLEMENT, J. K. 67, 92
CODEGONE, C. 194, 198
COHEN, E. S. 485
COHEN, L. 60, 62, 129, 154
COLE, D. J. 241, 244, 249, 479
COLLINS, R. D. 180, 193
COMINGS, E. W. 193
COOK, E. B. 120
COOPER, R. 337, 338
COREY, R. C. 382
CORNER, J. 307
CORRSIN, S. 187, 193
COTTRELL, T. L. 320
COWARD, H. F. 6, 13, 158, 161, 260, 263
COWLING, T. G. 358
CROCCO, L. 230, 234, 240
CROSNO, C. W. 403
CULLEN, R. E. 452
CURTISS, C. F. 113, 224, 228, 296, 307, 345, 346, 357, 358, 478
CYPHERS, J. A. 113, 358

DAHLER, J. S. 358
DAI, Y. B. 193
DAMKÖHLER, G. 240
DAMON, G. H. 129, 154
DAVIDSON, J. F. 386, 402
DAVIDSON, N. 19
DAVIES, P. 126
DAVIS, H. 129, 154
DAWS, L. F. 254
DECKERS, J. 281
DELBOURG, P. 250
DELFOSSE, J. M. 281, 286
DEMBROW, D. W. 113, 216, 430
DENNIS, W. R. 380
DENNISTON, D. W., Jr 402
DENTON, Miss E. J. 320
DICK, W. F. L. 126
DIEDRICHSEN, J. 161, 251, 378, 379
DIN, F. 125
DIXON-LEWIS, G. 46, 51, 379
DOBROKHOTOV, A. A. 480
DOERING, W. 329
DONNELLY, J. A. 384
DONOVAN, R. E. 248, 249
DOUSMANIS, G. C. 51
DOWS, D. A. 249
DUGGER, G. L. 128
DUNCAN, A. B. F. 403
DURR, M. 92

ECKERT, E. R. G. 452
EDMONSON, R. B. 430
EDSE, R. 280
EDWARDS, R. S. 115
EGERTON, A. C. 2, 25, 26, 46, 51, 118, 121, 122, 241, 249
EINBINDER, H. 340, 345
EINBINDER, J. 390, 403
EISENKLAM, P. 125
ELIASON, M. A. 352, 358
ELLINGTON, R. T. 484
ELLIS, H. H. 187, 193
ELTENTON, G. C. 403
EMMONS, H. 478
ENGLER, C. 69, 92
ERHARD, K. H. L. 117
ERMAN, G. 385, 402
EPSTEIN, F. 402
ESSENHIGH, R. H. 72, 93
EUCKEN, A. 359
EVANS, M. 113
EVANS, M. W. 452
EYRING, H. 114, 403

FAIN, J. 98, 101
FAIRBAIRN, A. R. 479
FAIRBANKS, D. 358
FARMER, F. B. 403
FARMER, J. B. 403
FARMER, R. H. 153
FAVIN, S. 478
FEILD, G. 485
FEIN, R. S. 430
FERGUSON, R. E. 58, 59, 431, 437
FESHBACH, H. 345
FILIPIEV, O. V. 116
FIOCK, E. F. 128, 280, 427, 430
FOERING, LOUISE 280
FONER, S. 113
FONER, S. N. 106, 403
FOORD, S. G. 25, 51
FORSTALL, W. 187, 190, 193
FORSYTH, J. S. 128
FORT, R. 28, 51
FOSTER, J. F. 13, 178
FOWLER, R. G. 395, 403

FOWLER, R. H. 386, 402
FRANCK, E. U. 358
FRANK-KAMENETSKY, D. A. 295, 298, 307, 358
FRASER, R. P. 119, 329
FRÉLING, E. 255
FREVERT, H. W. 71, 93
FRIAUF, J. B. 327, 329
FRIEBERTSHAUSER, P. E. 264
FRIEDMAN, R. 103, 113, 128, 294, 295 302, 307, 358, 452
FRISTROM, R. M. 102, 113, 217, 228, 357, 358, 430, 467, 478
FUHS, A. E. 229

GÁL, D. 404
GARDNER, J. B. 33, 51
GARNER, W. E. 402
GARSIDE, J. E. 128
GAYDON, A. G. 59, 252, 280, 388, 397, 401–403, 479, 487
GAYHART, E. L. 420, 430
GAYLORD, E. W. 187, 193
GHOSH, B. 73, 93
GIDDINGS, J. C. 114, 291, 295
GIGUÈRE, P. A. 49, 52
GILBERT, M. G. 250
GLASSTONE, S. 403
GLINKOV, M. A. 115
GODBERT, A. L. 70, 92
GODSAVE, G. A. E. 129, 154, 378
GOERCKE, P. 386, 402
GOLDSMITH, M. 384
GORDON, A. S. 19, 24, 113, 228
GOUY, G. 280
GRAF, E. G. 382
GRAHAM, T. E. 316, 320
GRAY, F. A. 116
GRAY, I. 62
GRAY, P. 59, 319, 320
GREEN, M. S. 346, 357
GREENE, E. F. 327, 329
GREENWALD, H. P. 6, 13, 64, 92, 260, 263
GREY, P. 279, 280
GRIFFIN, H. K. 70, 92
GRIMMETT, H. L. 193
GROSSE, A. V., Jr 483
GRUMER, J. 120, 170, 178, 253
GRUNFELDER, C. 102, 228, 358, 478

HABER, F. 385, 402
HAINER, J. H. 64, 92
HALL, A. R. 53, 59, 378
HARGER, J. 67, 92
HARRIS, M. E. 170, 178
HARTMANN, I. 64, 92, 480
HASELDEN, G. G. 126
HASS, H. B. 280
HAWKINS, J. M. 369, 378
HAWTHORNE, W. R. 183, 193
HEATH, D. F. 46, 51
HEDLEY, A. G. M. 126
HELLWIG, K. 98
HENDERSON, I. H. S. 403
HENKEL, M. J. 307
HERBERT, M. V. 360, 378
HERZBERG, G. 397, 403
HEUMANN, G. 402
HIDEO IKEGAMI. 199, 391, 403
HILSENRATH, J. 346, 358
HINSHELWOOD, C. N. 28, 51
HINZE, J. O. 182, 187, 193
HIPPLE, J. A. 403
HIRSCH, H. 121
HIRSCHFELDER, J. O. 113, 224, 228, 291 295, 296, 307, 345, 346, 352, 356–9, 478
HIRST, A. A. 355, 358
HOARE, D. E. 25, 36, 46, 51
HOLLIDAY, D. K. 250
HONIG, R. E. 403
HORN, G. 116, 193
HORNER, E. C. A. 51, 52
HOTTEL, H. C. 73, 93, 129, 154, 181, 183, 193, 485
HOTZWART, R. 69, 92
HOVERS, J. W. J. 64, 92
HOY, H. R. 129, 154
HU, S. 484
HUBBARD, E. H. 116, 485
HUDSON, R. 113
HUDSON, R. L. 403
HUGGILL, H. A. W. 126
HUHN, P. 419
HULSE, C. 179
HUMPHREYS, C. J. 246, 249
HUMPHREYS, N. B. 59
HURD, D. T. 430
HUSTRULID, A. 403

IBBS, T. L. 355, 358
IKEGAMI, H. 199, 391, 403
INGHRAM, M. G. 403
INGLE, H. 178, 263
INGOLD, K. U. 403
ISLES, G. L. 379

JACOBSON, M. 64, 92
JAECKEL, G. 65, 92
JAHN, G. 430
JEGG[redacted], K. E. 402
JENKINS, T. W. 452
JENSEN, R. A. 193, 452
JOHN, R. R. 401, 403
JOHNSTON, E. F. 357, 358
JOHNSTON, H. L. 324, 329
JOHNSTON, H. S. 280
JOHNSTON, W. 452
JOHNSTON, W. C. 128
JONES, E. 71, 93, 118
JONES, G. W. 158, 161, 452
JONES, S. 129, 154

JONES, W. R. D. 92
JOST, W. 401, 403
JOUGET, E. 329

KALLMAN, H. 403
KANT, A. 129, 154
KARABINOS, J. V. 280
KARLOVITZ, B. 338, 402
KASKAN, W. E. G. E. 452
KATAN, L. L. 466
KEAGY, W. R. 187, 193
KEBELY, V. 402
KELLER, G. J. 280
KENNEDY, R. E. 452
KENNEY, M. J. 115
KEYES, F. G. 355, 358
KHARASCH, M. S. 320
KIDDER, G. A. 358
KIMREY, Mrs J. S. 228
KINBARA, T. 199, 211, 390, 391, 403
KING, C. N. 363, 378
KING, I. R. 286, 389, 402
KINGMAN, F. E. T. 153, 154
KIRCHNER, J. G. 280
KIRKBY, W. A. 122, 254, 384, 486
KIRKWOOD, J. G. 321, 329
KISTIAKOWSKY, G. B. 98, 321, 324, 327, 329, 382
KLEIN, G. 296, 307, 342, 345
KLEIN, R. 59
KLIBANOV, T. M. 349, 358
KNAPSCHAEFER, D. H. 402
KNIGHT, H. T. 329
KNIPE, R. H. 24
KNOWLER, A. 383
KONDRATJEW, V. 19, 24
KONDRATJEWA, H. 19, 24
KOSCH, P. 403
KRASSA, P. 402
KREUTZ, C. D. 393, 403
KRUSZEWSKI, S. 485
KUCHTA, J. M. 129, 154
KURZ, P. F. 3, 13, 162, 178, 212, 216, 257, 263
KYDD, P. H. 382

LACY, B. S. 402
LADERMAN, A. J. 384
LAFFITTE, P. 255
LAIDLER, K. J. 46, 51, 397, 400, 403
LANGER, A. 403
LAYZER, D. 340, 345
LEAH, A. S. 126
LE BLANC, M. 358
LE CHATELIER, H. 6, 13, 260, 263
LEE, C. Y. 350, 358
LENARD, P. 403
LENHER, S. 98
LEVY, J. B. 317, 320
LEWIS, B. 2, 45, 46, 51, 59, 127, 128, 166, 178, 263, 280, 327, 329, 338, 385, 393, 402, 452
LINDSAY, A. L. 357, 359
LINNETT, J. W. 46, 51, 427, 430
LITTON, R. S. 216
LLEWELLYN JONES, F. 338
LOEB, L. B. 211
LONSDALE, H. K. 348, 358
LOSCHMIDT, J. 348, 358
LOSSING, F. P. 403
LOWRY, H. H. 129, 154
LUFT, N. W. 129, 154
LUKASIEWICZ, J. 383
LYN, W. T. 114

MCADAMS, W. H. 452
MCCOUBREY, J. C. 53
MACDONALD, R. D. 98
MCDOWELL, C. A. 403
MCGUIRE, J. H. 18
MACKENZIE, J. E. 358
MACLEOD, L. H. 384
MCNEELY, J. K. 390, 403
MAIER, E. 420
MALIN, M. E. 329
MALINOVSKII, A. E. 402
MANDELSHTAN, S. L. 397, 403
MANTON, J. 128, 392, 393, 403
MARSDEN, D. G. H. 403
MARTYNYUK, L. A. 403
MARVIN, C. F., Jr 430
MASCOLO, R. W. 402
MASON, E. A. 348, 350, 357, 358
MATSEN, F. A. 94, 98, 99, 101
MATTUCK, A. J. 113
MATTUCKS, G. R. 193
MAYER, E. 438, 452
MAYORCAS, R. 116, 485
MELVILLE, H. W. 358
MELTZER, T. H. 320
MILLER, C. H. 243, 249
MILLIKEN, B. B. 128
MILNE-THOMSON, L. M. 478
MINKOFF, G. J. 25, 26, 46, 51, 122, 241, 244, 249, 479, 482
MISCHUK, E. 384
MITCHELL, E. T. 327, 329
MOE, G. 384
MONTROLL, E. W. 346, 357
MORGAN, J. D. 66, 92
MORRIS, J. D. 402
MORSE, P. 345
MOUTET, H. 240
MOYERMAN, R. M. 387, 402
MUCKENFUSS, C. 358
MUELLER, K. H. 280
MULLINS, B. P. 378
MUSKAT, M. 154

NAGY, J. 92
NAKAMURA, J. 200, 211, 390, 391, 403

NAMIOKA, T. 403
NEEDHAM, B. P. 59
NEEDHAM, D. P. 248, 249, 320
NEEDHAM, H. C. 365, 378
NETTLEY, P. T. 358
NEWARK, H. E. 70, 92, 129, 154
NEWBY, M. P. 183, 193
NEWITT, D. M. 126
NICHOLLS, P. 382
NICHOLSON, A. J. C. 402
NICHOLSON, H. M. 368, 378
NORRISH, R. G. W. 25, 48, 51, 52, 117
NUDENBERG, W. 320

OLSEN, H. L. 420, 430
ORLICK, C. A. 320
ORNING, A. A. 73, 93
OSBERGHOUS, D. 403
OSTBORG, H. N. 70, 92
OXENDINE, J. R. 120, 253, 402

PAGE, F. M. 398, 403
PALMER, K. N. 14, 18, 129, 154
PARKER, W. G. 59, 161, 241, 249, 280, 430, 479
PARR, S. W. 70, 92
PARTINGTON, J. R. 280
PAYMAN, W. 6, 13, 260, 263, 383
PEARSE, R. W. B. 280
PEARSON, A. E. 116
PEARSON, S. W. 253
PEASE, R. N. 46, 51, 402
PENGELLY, A. E. 485
PENNER, S. S. 229, 230, 240, 290, 295, 304, 307, 345, 384
PERRIN, J. R. 384
PERRY, M. D. 153
PHILLIPS, V. D. 128
PICKERING, H. S. 430
PIETERS, H. A. J. 64, 92
PILCHER, J. M. 70, 92
PIMENTEL, J. C. 247, 249
PLYLER, E. K. 246, 249
POLING, R. E. 178
POMERANTSEV, V. V. 358
POPOVA, E. V. 116
PORTER, G. 117, 431, 437
PORTER, H. C. 70, 93
POTTER, A. E., Jr 128, 452
POTTER, R. L. 321, 329
POWLING, J. 59, 121, 241, 248, 249, 308, 320, 379
PRAUSNITZ, J. M. 357
PRESCOTT, R. 102, 113, 228, 358, 478
PRICE, D. J. 70, 93
PRICE, W. C. 249
PRIGG, J. A. 250
PROTOPOPOV, A. K. 403
PUTNAM, A. A. 380, 452

RADCLIFFE, A. 369, 378
RADIER, H. H. 62
RAEZER, S. D. 113, 467
RASBASH, D. J. 453, 466
REAGH, J. D. 48, 52
REID, T. J. 316, 320
REITER, S. H. 402
RENICH, W. T. 219, 420, 430
RICE, G. S. 64, 92
RICE, R. A. 362, 378
RICE, R. G. 280
RICE, W. E. 358
RICHARDS, R. 243, 249
RICHARDSON, J. M. 329, 339, 345
RICHMOND, J. K. 120, 253
RIGG, M. W. 384
RILEY, F. F. 280
RIVIÈRE, M. 116
ROBERTSON, A. D. 116
ROBERTSON, W. W. 59, 94, 98, 101
ROEDER, C. H. 403
ROFFEY, F. 402
ROGOWSKI, Z. W. 453, 466
ROSEN, B. 403
ROSEN, J. B. 339, 340, 345, 452
ROSEN, P. 110, 113, 478
ROSSIKHIN, V. S. 401, 403
ROSSINI, F. E. 329
ROTANOV, A. P. 402
ROTHMAN, A. J. 353, 358
ROUSE, H. 193
RUDEN, P. 187, 193
RUMPEL, W. F. 358
RUST, F. F. 320

SADOWNIKOW, P. 48, 52
SAENGER, E. 386, 402
SALOOJA, K. C. 25, 26, 46, 51, 52, 122
SANDERS, T. N. 51
SANITER, F. H. 193
SARJANT, R. J. 115
SATO, K. 402
SAUNDERS, M. J. 390, 403
SAUNDERS, O. A. 485
SAUNDERS, S. W. 385, 402
SAVEDOFF, L. 329
SCHAAF, V. P. 320
SCHÄFER, K. 349, 358
SCHAWLOW, A. L. 51
SCHEER, M. D. 51, 52, 59
SCHMIDT, R. 358
SCHOEN, L. J. 59
SCHOLL, J. R. 329
SCHOTTKY, W. F. 358
SCHRIESHEIM, A. 118
SCHUHMANN, K. 349, 358
SCHULTZ, H. 170, 178
SCHWERTZ, F. A. 228, 358
SCOTT, E. W. 280
SEARIGHT, E. F. 484

SEMENOFF, N. N. 295, 405, 415, 419
SEUBOLD, F. H. 320
SEWELL, R. 115
SHAFER, M. R. 230
SHAPIRO, A. H. 190, 193
SHAW, F. S. 478
SHAW, G. T. 320
SHEPHERD, W. C. F. 129, 154, 383
SHERMAN, R. A. 70, 92
SHULER, K. E. 46, 51, 387, 390, 397, 400, 402, 403
SCHULTZ, R. D. 384
SILVER, R. S. 129, 154
SILVERMAN, S. 19, 24
SIMMONS, R. F. 59, 155
SIMON, D. M. 128, 452
SIMPSON, P. 60
SINGER, J. M. 120, 253
SINNATT, F. S. 70, 92, 129, 154
SKALOV, B. 402
SKEET, G. 153
SLOTIN, L. 48, 52
SMALL, N. J. H. 413, 419
SMILEY, E. F. 355, 358
SMITH, A. G. 390, 403
SMITH, D. F. 70, 92
SMITH, R. W., Jr 392, 393, 403
SMITH, S. R. 113, 228
SMITH, W. A. W. 308, 320
SMITH, W. V. 46, 51
SMITHELLS, A. 178, 263
SNOWDEN, F. F. 51, 52
SOKOLIK, A. 402
SPAKOWSKI, A. E. 128, 452
SPALDING, D. B. 71, 93, 120, 129, 154, 161, 287, 295, 296, 381, 449, 450, 452
SPAULDING, W. P. 307
SPENCE, R. 98
SQUIRE, H. B. 187, 190, 193
STAPLES, C. W. 382
STARK, G. W. V. 466
STARKMAN, E. S. 384
STEACIE, E. W. R. 98, 320
STEELE, Miss P. 307
STEFAN, J. 348, 358, 478
STEIN, N. 358
STEINBERGER, R. 319, 320
STEINGRIMSSON, V. 358
STERN, O. 385
STEVENS, F. W. 424, 430
STEVENSEN, D. P. 403
STEVENSON, D. P. 437
STEWART, D. G. 360, 378
STEWART, I. McC. 73, 93
STEWART, R. D. 384
STOKES, C. S. 483
STOPS, D. W. 353, 358
STREHLOW, R. A. 349, 358, 427, 430
STUART, J. G. 427, 430
STYLE, D. W. G. 48, 51, 52
SUGDEN, T. M. 390, 398, 403
SUMMERFIELD, M. 401, 403
SUMMERS, D. 51, 52
SUNAVALA, P. D. 179, 182, 193
SWETT, C. C. 333, 338
SZABÓ, Z. G. 404, 419

TAFFANEL, J. 66, 92
TANFORD, C. 385, 402
TATE, J. T. 403
TAUBERT, R. 403
TAYLOR, G. B. 70, 93
TAYLOR, J. F. 187, 193
TENSMEYER, L. G. 114
THABET, S. K. 121, 241, 249
THOMPSON, H. W. 243, 249
THOMPSON, J. J. 199, 211, 402
THOMPSON, R. 280
THOMPSON, W. B. 13, 178, 263
THOMSON, G. P. 402
THRING, M. W. 115, 116, 129, 154, 179, 183, 193, 250, 253, 254, 485
THRUSH, B. A. 117, 390, 403
TIMKOVSKII, V. P. 402
TIMMERMANS, J. 161
TJULANDER, V. E. 384
TONKIN, P. S. 14, 153
TOSIRÔ KINBARA, 199, 200
TOWNEND, D. T. A. 100, 101, 128
TOWNES, C. H. 46, 51
TREON, J. F. 280
TROSTEL, L. J. 71, 93
TROUNCER, J. 190, 193
TSIEN, H. S. 230
TSUCHIYA, T. 403
TSYKORA, I. L. 403
TU, C. M. 129, 154
TUFTS, F. L. 385, 386, 402
TVERDOKHLEBOV, V. I. 385, 390, 402, 403
TYLER, J. D. 180, 193

UBBELOHDE, A. R. 2, 413, 419
UBBINK, J. B. 358
UBEROI, M. S. 187, 193

VAN DER HEGGE ZIJNEN, B. G. 193
VAN LANGEN, J. 116
VANPÉE, M. 41, 51
VANREUSEL, L. 281, 286
VAN TIGGELEN, A. 281
VAUGHAN, W. E. 320
VIEILLE, P. 383
VINES, R. G. 355, 358
VITAL, M. 69, 92
VOGT, K. 402
VOLTA, A. 385
VON ELBE, G. 45, 46, 51, 59, 127, 128, 166, 178, 263, 280, 338, 385, 402, 452
VON ENGEL, A. 403

VON KÁRMÁN, T. 120, 290, 295, 304, 307, 345
VON MEYER, R. 69, 92
VON NEUMANN, J. 329
VON OBERMAYER, A. 358

WAGNER, H. G. 401, 403
WALDMAN, L. 348, 358
WALKER, J. F. 320
WALKER, R. E. 349, 358
WALL, F. T. 358
WALSH, A. D. 24–26, 37, 46, 51, 413, 419
WARD, Miss M. 153
WARREN, D. R. 46, 51
WARREN, J. W. 402
WASSILJEWA, A. 355, 358
WATANABE, K. 402, 403
WATSON, W. R. 382
WATT, J. S. 403
WAYMAN, D. H. 321
WEAVER, E. R. 250
WEBER, J. 387, 390, 402
WEDDELL, D. S. 183, 193
WEHNER, J. F. 339, 452
WEIL, S. A. 484
WEINBERG, F. J. 124, 358
WEIR, A. 482
WELLER, A. E. 187, 193
WELLS, F. E. 402
WESTBROOK, E. A. 98
WESTENBERG, A. A. 113, 217, 346, 349, 358, 467, 478
WHEATLEY, P. J. 430
WHEELER, R. V. 70, 92
WHEELER, W. H. 329
WHITE, A. G. 71, 93
WHITE, D. W. 153
WHITE, E. C. 70, 93
WHITE, H. 337, 338
WHITE, J. R. 280
WHITTINGHAM, G. 129, 154
WHITTLE, E. 249
WIDDAS, W. 69, 92
WILD, N. E. 358
WILDE, K. A. 304, 307
WILHELM, R. H. 344
WILKE, C. R. 271, 280, 350, 357, 358
WILLIAMS, R. P. 64, 92
WILSON, H. A. 199, 211, 403
WISEMAN, L. A. 320
WOHL, K. 127, 128, 273, 280, 452
WOLF, I. W. 330
WOLFHARD, H. G. 53, 59, 155, 161, 241, 249, 251, 277, 280, 379, 388, 397, 401, 402, 403, 430, 479
WOLFROM, N. L. 280
WOOD, W. W. 321, 329
WRIGHT, W. A. 219
WUEST, W. 187, 193
WUPPERMAN, G. 358
WYCKOFF, R. D. 154

YOFFE, A. D. 279, 280, 319, 320
YOKLEY, C. R. 437

ZELDOVICH, Y. B. 295, 298, 307, 329
ZENON, Z. 338
ZIJNEN, B. G. v. D. H. 182, 193
ZONNERBERG, G. J. O. 64, 92
ZUKOSKI, E. E. 384, 485